2016

Interfacing of neuromorphic vision, auditory and olfactory sensors with digital neuromorphic circuits

Anup Vanarse
Edith Cowan University

Edith Cowan University

Copyright Warning

Interfacing of Neuromorphic Vision, Auditory and Olfactory Sensors with Digital Neuromorphic Circuits

This thesis is presented in partial fulfilment of the degree of

Master of Engineering Science

ANUP VANARSE

(B.E. (Computer Science and Engineering), Visvesvaraya Technological University, India)

Edith Cowan University

School of Engineering

2016

CONTENTS

ABSTRACT v
STATEMENT OF ORIGINALITY vii
ACKNOWLEDGEMENTS ix
CONVENTIONS xi
PUBLICATION xiii
LIST OF FIGURES xv
LIST OF ABBREVATIONS xvii

CHAPTER 1. INTRODUCTION 1
1.1. MOTIVATION 2
1.2. RESEARCH QUESTIONS: 2
1.3. RESEARCH CONTRIBUTION: 3
1.4. THESIS ORGANISATION: 4

CHAPTER 2. LITERATURE REVIEW 5
2.1. NEUROMORPHIC ENGINEERING 5
2.2. SILICON NEURON: ESSENTIAL COMPONENT OF NEUROMORPHIC SYSTEMS 8
2.3. NEUROMORPHIC VISION SENSING 13
2.4. NEUROMORPHIC AUDITORY SENSORS 24
2.5. NEUROMORPHIC OLFACTION SENSING 32
2.6. SUMMARY 42

CHAPTER 3. COMPARISON BETWEEN CURRENT STATE-OF-THE-ART NEUROMORPHIC VISION, AUDITORY AND OLFACTORY SENSORS 43
3.1. CURRENT DEVELOPMENTS IN NEUROMORPHIC ENGINEERING 43
3.2. NEUROMORPHIC VISION SENSORS 44
3.3. NEUROMORPHIC AUDITORY SENSORS 46
3.4. NEUROMORPHIC OLFACTORY SENSORS 48

CHAPTER 4. METHODOLOGY 51

4.1. ADDRESS EVENT REPRESENTATION 51
4.2. PROPOSED APPROACH 53
4.3. SUMMARY 59

CHAPTER 5. JAVA SIMULATION AND MODELLING 61
5.1. JAVA BASED MODEL OF OLFACTORY SENSOR 61
5.2. SIMULATION AND RESULT ANALYSIS 67
5.3. COMPARISON WITH NENGO SIMULATION MODEL 69

CHAPTER 6. CONCLUSION 75
6.1. APPLICATION 77
6.2. FUTURE DIRECTIONS 77

REFERENCES 79

ABSTRACT

The conventional Von Neumann architecture imposes strict constraints on the development of intelligent adaptive systems. The requirements of substantial computing power to process and analyse complex data make such an approach impractical to be used in implementing smart systems. Neuromorphic engineering has produced promising results in applications such as electronic sensing, networking architectures and complex data processing. This interdisciplinary field takes inspiration from neurobiological architecture and emulates these characteristics using analogue Very Large Scale Integration (VLSI). The unconventional approach of exploiting the non-linear current characteristics of transistors has aided in the development of low-power adaptive systems that can be implemented in intelligent systems.

The neuromorphic approach is widely applied in electronic sensing, particularly in vision, auditory, tactile and olfactory sensors. While conventional sensors generate a huge amount of redundant output data, neuromorphic sensors implement the biological concept of spike-based output to generate sparse output data that corresponds to a certain sensing event. The operation principle applied in these sensors supports reduced power consumption with operating efficiency comparable to conventional sensors. Although neuromorphic sensors such as Dynamic Vision Sensor (DVS), Dynamic and Active pixel Vision Sensor (DAVIS) and AEREAR2 are steadily expanding their scope of application in real-world systems, the lack of spike-based data processing algorithms and complex interfacing methods restricts its applications in low-cost standalone autonomous systems.

This research addresses the issue of interfacing between neuromorphic sensors and digital neuromorphic circuits. Current interfacing methods of these sensors are dependent on computers for output data processing. This approach restricts the portability of these sensors, limits their application in a standalone system and increases the overall cost of such systems. The proposed methodology simplifies the interfacing of these sensors with digital neuromorphic processors by utilizing AER communication protocols and neuromorphic hardware developed under the Convolution AER Vision Architecture for Real-time (CAVIAR) project. The proposed interface is simulated using a JAVA model that emulates a typical spike-based output of a neuromorphic sensor, in this case an olfactory sensor, and functions that process this data based on supervised learning. The successful implementation of this simulation suggests that the methodology is a practical solution and can be implemented in

hardware. The JAVA simulation is compared to a similar model developed in Nengo, a standard large-scale neural simulation tool.

The successful completion of this research contributes towards expanding the scope of application of neuromorphic sensors in standalone intelligent systems. The easy interfacing method proposed in this thesis promotes the portability of these sensors by eliminating the dependency on computers for output data processing. The inclusion of neuromorphic Field Programmable Gate Array (FPGA) board allows reconfiguration and deployment of learning algorithms to implement adaptable systems. These low-power systems can be widely applied in biosecurity and environmental monitoring. With this thesis, we suggest directions for future research in neuromorphic standalone systems based on neuromorphic olfaction.

COPYRIGHT AND ACCESS DECLARATION

I certify that this thesis does not, to the best of my knowledge and belief:

(i) incorporate without acknowledgement any material previously submitted for a degree or diploma in any institution of higher education;

(ii) contain any material previously published or written by another person except where due reference is made in the text; or

(iii) contain any defamatory material.

Signed (signature not included in this version of the thesis)

Date…….

STATEMENT OF ORIGINALITY

I certify that this thesis does not, to the best of my knowledge and belief:

i. Incorporate without acknowledgment any material previously submitted for a degree or diploma in any institution of higher education;
ii. Contain any material previously published or written by another person except where due reference is made in the text of this thesis; or
iii. Contain any defamatory material;

Anup Vanarse

To my family, for their endless trust, support, encouragement and love.

ACKNOWLEDGEMENTS

I would like to take this opportunity to thank all the people who have helped me directly or indirectly during my Masters studying career.

I would like to thank my supervisor A/Prof. Adam Osseiran for constant motivation and encouragement. His invaluable advice during the course of my Masters studies has guided me to accomplish this task. He held me to the highest of standards, but also had the faith that I would be able to achieve them. None of the work in this thesis would have happened without him.

I wish to thank my co-supervisor Dr. Alex Rassau for his valuable inputs during the course of this research. His guidance for documenting this research has been instrumental.

I would also like to thank the Graduate Research School support staff especially Heather Williams for her constant support and encouragement. I am also thankful to Dr. Greg Maguire (research writing consultant at ECU) for his support to improve my academic writing. It is a privilege for me to have worked with each one of them.

I am grateful to all with whom I have spent my time as a post-graduate research student at ECU.

I would like to express my earnest gratitude to my parents for their love and countless sacrifices to give me the best possible education. I cannot thank them enough for giving me the opportunity to freely pursue my interests and career. Without their patience and unreserved support, it would not have been possible to reach this stage in my career. I owe a debt of gratitude to my wife Komal and my cousin Nikhil, who have always believed in me and my abilities, and supported me throughout this research and my life.

This page has been left blank intentionally

CONVENTIONS

Typesetting

This thesis is typeset in Times New Roman using Microsoft Word 2013. Referencing and citation style are based on the Institute of Electrical and Electronics Engineers (IEEE) Transaction style.

Spelling

English spelling in this thesis is based on Australian English.

This page has been left blank intentionally

PUBLICATION

Journal

Vanarse A., Osseiran A. and Rassau A., (2016), “A Review of Neuromorphic Vision, Auditory and Olfactory Sensors,” Frontiers in Neuroscience, doi: 10.3389/fnins.2016.00115

This page has been left blank intentionally

LIST OF FIGURES

Figure 2.1. Current-Voltage plots by Carver Mead to compare the ubiquitous exponential characteristics between membrane potentials and analogue transistors (adapted from [4]) .7
Figure 2. 2. Basic anatomical part of a neuron (Adapted from [18]).....9
Figure 2.3. Light microscope photograph of a stained neuron (Adapted from [18]).....9
Figure 2.4. High-level conceptual model of an Integrate and Fire neuron (Adapted from [18]) 11
Figure 2.5. Integrate-and-Fire neuron model by Carver Mead (Adapted from [22]).....11
Figure 2.6. Schematics of HH-soma implementation in CMOS (Adapted from [23]).....12
Figure 2. 7. Signal time course of a HH-soma implementation (Adapted from [18]) 13
Figure 2.8. Cross section of primate retina (Adapted from [11]) 14
Figure 2.9. Key components of biological retina that are emulated in silicon retina (Adapted from [24]) 15
Figure 2.10. Schematic of pixel from Mahowald retina (Adapted from [4]) 17
Figure 2.11. Adaptive retina pixel circuit by Carver Mead (Adapted from [4]).....18
Figure 2.12. A 128 × 128 Dynamic Vision Sensor by Tobi Delbruck (Adapted from [37]).....20
Figure 2.13. Three layer model of biological vision and corresponding DVS pixel circuit (Adapted from [24]) 21
Figure 2.14. Waveforms of DVS pixel circuit (Adapted from [24]) 21
Figure 2.15. Output image from DVS (Adapted from [12]) 22
Figure 2.16.ATIS pixel circuit, operation principle of ATIS and its output frames (Adapted from [24]).....23
Figure 2.17. DAVIS pixel circuit with APS and DVS pixel fusion (Adapted from [27]) 23
Figure 2.18. DAVIS vision sensor (Adapted from [27]) 24
Figure 2.19. Human auditory system (Adapted from [12]) 25
Figure 2.20. Cross-section of biological cochlea (Adapted from [5]) 26
Figure 2.21. Silicon cochlea design by Mead and Lyon (Adapted from [5]).....28
Figure 2.22. Block diagram representation for bionic ear processor by Sarpeshkar et al. (Adapted from [62]) 29
Figure 2.23. Operating principle of AEREAR (Adapted from [65]).....30
Figure 2. 24. Block diagram representation of working of AEREAR2 (top) and AEREAR2 sensor board (bottom) 31
Figure 2.25. Cross-section of human olfactory system (Adapted from [71]) 33
Figure 2.26.Cross-section of biological olfactory epithelium (Adapted from [72]).....33
Figure 2.27. Detailed pathway for biological olfaction (Adapted from [72]) 34
Figure 2.28. Typical biomimetic olfactory sensor design (Adapted from [74]).....36
Figure 2.29. Block diagram of aVLSI implementation of adaptive olfactory system (Adapted from [77]) 37
Figure 2.30 Sensor interface PCB (Adapted from [77]) 38
Figure 2.31. System implementation diagram for olfactory sensor based on SNN (Adapted from [82]) 39
Figure 2.32. System architecture for electronic nose chip in [83].....40

Figure 2.33. Key components and working of 4 × 4 gas sensor described in [88] 41

Figure 4.1. Conceptual diagram of working of AER (Adapted from [11]).....51
Figure 4.2. AER sender and receiver architecture (Adapted from [12]).....52
Figure 4.3. AER-SWITCH board (Adapted from [10]).....54
Figure 4.4. USB-AER board (Adapted from [10]).....55
Figure 4.5. A block diagram representing connection between AER-SWITCH and USB-AER..56
Figure 4.6. DVS128 PAER commercial vision sensor based on DVS pixel design (Adapted from [105]).....57
Figure 4.7. Interfacing of neuromorphic vision sensor with USB-AER FPGA board 57
Figure 4.8. DAS1 commercial neuromorphic auditory sensor (Adapted from [107]) 58
Figure 4.9. Interfacing of neuromorphic auditory sensor with USB-AER FPGA board.....58
Figure 4.10. Typical interfacing method for CMOS olfactory sensor in [108] 59
Figure 4.11. Interfacing of neuromorphic olfactory sensor with USB-AER FPGA board using AER SWITCH board.....59
Figure 4.12. Block diagram of the proposed interfacing method 60

Figure 5.1. ORN sensor array panel for JAVA simulation system 62
Figure 5.2. JAVA simulation system window 62
Figure 5.3. Selection of ORN for supervised learning for gas1 63
Figure 5.4. Selection of ORN for supervised learning for gas2 64
Figure 5.5. Selection of ORN for supervised learning for gas3 64
Figure 5.6. Selection of ORN for supervised learning for gas4 65
Figure 5. 7. Output spike data at time=9 sec.....66
Figure 5. 8. Gas concentration graph at time=9 sec 66
Figure 5. 9. Initial values for simulation. Simulation at time=0 sec.....67
Figure 5.10. Simulation at time=5 sec 68
Figure 5.11. Simulation at time=9 sec 68
Figure 5. 12. Nengo simulation network with 2D array of 16 neurons 71
Figure 5.13. Nengo generated simulation window with two controls for concentration of gases as input and voltage grid, output values and spike raster for output.....71
Figure 5.14. Output response for increase in gas2 concentration 72
Figure 5.15. Output response for maximum concentration of gas2 72
Figure 5.16. Output response for increase in gas concentration of gas1 and gas2 73
Figure 5.17. Output response for stable concentration of gas1 and gas2 73

LIST OF ABBREVATIONS

ADC	Analogue to Digital Conversion
AER	Address Event Representation
AGC	Automatic Gain Control
APS	Active Pixel Sensor
ATIS	Asynchronous Time-based Image Sensor
aVLSI	Analog Very Large Scale Integration
BDJ	Buried Double Junction
CAVIAR	Convolution AER Vision Architecture for Real-time
CCD	Charge Couple Device
CB Polymer	Carbon Black Polymer
CLBT	Compatible Lateral Bipolar Transistors
CMOS	Complementary Metal-Oxide Semiconductor
DAC	Digital to Analogue Conversion
DAQ	Data Acquisition
DAS1	Dynamic Audio Sensor 1
DAVIS	Dynamic and Active pixel Vision Sensor
DSP	Digital Signal Processing
DVS	Dynamic Vision Sensor
FIFO	First-In First-Out
FPGA	Field Programmable Gate Array
FPN	Fixed Pattern Noise
IEEE	Institute of Electrical and Electronics Engineers
IHC	Inner Hair Cells
ITD	Inter-aural Time Difference
KNN	K-Nearest Neighbour
LIF	Leaky Integrate and Fire
LTP/LTD	Long Term Potentiation/Long Term Depression

MEMS	Micro-Electro-Mechanical Systems
MOSFET	Metal Oxide Semiconductor Field-Effect Transistor
ORN	Odour Receptor Neuron
PFM	Pulse Frequency Modulation
QVGA	Quarter Video Graphics Array
SNN	Spiking Neural Network
SNR	Signal-to-Noise Ratio
STDP	Spike Time Dependent Plasticity
SVM	Support Vector Machine
TTFS	Time to First Spike
VLSI	Very Large Scale Integration
USB	Universal Serial Bus
UV	Ultra-Violet

CHAPTER 1. INTRODUCTION

The need for intelligent machines is rising as technology continues to evolve. To embed intelligence in electronic devices, it is necessary to equip them with sensors and efficient processors. Currently, the operating principle in most electronic sensors and processors is based on the Von Neumann architecture where memory and data processing are two different units. Systems based on this architecture tend to consume excessive power with the operating frequencies increase and as the data is transmitted back and forth between memory and processor during data operations. The ever growing number of sensors in modern systems results in a huge amount of redundant data that requires substantial computing power to implement complex data processing strategies. However, increasing the number of transistors on a chip to increase processing power is impractical due to the physical limitations of silicon and heat dissipation issues [2].

Extensive research in neuroscience has revealed that animals and humans perform cognitive tasks such as grasping, smelling and recognising voices, with utmost ease. The operating principles of neurobiological architecture depend on asynchronous processing that ensures real-time response to stimuli. The unification of memory and processing as a single unit dramatically reduces power consumption. An essential characteristic of neurobiological architecture is extensive connectivity between neurons and synaptic weight changes that form the basis of learning rules in biological systems. The idea of reverse-engineering this biological phenomenon using electronics gave an impetus towards the development of an interdisciplinary science called neuromorphic engineering.

Scientists including Max Delbruck, Richard Feynman, John Hopfield and Carver Mead collaborated to study the non-linear current characteristics of transistors [3]. Carver Mead in his path-breaking paper, 'Neuromorphic Electronic Systems', exposed the drawbacks of using the transistor merely as a digital switching device. He proposed that the analogue properties of transistors can be exploited to implement adaptive circuits that mimic neurobiological architecture. He highlighted the advantages of this approach including low-power consumption and efficiency and presented a prototype for an adaptive silicon retina and cochlea [4, 5].

Since the development of neuromorphic engineering, these concepts have been applied in data processing, the design of network architecture, and, most successfully, in electronic sensing [6]. The properties of human sensory systems such as vision, audition and olfaction are

emulated by using analogue VLSI. Recent developments have adopted an analogue-digital hybrid approach to implementing the state-of-the-art neuromorphic vision, auditory and olfactory sensors.

1.1. MOTIVATION

An important characteristic of neuromorphic sensors is low-power consumption and asynchronous spike-based output. This unique format of the output is analogous to asynchronous action potentials generated in biological sensory systems to detect an occurrence of an event independent of time. Hence, conventional interfacing protocols that depend on external clocking circuits cannot be applied for transmission of outputs from neuromorphic sensors. To overcome this limitation, neuromorphic sensors use Address Event Representation (AER)-based communication that facilitates transmission of address events in the form of spikes. Neuromorphic sensors are provided with interfaces such as AER, Universal Serial Bus (USB) and Data Acquisition (DAQ) to communicate the output data with a processing unit.

The output data processing of these sensors is mainly implemented on computers due to the limitations on processing algorithms that can be deployed on a low-power system. In such cases, a USB interface is used to connect these sensors and transmit time-stamped AER spikes. This interfacing technique restricts the portability of these sensors as well as incurring high costs for output data processing and, thus, limits large-scale application. Development towards standardisation of AER interfaces has enabled direct connection between neuromorphic sensors and rapid-prototyping development boards [7]. Accordingly, neuromorphic processing boards such as SpiNNaker [8], BrainScaleS [9] and CAVIAR [10] have been developed that can process spike-based data and can be reconfigured for application specific tasks by using on-board FPGAs.

This research project addresses the issue of interfacing neuromorphic vision, auditory and olfactory sensors with digital neuromorphic circuits. This project will encourage the use of neuromorphic sensors in stand-alone autonomous systems and eliminate their dependency on computers for output data processing.

1.2. RESEARCH QUESTIONS:

This research project focuses on establishing a direct interface between neuromorphic vision, auditory and olfactory sensors with digital neuromorphic circuits. An important issue this project addresses is: "What methodology should be adopted to establish an efficient interface between neuromorphic vision, auditory and olfactory sensors and digital neuromorphic circuits?"

The answer to this research question will be the result of a series of answers for the questions below:

- Which learning algorithm is best suited for implementation in an autonomous system with neuromorphic sensors?
- Which neuromorphic sensors are compatible with AER interfacing?
- Which digital neuromorphic processing board facilitates AER interfacing with rapid prototyping and upscaling?
- How will the system implement correlation of output from multiple sensors?
- How can a simulation of this interface be implemented using standard programming environments?
- Which application areas can benefit from this interface and how?

These research questions will focus on determining appropriate learning methods for autonomous systems implementing neuromorphic sensors, selection of sensors based on their output data format, correlation of output from multiple sensors and selection of appropriate neuromorphic FPGA development board.

1.3. RESEARCH CONTRIBUTION:

This thesis focuses on eliminating the dependency on computers for interfacing of neuromorphic sensors. The original contribution of this research lies in establishing a simplified model of interfacing neuromorphic sensors with digital neuromorphic circuits that can be readily adopted in the design of autonomous systems based on neuromorphic sensing. This model will provide a platform for stand-alone autonomous systems to integrate multiple sensors and correlate their output data. The digital neuromorphic circuits can be used as a learning unit and tend to improve the performance of the system during the course of time. The proposed interfacing method will extend the scope of application of neuromorphic sensors for bio-security and other advanced applications.

1.4. THESIS ORGANISATION:

This introductory chapter is followed by a literature survey in Chapter 2. The literature review starts with a detailed description of developments in neuromorphic engineering and investigates state-of-the-art neuromorphic sensors and their operating principles. Chapter 3 is adapted from the author's manuscript "A Review of Current Neuromorphic Approaches for Vision, Auditory and Olfactory Sensors". This chapter will introduce current benchmarks in neuromorphic sensing and compare them. Chapter 4 describes the proposed methodology and explains each component of the interface. Chapter 5 describes the JAVA modelling and simulation of the interface and compares the JAVA model with a standard simulation tool, Nengo. Chapter 6 comprises of conclusion, application and future direction for this project.

CHAPTER 2. LITERATURE REVIEW

Neuromorphic engineering is a rapidly evolving field that takes inspiration from unconventional biological computing concepts like asynchronous processing, hybrid analogue/digital components and the combination of computing and memory components. Since the last decade, there have been path-breaking research activities in neuromorphic sensing and that has led to sophisticated designs of neuromorphic sensors. This literature survey is focused on studying prominent work in neuromorphic vision, auditory and olfactory sensing, in order to determine digital interfacing methodology for neuromorphic sensors.

During this literature review, most of the work was referred from IEEE Xplore digital library. Other libraries like Springer Link, Science Direct and Elsevier were also used. Some of the keywords used were “neuromorphic vision”, “neuromorphic auditory sensors”, “neuromorphic olfaction”, “neuromorphic engineering” and “biomimetic sensors”. This literature review, highlights key contributions from researchers like Tobi Delbruck, Shih-Chii Liu, André van Schaik, Thomas Jacob Koickal and Carver Mead.

2.1. NEUROMORPHIC ENGINEERING

Neurobiological architecture is an example of a well-organized and efficient computing approach. Biological methods of processing certain complex data can be more efficient than any digital system attempting to perform similar tasks. For example, a bee’s flight motor skills and cognitive behaviour cannot be matched by even the most sophisticated aerial vehicles. The bee’s ability to sense and scan a large area for navigation between beehives and flowers, dissipates only 10 mW of energy [11]. Similar digital systems that use sensory data and Global Positioning Systems (GPS) consume approximately 1kW of computing power [11]. This shows that even though biological systems implement slow, inhomogeneous and stochastic computing elements, they tend to outperform today’s powerful digital systems at processing sensory data and motor control. Research has shown that neurobiological systems utilise the advantages of massively parallel mechanisms, both analogue and digital signal representations, and distributed processing. The combination of computing and memory elements, allows biological systems to learn, adapt and improvise in varied tasks [2]. However, state-of-the-art digital systems rely on Boolean logic, synchronous processing and precise digital formats. Even the simulation of neuronal computing methods requires supercomputers that rely on fast,

clocked and multi-processor digital hardware that involves high-power consumption [6]. The Von Neumann architecture based on digital systems require several data transfer iterations from memory chips to processing units, as memory and computing elements are implemented as different entities. This technique is not ideal for complex data processing like image and sound processing [12]. Understanding the intelligent computation principles in neurobiological systems will boost the development of novel computing models that are both power-efficient and intelligent.

The quest to develop custom hardware, that takes inspiration from neurobiological architecture, started since the development of the perceptron and electronic retina. In the late 1980s, Carver Mead utilised the non-linear current characteristics of transistors and analogue VLSI concepts, to develop circuits that somewhat mimic human sensory systems. Such systems were called neuromorphic, describing their ability to emulate the neurobiological architecture for effective processing and sensing. Carver Mead quantified the energy loss to be 10,000 times in excess when transistors are operated as digital switches, especially, when simple digital calculation causes numerous ON-OFF switching of millions of transistors. In [4], Mead particularly highlighted the voltage-dependent exponential behaviour of a transistor in the subthreshold region. As illustrated in Figure 2.1, these characteristics are analogous to the exponential dependence of active populations of voltage-sensitive ionic channels as a function of the potential across the membrane of a neuron. This similarity facilitates the implementation of voltage-controlled conductance-based electronic models of neurons and synapses. These concepts were also applied to construct useful computational biological primitives such as phototransduction, logarithmic functions, inhibition, correlation amplification, multiplication, thresholding, and winner-takes-all selection [6].

Biological structures depend on analogue computing to process sensory data. This computing is carried out by the physics of these special-purpose structures. For example, the natural structure of the ear provides physical properties that can perform frequency analysis, signal modulation and filtering, eventually relaying the signals to the brain. Developments in neuromorphic engineering have boosted research in biological sensing. Although biological sensing depends on analogue computation, there is a certain digital aspect to it. A brain cell or neuron receives certain patterns of voltage from other neurons at its membrane, integrates these voltages in an analogue manner and produces a spike-based output when the voltage exceeds a certain threshold. This output is analogous to digital information which denotes the presence

(1) or absence (0) of a voltage spike [13]. These spikes act as an input to more neurons and this process, when amplified to involve millions of neurons, leads to sensing and motor movements.

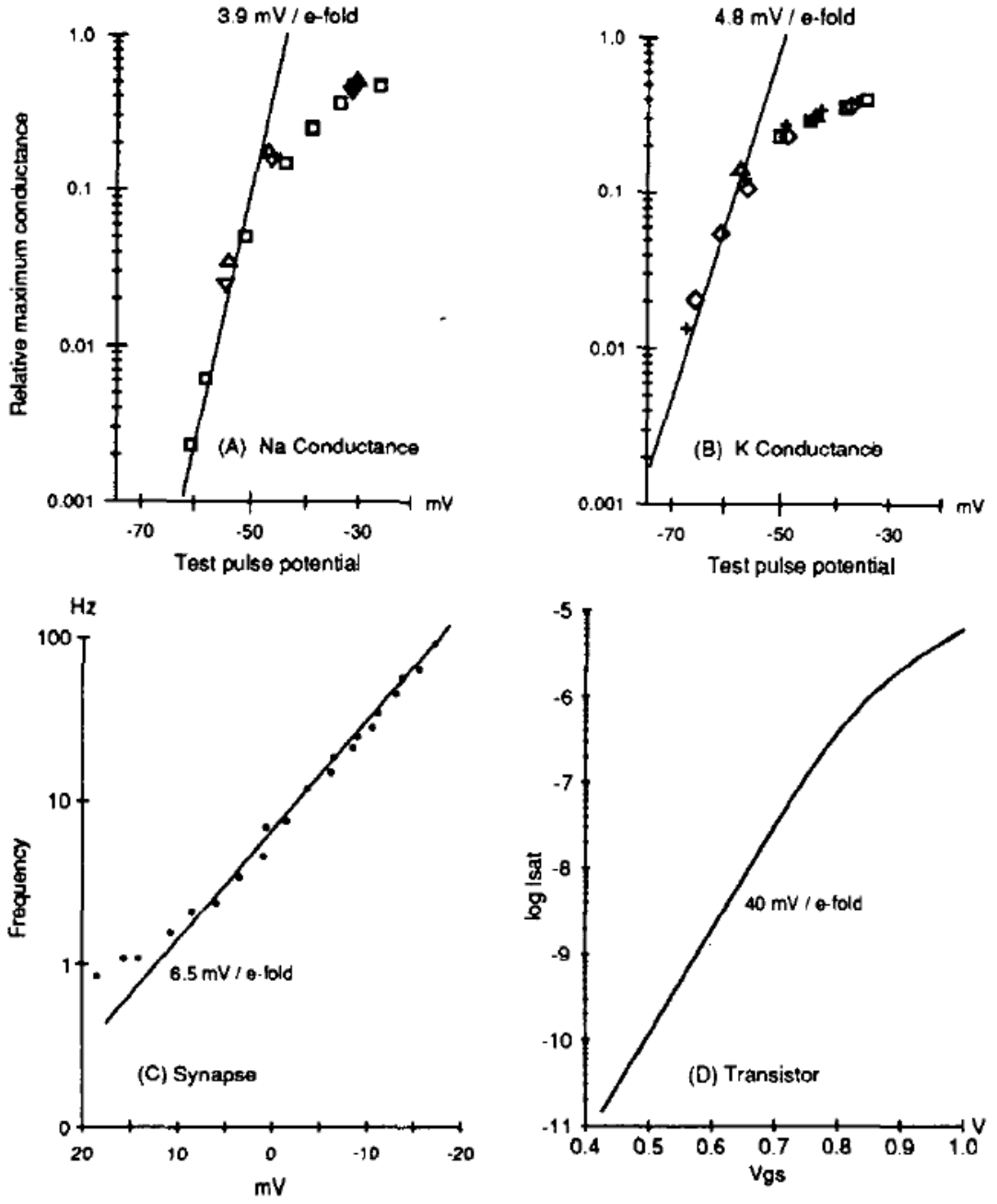

Figure 2.1. Current-Voltage plots by Carver Mead to compare the ubiquitous exponential characteristics between membrane potentials and analogue transistors (adapted from [4])

Initially, Carver Mead proposed the use of only aVLSI to construct neuromorphic hardware [14]. He attempted to include most of the functionality of a retina and a cochlea in silicon. These experiments aimed at replicating the actual working of these sensory structures but they failed to fully implement the underlying operating principles. The application of analogue concepts ensured that only a few transistors had to be used to carry out computations

and operation in the subthreshold region evaded excessive power consumption. Analogue implementations can be more accurate than digital systems within a given power budget as precise values can be computed using the analogue format unlike in digital implementations that are restricted to only two values 1 or 0. Although analogue implementations provide these advantages, the analogue properties of every transistor are intrinsically different, which leads to transistor mismatch. This mismatch introduces errors in computation and the output is compromised. Analogue implementations are prone to noise due to temperature variations and voltage supply variance [15]. The restriction of digital representation to two values provides much greater immunity to erroneous signal alteration due to noise. Digital systems are robust to noise from temperature variance, supply voltage variance, fluctuations in the flow of current and thermal noise [2]. Digital systems also tend to be relatively easy to program and upscale. These advantages were noticed and reported in early implementations in [16]. Recent neuromorphic implementations include a hybrid approach that leverages the advantages of both analogue and digital approaches [2].

Extensive research on the computational power of biological systems to the abstraction level of a single neuron and its associated synapses has facilitated the development of sophisticated designs of neuromorphic systems. This has sparked advanced research in developing large-scale neural systems that exhibit adaptive characteristics rather than the largely used feed-forward and reactive systems [12].

2.2. SILICON NEURON: ESSENTIAL COMPONENT OF NEUROMORPHIC SYSTEMS

2.2.1. REAL NEURONS

A neuron is a fundamental functional block in a neural system that is responsible for many chemical and electrical processes. There are approximately 10^{11} neurons in the human brain, each with about 10^{4} connections to others of its kind [17]. The connections between the axons and dendrites of neurons are called synapses. The output pulse of a neuron, the so-called action potential, is carried by the axon. Dendrites receive this input current that flows to the soma within which it is eventually integrated. The axon hillock is responsible for initiation of an action potential as the integrated input current (often referred to as the membrane voltage

V_m) amounts to a voltage higher than some threshold. Figure 2. 2 shows the basic anatomy of the biological neuron.

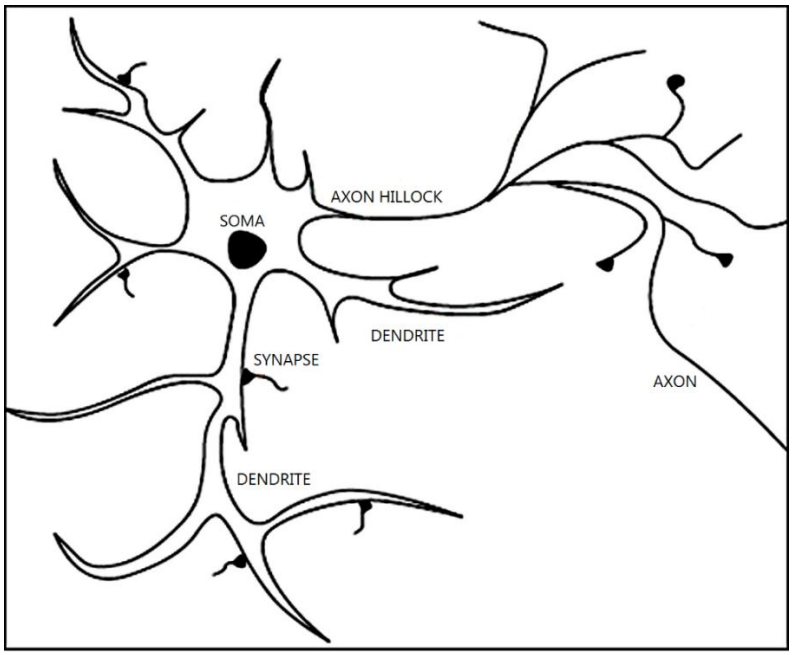

Figure 2. 2. Basic anatomical part of a neuron (Adapted from [18])

Figure 2.3, gives an impression of a real neuron. This image is a light microscope photograph by John Anderson, Institute for Neuroinformatics, Zurich, Switzerland.

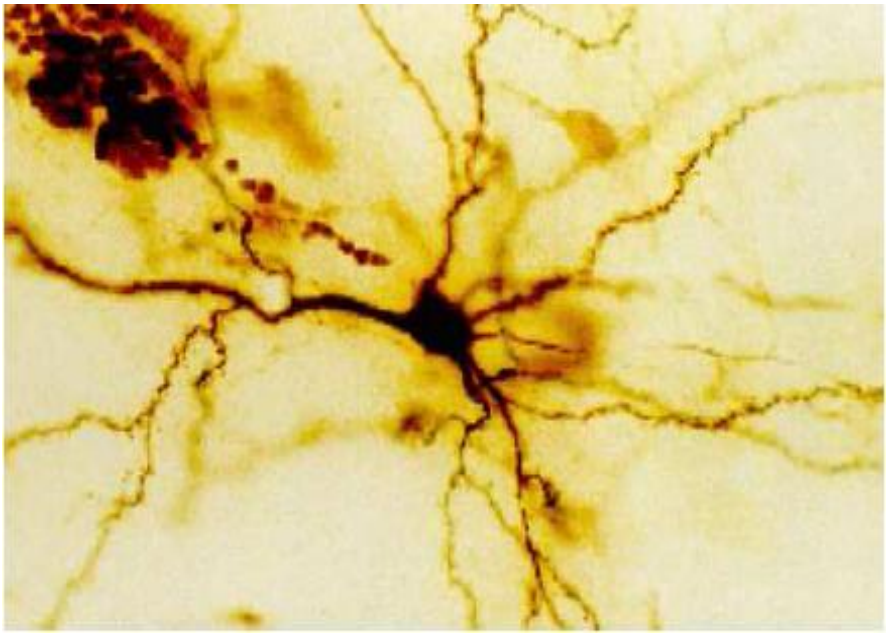

Figure 2.3. Light microscope photograph of a stained neuron (Adapted from [18])

The synapses are responsible for storing the learning information in the brain. The amount of charge deposited on the post-synaptic cell per input spike is identified as the connection strength between synapses. These connection strengths can change permanently

and alter the behaviour of an entire network. These long-term connection changes in synaptic weights are termed as Long-Term Potentiation/Depression (LTP/LTD) [19]. Spike Timing Dependent Plasticity (STDP) is a term coined to describe changes in the synaptic strength that are triggered by temporal spiking patterns of a pre- and post-synaptic neuron.

2.2.2. aVLSI MODELS OF NEURONS

Recent developments in neuromorphic engineering have sparked interest in the physiological model of a neuron that describes its functionality and can be realised in aVLSI circuits. As biological neurons depend on voltages and currents, it has been relatively easy to model neurons in VLSI electronic circuits [15]. There are several aVLSI models of neurons based on their level of detail. The simplest way of representing a neuron in electronics is by representing them as electrical nodes where a voltage or current represents a neuron's activity, and the input and output are identical with no transfer function [20].

2.2.2.1. PERCEPTRONS

A perceptron is a simple representation of a neuron, mostly implemented as a mathematical model. A perceptron, also known as a sigmoid neuron, models the multiple input-single output property of real neurons. The output of a perceptron is computed by an activation function of the weighted sum of its inputs [21]. The idea of a perceptron is limited to mathematical modeling and is rarely implemented using aVLSI. Perceptron implementation in digital hardware and traditional computers, provide the advantages of a fully parallel, space and energy conservative implementation [18]. Equation 2.1 is a representation of a perceptron as an activation function that performs summation of X_i inputs with W_i weights.

$$\sum_i f(W_i X_i)$$

Equation 2.1. Mathematical model of a perceptron (Adapted from [18])

2.2.2.2. INTEGRATE AND FIRE NEURONS

An integrate-and-fire neuron performs integration of weighted charge, triggered by presynaptic spikes. The neuron fires an output pulse when the voltage reaches a certain threshold, and the integrator is reset. This type of neuron is widely implemented in aVLSI as shown in Figure 2.4 [18]. The spike-based communication in this model provides distinct advantages in noise robustness.

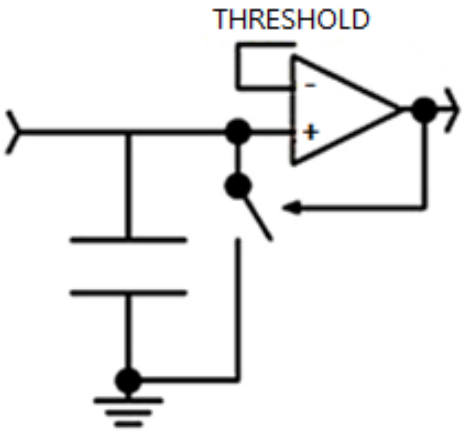

Figure 2.4. High-level conceptual model of an Integrate and Fire neuron (Adapted from [18])

Figure 2.5 presents a model of an integrate-and-fire neuron proposed by Carver Mead [14]. This neuron comprises an integrator capacitor that represents the membrane potential of a neuron, a high gain amplifier that switches as the integrated input current exceeds the threshold voltage, and a stabilising feedback capacitor to maintain the membrane capacitance by adding the extra charge to stabilise the firing state.

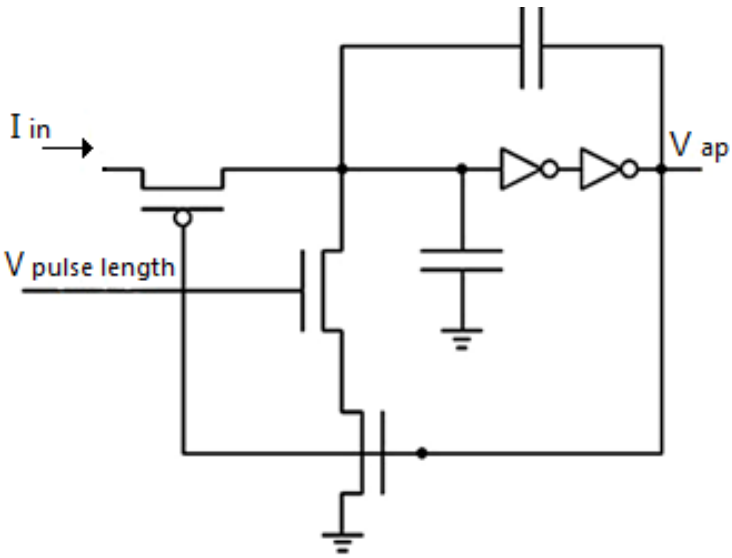

Figure 2.5. Integrate-and-Fire neuron model by Carver Mead (Adapted from [22])

2.2.2.3. SILICON NEURONS

Silicon neurons extend the level of detail to model neurons. This model includes the details of varying properties and states along the dendrites and the axons of the neuron. The action potentials are generated as a sharp voltage rise when the membrane potential reaches a threshold.

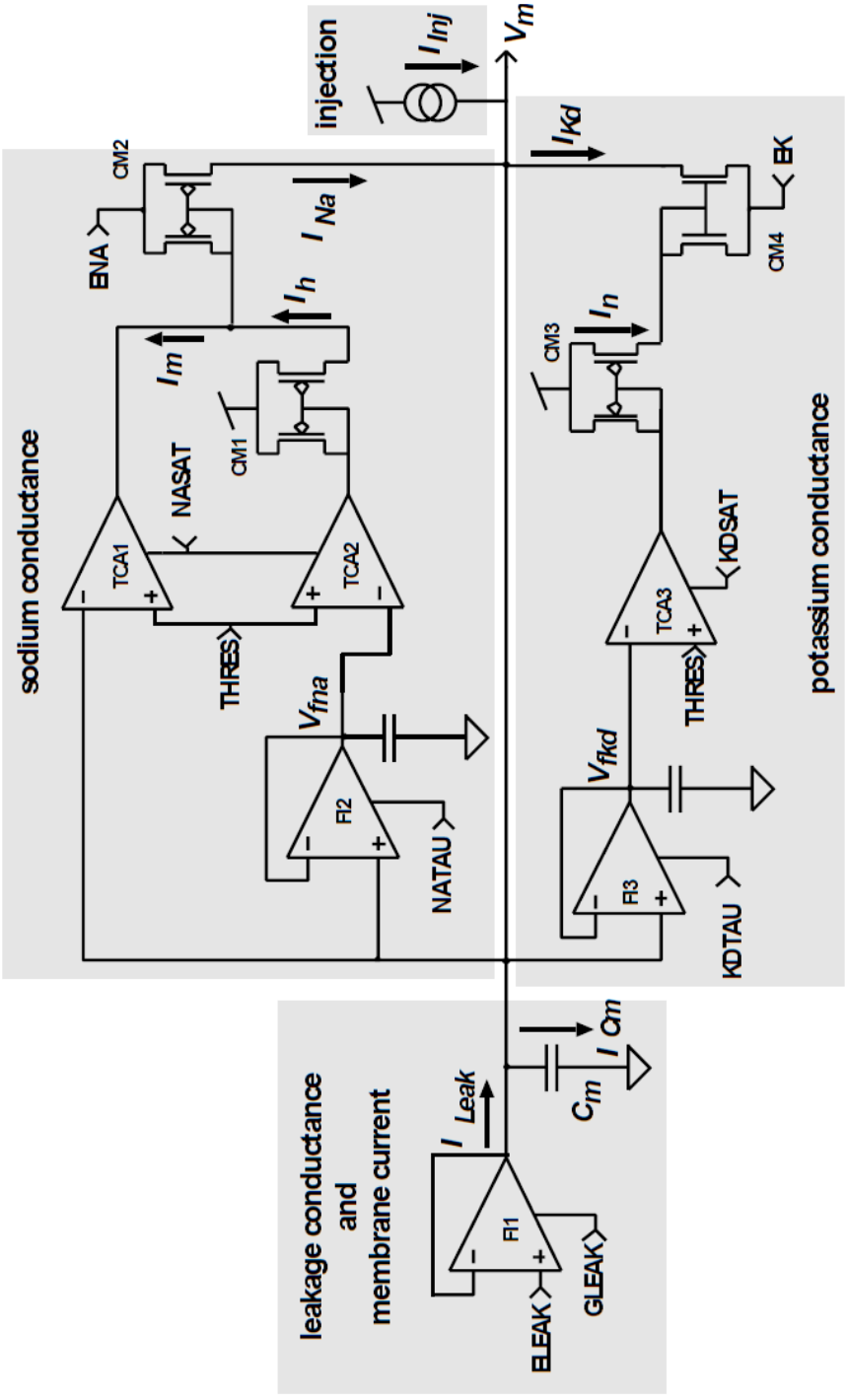

Figure 2.6. Schematics of HH-soma implementation in CMOS (Adapted from [23])

This modelling of the action potential generation is based on the Hodgkin- Huxley model [23]. This model was initially limited to the mathematical formulas, but with developments in electronic modelling, this model has been implemented in aVLSI and verified using simulations. A CMOS implementation of Hodgkin-Huxley soma that emulates the sodium and potassium conductance in real neurons is shown in Figure 2.6. The red graph line shown in Figure 2. *7*, depicts the typical behaviour of membrane voltage (V_m) that is activated once the voltage increases beyond threshold (THRES). The delayed activation (V_{fkd}) introduced by RC-type delay filter/integrator circuit causes some delay for the turning off action of the spike. This results in the membrane potential falling below resting potential before returning to the normal values.

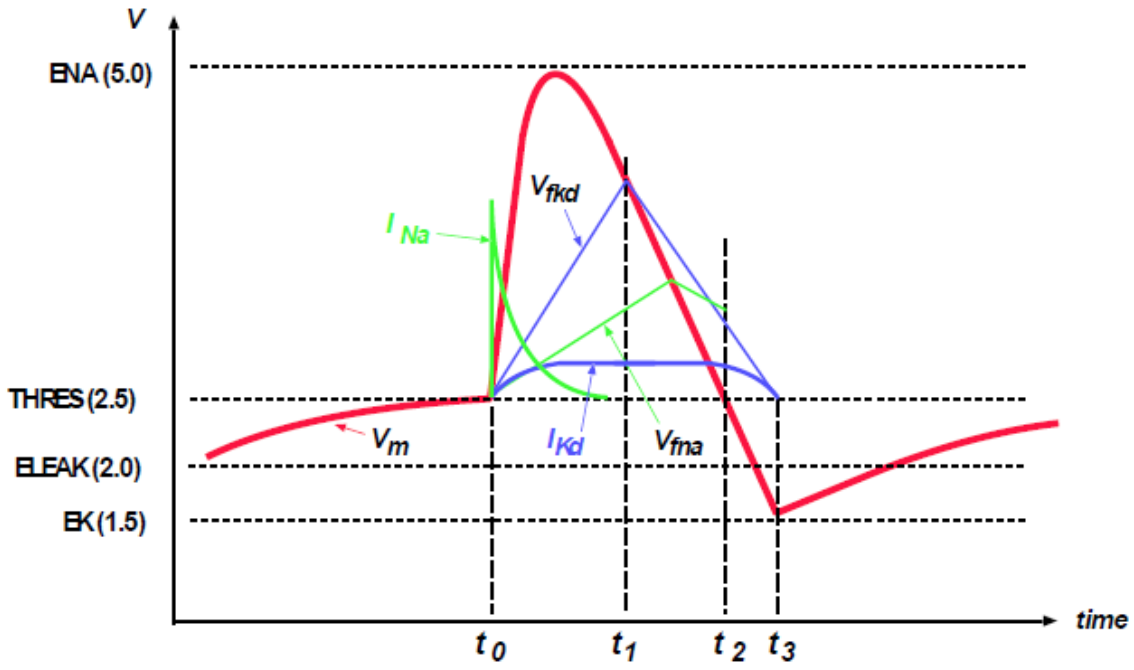

Figure 2. 7. Signal time course of a HH-soma implementation (Adapted from [18])

2.3. NEUROMORPHIC VISION SENSING

The extensive research in neuromorphic engineering has led to the development of several neuromorphic devices such as neural processors, neural network architectures and the most successful being neuromorphic sensors. The silicon retina is the most prominent example of effective emulation of a biological sensory system using neuromorphic concepts [24]. It is necessary to study the biological retina and underlying concepts of biological vision sensing in order to understand the working of the silicon retina.

2.3.1. BIOLOGICAL RETINA

The human visual system is a complex sensory system that is responsible for relaying optical information to the brain [25]. This process of sensing light starts with appropriate pre-processing at the eyeball and ends with the optic cranial nerve that sends action potentials to the brain's visual cortex. The essential processing of the visual data is carried out by the retina. The retina is a thin tissue with a dense neural network that lines the inner surface of the eye. As shown in the Figure 2.8 and Figure 2.9, the retina comprises of three primary layers, the inner and outer plexiform layer and the photoreceptor layer. The photoreceptor layer further contains cone cells and rod cells that are responsible for the conversion of incident light into action potentials. These photoreceptor cells control the functionality of bipolar cells and horizontal cells of the outer plexiform layer.

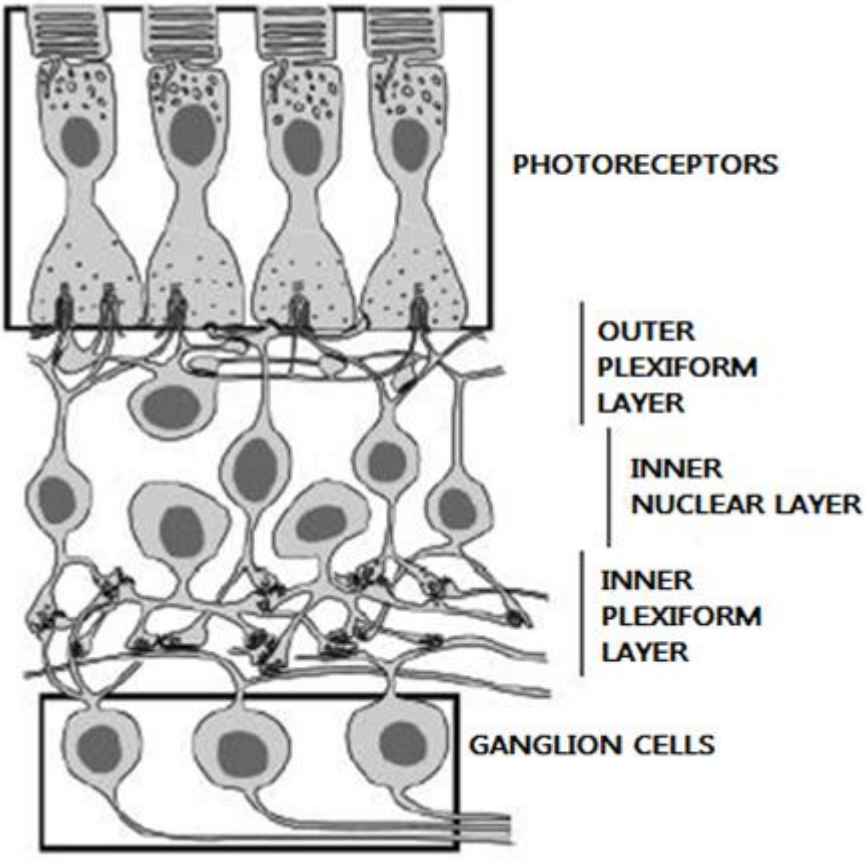

Figure 2.8. Cross section of primate retina (Adapted from [11])

The horizontal cells are arranged in a resistive mesh and carry out computation of spatio-temporal averages. The bipolar cells are divided into ON and OFF cells that are capable of distinguishing between bright spatio-temporal contrast and dark spatio-temporal contrast. Thus, the bipolar cells are controlled by the difference between photoreceptor and horizontal

cell output. These ON and OFF bipolar cells further join onto different amacrine cells and, ON and OFF ganglion cells in the inner plexiform layer [11, 12]. The communication signals between the ganglion and bipolar cells are mediated by the amacrine cells.

The ganglion cells and bipolar cells can be further differentiated into cells with more sustained responses and cells with more transient responses. The information related to transient and sustained responses is carried along separately in two parallel pathways: the parvocellular pathway is sensitive to spatial changes, and the magnocellular pathway is sensitive to temporal changes. Although there are several other pathways of the visual input, the simplified classification of sustained and transient pathways is relatively easy to understand and emulate in aVLSI [24]. Temporal changes provide the "where" information of the visual scene, and spatial information provides the "what" information. For example, the information related to motion parameters like the direction of a moving object is provided by temporal change, whereas details of the object such as colour and shape is provided by spatial vision [11]. The retina encodes the spatio-temporal information of the visual scene into action potentials that are communicated to the visual cortex of the brain. This information is carried through retinal ganglion cells and undergoes advanced adaptive filtering and sampling.

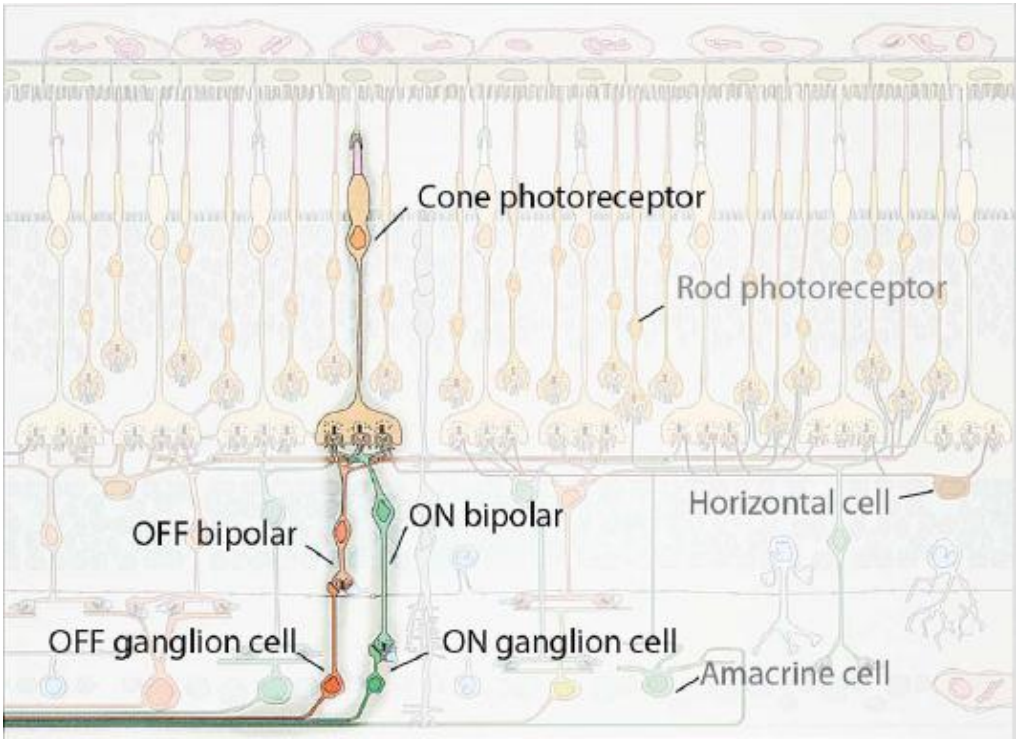

Figure 2.9. Key components of biological retina that are emulated in silicon retina (Adapted from [24])

2.3.2. LIMITATIONS OF CONVENTIONAL VISION SENSING

To match the performance parameters of human vision like high photopic range (>100 dB), spatial and temporal resolution, and field of view, requires a conventional vision sensor to capture images at Nyquist rate and transmit them at 20 GB/s. Biological vision carries out this functionality by coding 2 bytes of visual scene information per spike. The optic nerve communicates these spikes to the visual cortex at about 20 MB/s, which is a thousand times less than conventional vision sensing [11, 12, 24].

The frame-based operation principle of conventional Charge Couple Device (CCD) and Complementary Metal-Oxide Semiconductor (CMOS) imagers imposes several limitations on efficient processing of visual data. Images are taken at a predetermined rate; this data undergoes appropriate image processing depending on the application. As events in the real world occur in an asynchronous manner and in continuous time, the concept of capturing visual data using a frame-based approach can lead to sampling inconsistencies. If frames are captured at a slow rate, changes in visual data between two consecutive frames is lost. This problem of undersampling can prove to be intolerable for applications such as machine vision and visual feedback systems [26].

Conversely, oversampling can lead to huge volumes of redundant data where there is no significant change in several frames. When the frame-based approach is applied, information is recorded from all the pixels regardless of any change in their values. Acquisition and processing of this large data set is complex, incurs high power consumption, and requires a lot of resources like wide channel bandwidth and large amounts of memory [27].

2.3.3. SILICON RETINA

Biological vision is asynchronous and controlled by changes occurring in the visual scene. This approach is contrary to the one used in traditional vision sensors, where information is captured by synchronous timing and control signals without any change in visual information and its dynamics. In order to apply a biological vision approach, it is necessary to eliminate the external synchronous clock for acquisition of visual information and allow each pixel to relay its information as per the changing light exposure [28, 29]. By implementing such a frame-free approach and computation at an individual pixel-level, the problems of frame based conventional vision sensing can be solved.

Mahowald was the first to implement vision chips that follow the operating principles of biological vision in silicon [30, 31]. Through this design, she tried to replicate the functionality of the cone cells to detect light, horizontal cells to compute the spatial and temporal average from cone cells output, and the bipolar cells that can compute the difference between average output and incoming input. In this silicon retina, the cone cell functionality has been demonstrated by using parasitic phototransistors and MOS-diode logarithmic current to voltage converters. As observed in the Figure 2.10, the averaging functionality of horizontal cells is implemented using a hexagonal network of active resistors. Finally, the potential difference between the hexagonal resistive network and the local receptor is computed. However, the mismatches in transistors affected the performance of the sensor under uniform lighting conditions, and the resulting output was compromised.

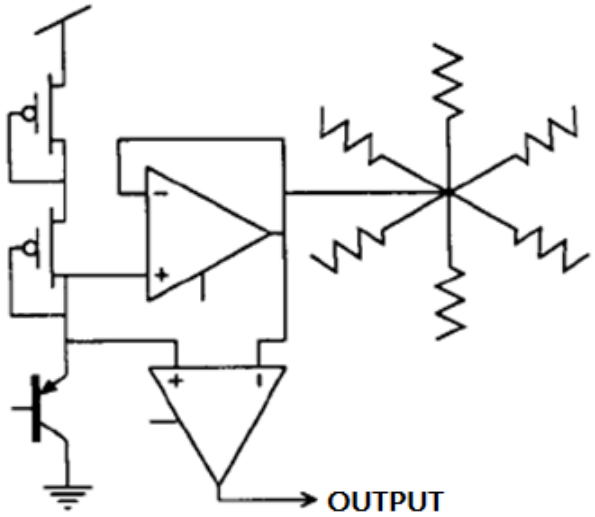

Figure 2.10. Schematic of pixel from Mahowald retina (Adapted from [4])

Mead pointed out that the drawbacks of transistor mismatch in Mahowald's retina are also observed in biological vision as no two photoreceptors or synapses have a similar sensitivity or synaptic weights [29]. He suggested that biology applied adaptive techniques to overcome the mismatch drawbacks and improve its precision. He enhanced the Mawhold's retina by using a floating gate Metal Oxide Semiconductor Field-Effect Transistor (MOSFET) as a feedback element to correct the offset and mismatch between the transistors. This is applied by adding a Ultra-Violet (UV) activated coupler of a poly-1-poly-2 structure. This UV coupler would close the feedback loop when exposed to UV light and hold the output voltage for a certain input current [4, 31, 32]. Figure 2.11 shows the circuit for the adaptive retina pixel by Carver Mead.

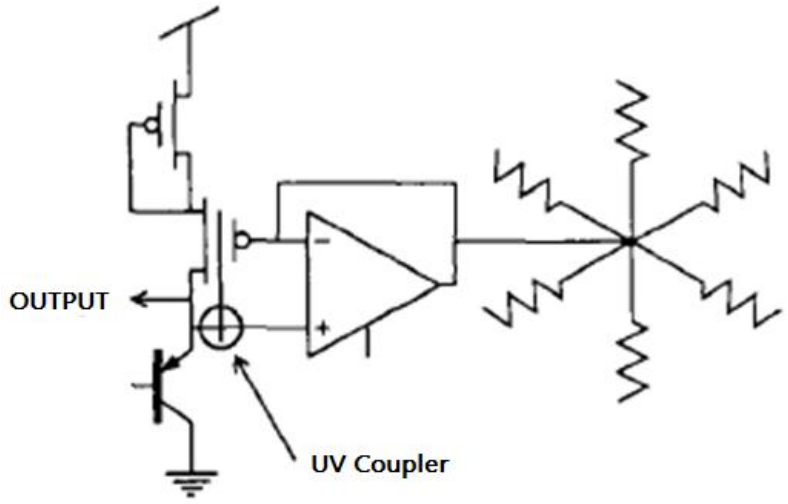

Figure 2.11. Adaptive retina pixel circuit by Carver Mead (Adapted from [4])

Zaghloul and Boahen improved the silicon retina by Mahowald and Mead, by adding both sustained (parvo) and transient (magno) cellular pathway functionalities [33, 34]. This simplified model of all five layers of retina comprised of both outer and inner retina functionalities. The inner retina model added the functionality of contrast gain control and the outer retina model could effectively carry out spatio-temporal bandpass filtering and local gain control. This model exhibited biological retina-like ability to adapt to varying light and contrast conditions and dynamically realign spatial and temporal filtering. The 3.5×3.3 mm^2 chip they designed could accommodate 5760 phototransistors at a density of 722 per mm^2 and 3600 ganglion cells at a density of 461 per mm^2. This implementation provides an output of spike trains which is analogous to ON and OFF centre wide-field transient and narrow-field sustained ganglion cells. This approach emphasised extensively on modelling biological retina closely, but the large mismatch, and 1-2 decades of Fixed Pattern Noise (FPN) restricted its application to laboratory experiments.

2.3.4. RETINOMORPHIC VISION DEVICES

Early silicon retina implementations emphasised on emulating the biological retina pathway for vision sensing. However, it was realised that the modelling of retina introduced drawbacks like large mismatch and FPN. This resulted in silicon retinas being developed only to study retina functionalities, but failed to prove useful for wider application. It is found that rather than emulating the entire retina pathway, only the essential characteristics of the retina can be implemented using aVLSI to achieve a result that is more reliable than the previous

silicon retina. Further developments in spike-based communication techniques like AER supported the implementation of event-based retinomorphic vision sensors.

Neuromorphic engineering concepts have been successfully applied in developing neuromorphic vision sensors like DVS [35], Asynchronous Time-based Image Sensor (ATIS) [36] and DAVIS [27]. Before the development of these sensors, several promising designs were explored that underpinned further study in neuromorphic vision. Researchers at CSEM Neuchatel developed a device that provides an event-based output that encodes high-to-low spatial contrast changes [37]. This enables early termination of readout without the loss of critical high-contrast changes especially when time constraints are applied for processing this information. With features such as 2% contrast mismatch and six-decade dynamic range, this device was commercially applied in the automotive industry. The temporal resolution of this device was limited to the frame rate that resulted in failure to reduce temporal redundancy. Mallik et al. [38] developed a temporal change detector Active Pixel Sensor (APS) imager that can detect a quantised absolute change in illumination and thus detect temporal changes. This design led to the development of a synchronous AER implemented by storing the addresses of the changed pixels in a First-In First-Out (FIFO) format. A limited dynamic range of 2.5 decades and absolute illumination-detection threshold restricted the use of this imager to uniform lighting conditions. The frame-based approach added the disadvantages of the sampling rate.

Several other applications like [39-41], contributed towards development in AER utilisation to communicate pixel address, spatial-contrast vision sensors, Time to First Spike (TTFS) images and time-based imagers. However, most of these designs suffered from transistor mismatch and leakage current in the transistor feedback circuit which resulted in failure to respond to slow changes in the visual scene. Developments by Kramer et al. in [42, 43], underpinned further research in vision sensors where individual pixels could compute and respond to positive and negative luminosity changes. The 48 × 48-pixel imager developed in [42], was further improved in [43] by using advanced pixel circuits with better performance to symmetrical ON-OFF responses. As the image contrast undergoes temporal differentiation, this imager can substantially reduce redundancy. This design exhibited a 32 × 32-pixel array with a pixel size of 40 × 40 μm^2 and dynamic input range of 100 dB. These contributions along with [26, 44-46], facilitated the development of DVS.

In 2008, Lichtsteiner, Posch and Delbruck presented the first practically usable device, DVS, in their path-breaking paper [35]. This 128 × 128 pixel frame-free CMOS vision sensor has been widely accepted as a benchmark in neuromorphic vision sensors. Each DVS pixel is designed to compute local relative luminosity changes and respond to temporal contrast changes in real-time. The dynamic range of DVS is > 120dB and the power consumption of this sensor is about 23 mW. DVS is built in a 0.35 µm 4M2P process with a pixel area of 40 × 40 μm^2 and 9.4% fill factor. The AER implementation ensures that the illuminance changes are reported with a precision timing of sub-millisecond. The events generated are directly proportional to the dynamic content of the scene that makes the operation of DVS independent of any external timing circuit.

Figure 2.12. A 128 × 128 Dynamic Vision Sensor by Tobi Delbruck (Adapted from [37])

DVS models key properties of biological vision: sparse and event-based output, pixel-level computation of relative luminosity change and the rectification of ON and OFF signals in the separate pathway [24]. These properties are analogous to the photoreceptor-bipolar-ganglion cell information flow in the biological retina as shown in Figure 2.13.

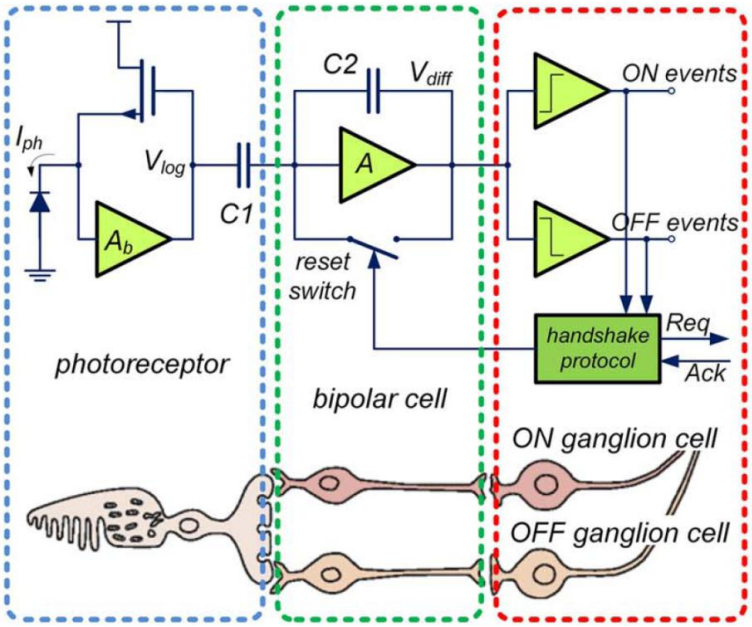

Figure 2.13. Three layer model of biological vision and corresponding DVS pixel circuit (Adapted from [24])

The principle of operation of DVS is plotted below in Figure 2.14. The upper graph represents a voltage waveform at point V_{log}. This voltage is computed by tracking the photocurrent of the photoreceptor circuit. The lower graph denotes the response from the bipolar circuit where spikes of different polarities are generated that are further communicated by the ganglion cells circuit to the next processing stage. These spikes represent the number of events. The output of the array of pixels is as shown in Figure 2.15. The events are recorded at an interval of tens of milliseconds. The dark pixels denote the OFF events, and the bright pixels denote the ON events. The main application areas of DVS are high-speed low-bandwidth imaging, wireless sensor networks, autonomous navigation systems and many more [47, 48].

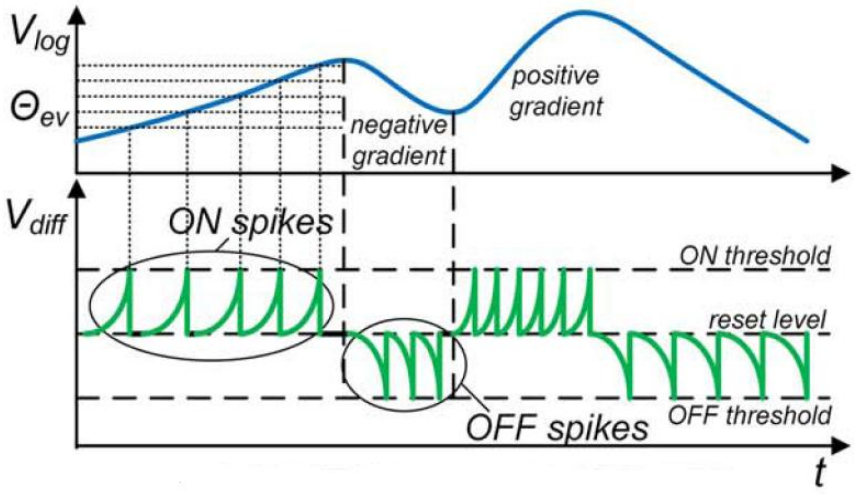

Figure 2.14. Waveforms of DVS pixel circuit (Adapted from [24])

Figure 2.15. Output image from DVS (Adapted from [12])

Implementation of the DVS underpinned further study, specifically in temporal change detection. Developments mentioned in [49] add features like colour vision to DVS pixels by utilising properties of Buried Double Junction (BDJ) photodiodes. Such an implementation can be used to detect light wavelength variation up to 15 nm. Improvements reported in [50], provided an impetus to extend the application of DVS. Serrano-Gotarredona and Linares-Barranco used a novel per-pixel photo sensing and transimpedance preamplifiers to improve the contrast sensitivity of DVS pixels by one order of magnitude i.e. down to 1.5% from 10-15% of the original DVS pixel. This also resulted in reduced power consumption to 4 mW, FPN to 0.9% and thus reduced the overall pixel size to 30 × 31 μm^2. The dynamic range and latency were maintained at 120 dB and 3 µs respectively. This improved design has the only drawback of a limited intra-scene dynamic range of three decades.

Christoph Posch et al. developed ATIS, a Quarter Video Graphics Array (QVGA) neuromorphic CMOS vision sensor based on the event-based DVS approach and a PWM-based conditional exposure measurement circuit [36]. In this design, a pixel can individually initiate exposure measurements when luminosity changes are detected. ATIS is asynchronous and event driven, and there are no external timing circuits that control its output readout. Any change in temporal and grey scale values of pixels are communicated using AER by requesting access to an asynchronous output channel. As the luminosity change information is encoded in a time-based manner, the high-dynamic range of 125-143 dB is achieved depending on visual scene activity. By implementing TCDS methods, the array FPN of <0.25% RMS and Signal-

to-Noise Ratio (SNR) of >56 dB is achieved at >10 Lux of illuminance. The greyscale output of ATIS overcomes the limitation of object recognition and identification.

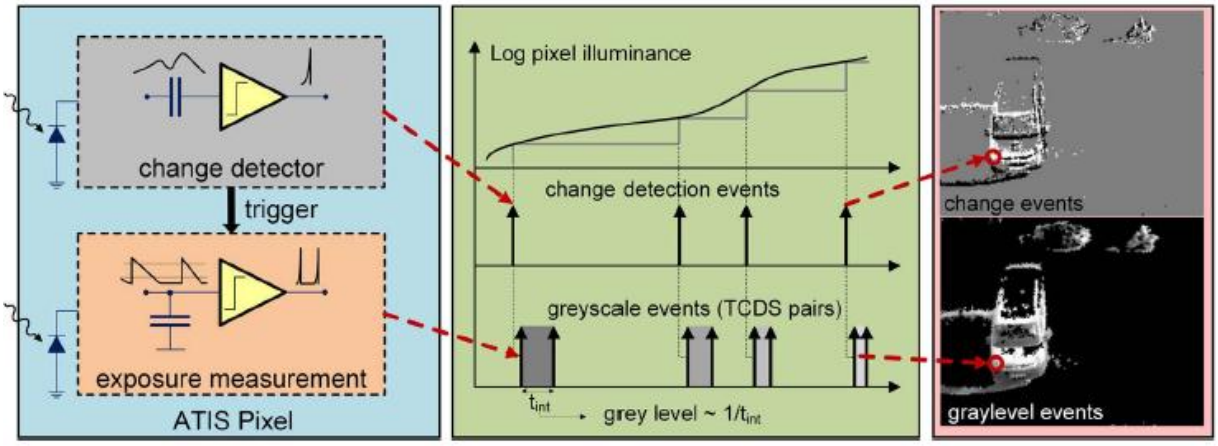

Figure 2.16.ATIS pixel circuit, operation principle of ATIS and its output frames (Adapted from [24])

Implementation of ATIS sparked the idea of a hybrid approach between frame-based and frame-free imaging to obtain static and dynamic scene information. Also, it was difficult to apply traditional computer vision algorithms to sparse DVS output because no static visual scene information was acquired. Drawbacks of ATIS such as non-uniform exposure restricting its ability to capture dark, narrow and slow moving objects, inspired the development of DAVIS.

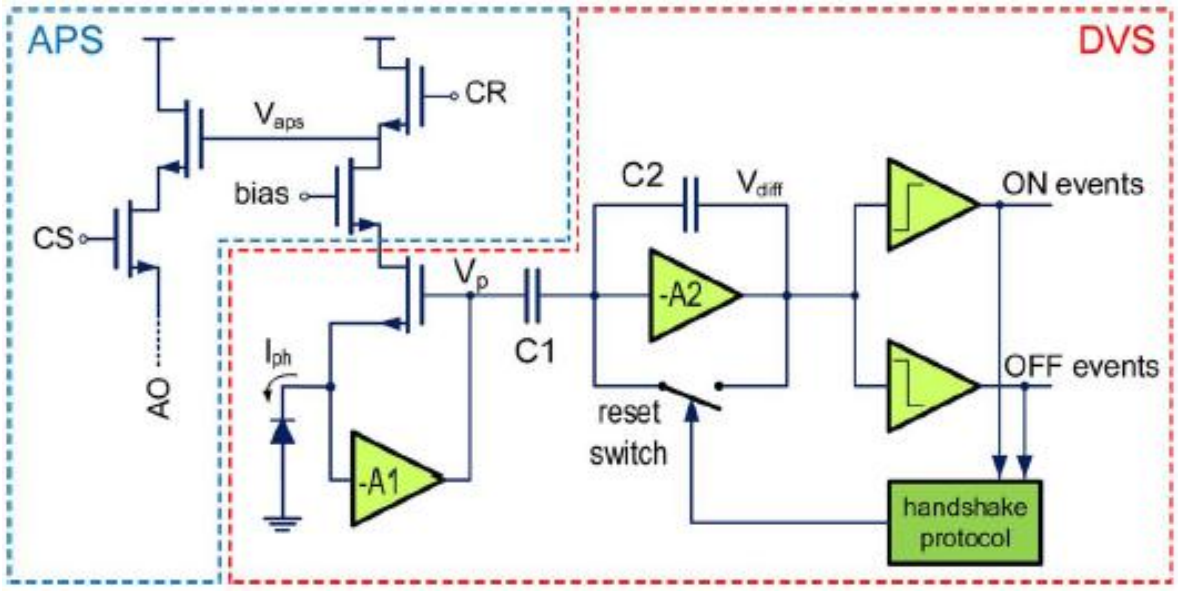

Figure 2.17. DAVIS pixel circuit with APS and DVS pixel fusion (Adapted from [27])

Developing from [51], DAVIS overcomes the limitation of motion artefacts by using a global shutter. This 240 × 180-pixel spatio-temporal vision sensor utilises the novel

combination of DVS pixel with an APS at the pixel level. This enables it to capture synchronous frame data along with asynchronous DVS events, and thus conventional machine vision algorithms can be applied to detect and identify objects in the scene.

Figure 2.18. DAVIS vision sensor (Adapted from [27])

The pixel size of DAVIS is 18.5 μm^2 and it is fabricated in a 0.18 µm 6M1P CIS technology [27]. The DVS pathway in DAVIS exhibits features such as a dynamic range of 130 dB, 3µs latency and 11% contrast detection threshold. The dynamic range of APS readout is 51 dB and adds 0.5% of FPN. The images captured using conventional methods can be easily used for further processing using traditional machine vision algorithms. Thus, DAVIS has set a new benchmark for a hybrid approach and will trigger further research in improving fill factor and resolution.

2.4. NEUROMORPHIC AUDITORY SENSORS

As mentioned by Carver Mead in [4], we can build intelligent and efficient machines if we can extend brain-like auditory sensing and processing capabilities to these machines. Neuromorphic auditory sensors mimic the working principle of the biological cochlea and attempt to implement it using aVLSI concepts. Research on silicon cochlea started in parallel

with silicon retina, but more efficient AER-based implementations have been developed in the last decade [52]. Biological audition concepts are also applied in designing front-ends for speech recognition and bionic ear processors.

2.4.1. BIOLOGICAL COCHLEA

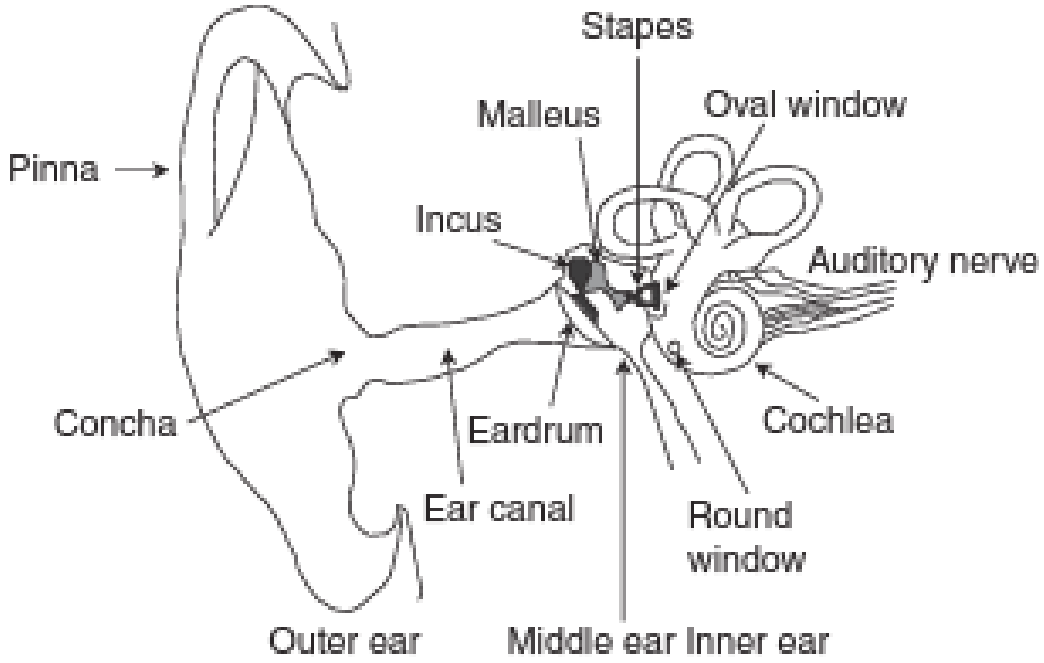

Figure 2.19. Human auditory system (Adapted from [12])

Over millenia the auditory sense in animals has evolved to adapt to changing frequencies of sound, identify the speaker, and even localise the source of sound on the basis of inter-aural time delay. The outer, middle and inner ears adapt to changing sound levels by amplifying the soft sound and suppressing loud sounds. The outer ear helps to focus towards the direction of the sound. The middle ear detects and reduces the signal strength of loud sounds before transferring it to the inner ear. If the sound detected is soft, the inner ear amplifies it by using hair cells that add energy back to the auditory system to strengthen the sound signals. The cochlea is an essential organ that is responsible for the conversion of sound waves that are the incident on outer ears, into action potentials that are communicated to the auditory cortex of the brain [11, 18]. It is necessary to study biological cochlea to understand the helical structure and functions. A cross-section of a human cochlea is shown below in Figure 2.20.

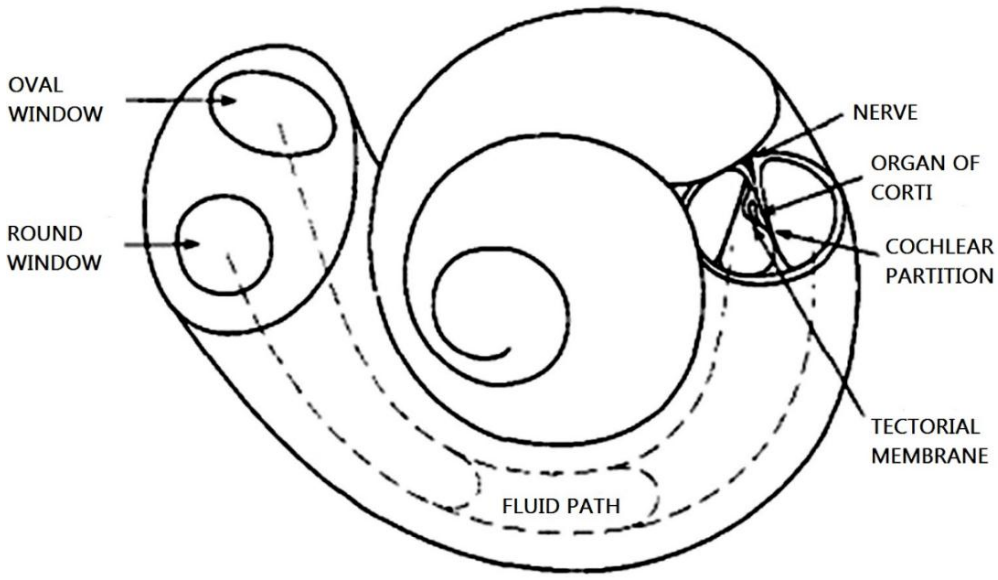

Figure 2.20. Cross-section of biological cochlea (Adapted from [5])

A cochlea is a spiral bony fluid-filled tube structure that is an essential part of the inner ear. The wide end of the unwound cochlea is called the base and the tapered end is called the apex. The interior of the cochlea is divided by Reissner's membrane and the Basilar membrane. The organ of Corti that contains the inner hair cells and the outer hair cells are situated on top of the Basilar membrane. The biophysics of the Basilar membrane produces deflections in the inner hair cells that cause generation of action potentials that travel to the auditory cortex of the brain. The oval window and the round window connects the cochlea to the middle ear. The vibrations created by the sound waves in the eardrum causes movements in the stapes. The movement of stapes pushes the oval window that further causes the fluid in the cochlea to move. The round window allows the fluid to bulge back as it moves in the opposite direction of the initial movement of the oval window.

The properties of Basilar membrane vary along its length as the base is sensitive towards the high-frequency sound, and the tapered apex is sensitive towards the low-frequency sound. The distortion in the fluid results in the formation of a sound wave that propagates from the base of the Basilar membrane to the apex. The high frequencies are strongly attenuated, and the low sound frequencies are amplified as the wave propagates through the Basilar membrane. Thus, only particular parts of the Basilar membrane exhibit maximum deflection to a given frequency. The biophysics of the membrane causes the inner hair cells and outer hair cells to fire action potentials to the brain as a result of the wave propagation within the membrane [53]. The disruptions within the fluid and the partition can be viewed as a distributed low-pass filter and the membrane velocity detected at each hair cell can be considered as a

bandpass-filtered sound wave. These low-pass and bandpass filtering mechanisms are an essential component of an auditory system. Research in auditory sensing has calculated the overall power consumption of biological cochlea to be around 14 µW with a dynamic range of 120 dB [54]. By applying neuromorphic engineering concepts, low-power high dynamic range auditory systems can be implemented.

2.4.2. SILICON COCHLEA

Conventional auditory sensing requires regular digital sampling of the input sound signal at certain Nyquist frequencies. The generation of auditory frames from this input data requires the processing to be carried out at the same input sampling rate. The prime sampling rate and high-resolution Analogue to Digital Conversion (ADC) may result in a substantial amount of power consumption as per application requirements. As observed in conventional vision sensing, the data storage and computation costs for redundant auditory data can be high regarding processing power. Although digital processing of sound is highly improved for certain applications it involves tremendous complexity [1]. In order to overcome these limitations of conventional auditory sensing and processing, neuromorphic concepts are applied to develop auditory sensors and processors that emulate the functionality of biological cochlea.

As described by Mead and Lyon in [5], a silicon cochlea should take real auditory signals as input, process it in real-time and provide an output that is analogous to the spike-based output given to the cochlear cranial nerve. They proposed that the filtering action of the Basilar membrane could be implemented using a cascade of low-order filters. Similarly, the cochlear's ability to adapt to changing sound environments can be modelled using some form of coupled Automatic Gain Control (AGC). This implementation introduced the essential quality factors for silicon cochlea such as latency, high-gain pseudo resonance and sharp roll-off. Figure 2.21, shows a floorplan of this 100 stage cochlea chip. This design suffered from transistor mismatch, limited dynamic range and high latency caused by a large number of cascades. If one of the second-order sections fails, the entire cascade becomes unusable which is another major drawback of 1D designs.

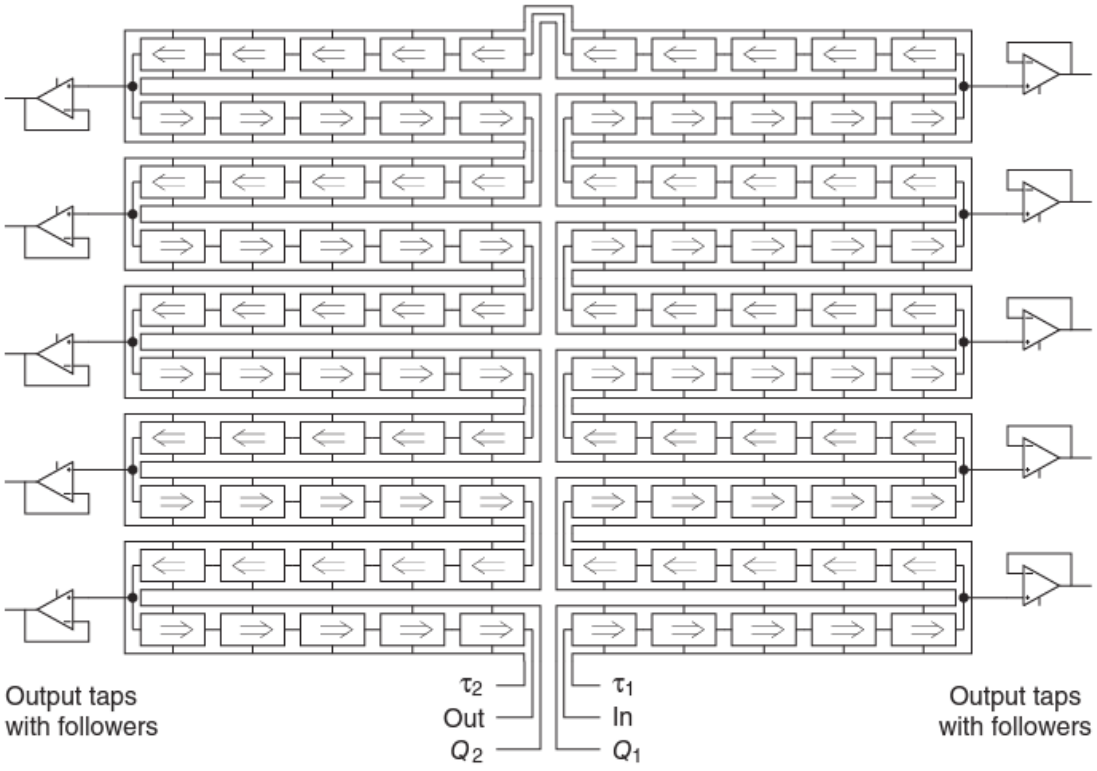

Figure 2.21. Silicon cochlea design by Mead and Lyon (Adapted from [5])

This design is further improved in [55]. Watts et al. pointed out the issues of the original design in [5] and proposed a 51 stage cascaded structure for improved silicon cochlea that consumed only 7.5 mW. Although this design was compact and consumed much less power, it did not address any issues that are related to 1D cascade design flaws and dependency on temperature, process and voltage variations. By improving the designs mentioned in [56], Sarpeshkar et al. presented an analogue VLSI Cochlea that dissipates 0.5 mW and can work in the auditory range of 100 Hz to 10 KHz. The prime focus in developing this design was to improve the dynamic range by using a novel wide-linear-range transconductance amplifier, low-noise second order filters, integrating dynamic gain control and implementing these in an architecture of overlapping cochlear cascades. A dynamic range of 61dB is achieved by implementing this analogue VLSI Cochlea in 117 stages of second-order sections. These early designs underpinned further research in improving the dynamic range of silicon cochlea and keeping the latency and power consumption to a minimum value.

A noteworthy contribution by Hamilton et al. is described in [57, 58]. This implementation was based on 2D architecture i.e. the modelling of cochlear fluid is the prime focus rather than modelling just the Basilar membrane as a cascade of filters. The system-level effect of the failure of a single unit in a cascade is minimised when a 2D architecture is used.

The power consumption of this chip is 16.72 mW, and the dynamic range is about 46 dB. The chip is fabricated using MOSIS AMI 0.5µm CMOS technology and has a die size of about 5mm^2.

Conventional cochlear implants convert sound frequencies into electrode-stimulation patterns for the auditory nerve. Although there has been steady improvement in performance of these implants, power consumption of these processors will be a critical issue if these devices are to be completely implanted inside the body. The neuromorphic concepts used in the development of silicon cochlea are also applied to develop bionic ear processors that are ultra-low-power consuming. Based on developments in [56, 59-62], Sarpeshkar et al. developed a bionic ear processor with a dynamic range of 77 dB and power consumption of 211 µW, which was 25 times less power consuming than state-of-the-art ADC and Digital Signal Processing (DSP) speech processors [54]. This processor operates over 16 programmable spectral channels at an internal dynamic range of 57 dB. A microphone preamplifier is used as an audio front end to capture input sound frequencies. With appropriate processing hardware/software architecture, these processors can be used in portable speech-recognition systems. The authors claim that these processors can, theoretically, function for 30 years on a 100 mAh rechargeable battery [54]. The architecture of this implementation is as given below.

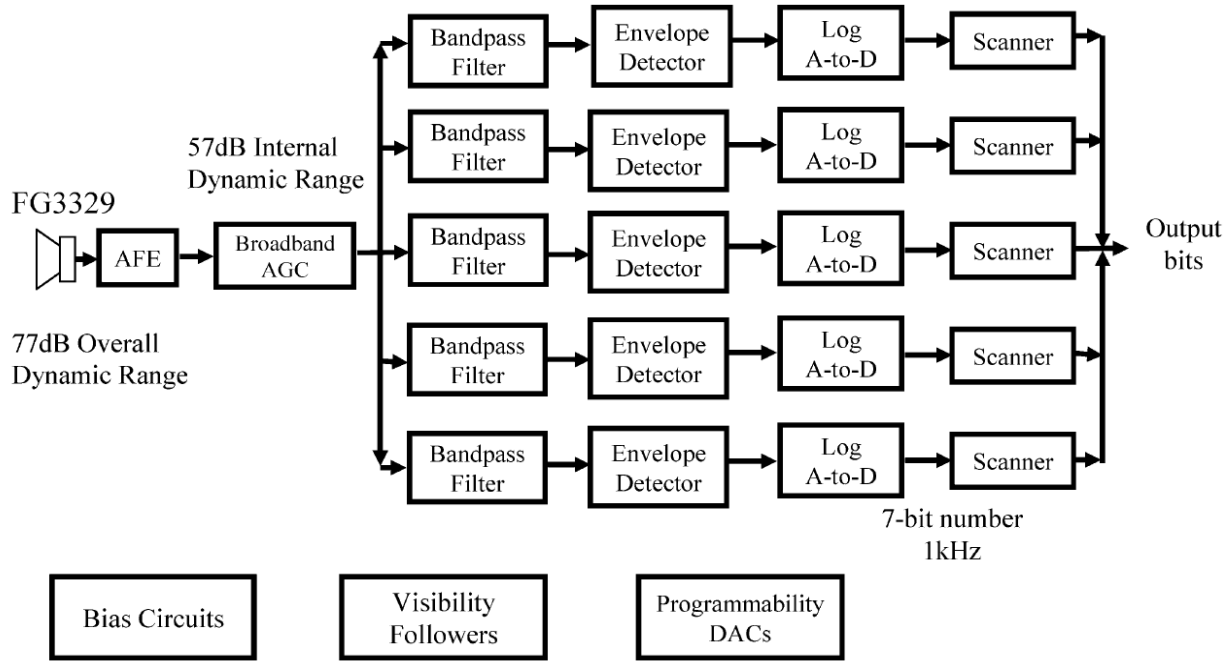

Figure 2.22. Block diagram representation for bionic ear processor by Sarpeshkar et al. (Adapted from [62])

2.4.3. EVENT-BASED SILICON COCHLEA

The spike-based output of biological cochlea ensured that each section of the Basilar membrane can respond to its specific sound frequency by generating action potentials. Developments in implementing spike-based communication using AER, Micro-Electro-Mechanical Systems (MEMS) technology and more precise CMOS technology supported more sophisticated implementations in silicon cochlea. A major drawback of Carver Mead's design in [5] was transistor mismatch that led to inaccurate results. Andre van Schaik et al. [63], proposed a solution to this problem by using Compatible Lateral Bipolar Transistors (CLBTs) for the current sources and thus ensured that the spacing of the cochlear filters was consistent. This design also eliminated the dependency of temperature variance on biasing of the cut-off frequency. Another contribution by van Schaik in [64], introduced the concept of binaural audition and use of MEMS technology in a neuromorphic audition to develop a low-power aVLSI sound localiser. These implementations demonstrated promising results in localisation and sound processing applications [12, 64].

The development of AER gave an impetus to research on silicon cochlea. An AER interface was provided to the matched silicon cochlea pair mentioned in [64]. This 32 stage silicon cochlea is modelled using second-order low-pass filters followed by a simplified Inner Hair Cells (IHC) circuit and a circuit that generates output spikes. The second-order sections employed in this model can be tuned to respond to frequencies ranging from 50 Hz to 50 KHz [65]. This model was used for localisation applications by computing Interaural Time Difference (ITD) [66]. This model laid a concrete foundation for research in silicon cochlea using AER. The IHC and spiking neuron circuit improvements were marked for future versions of this model.

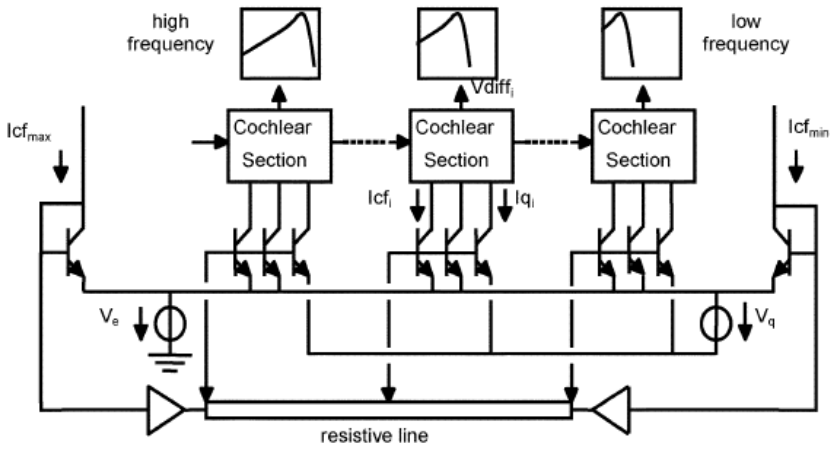

Figure 2.23. Operating principle of AEREAR (Adapted from [65])

The development of AEREAR2 has set a benchmark in neuromorphic auditory sensing. AEREAR2 [1] is a binaural silicon cochlea that comprises of 64-stage cascaded analogue second-order filter banks that can be digitally calibrated. Each channel consists of 4 Pulse Frequency Modulation (PFM) outputs that generate address-event spikes. The 5 bit Digital to Analogue Conversion (DAC) is used to adjust quality factors of each channel individually. The front-end microphones are used to capture incident sound frequencies with onboard preamplifiers to amplify low sound frequencies [59]. This binaural Cochlea provides spike-based output by modelling the Basilar membrane biophysics using a large number of coupled filters followed by half-wave rectification.

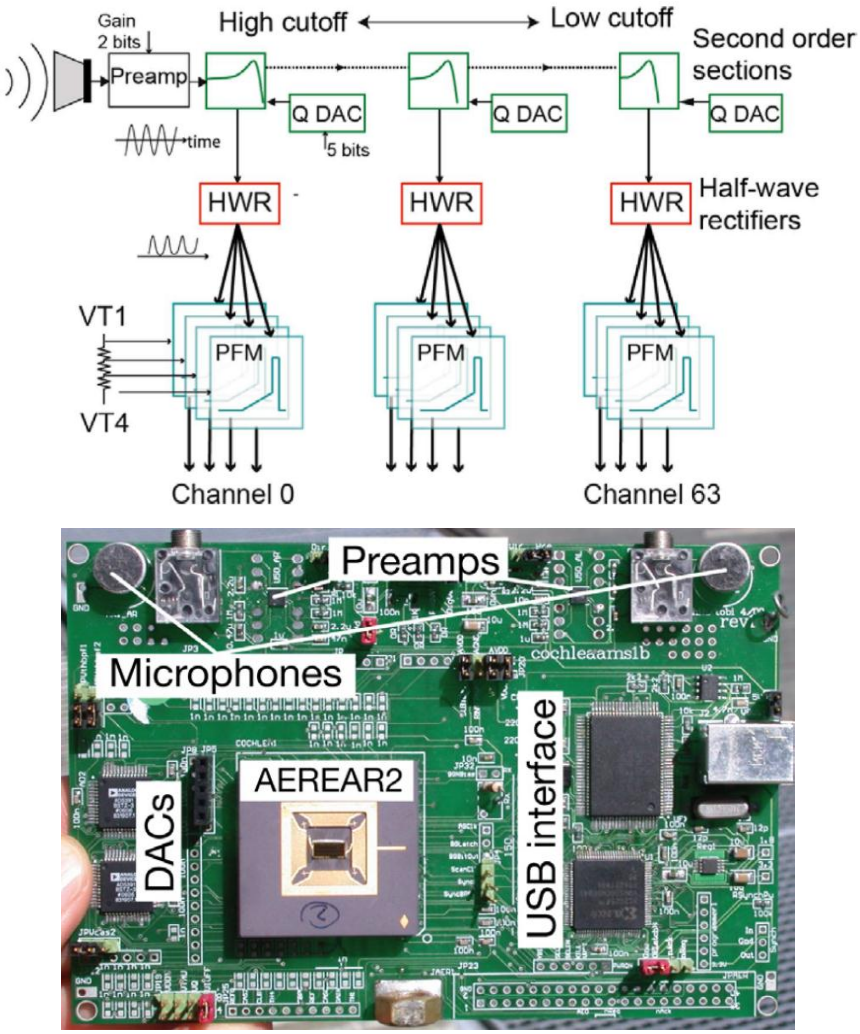

Figure 2. 24. Block diagram representation of working of AEREAR2 (top) and AEREAR2 sensor board (bottom) (Adapted from [1])

The local gain adjustment and biasing circuits ensure the operation of the cochlea is independent of temperature, voltage and process variations. When combined with preamplifier gain control, the total dynamic range of this cochlea is 52dB with power consumption between

12 and 22 mW. A USB interface is provided to enable easy digital interfacing to PCs and host microcontrollers. AEREAR2 is 40 times less computationally demanding than conventional cross-correlation method for localisation applications [1]. Features like being robust to mismatch and easy programmability has promoted the application of AEREAR2 in auditory scene analysis applications [67].

We can learn from these implementations that future research in neuromorphic auditory sensing will be directed towards sound reconstruction from spike data and deriving efficient solutions for the cocktail-party auditory scene analysis problem. Research towards developing neuromorphic auditory front-ends [68] will expose several other avenues to implement a complete neuromorphic auditory system.

2.5. NEUROMORPHIC OLFACTION SENSING

The biological sense of smelling aromatic compounds is termed as olfaction. Olfaction is among the most complex sensory system to decode and understand entirely because millions of receptor neurons exhibits phenomenal redundancy to appropriately identify and distinguish between odours. Gustatory sensing is mainly dependent on the ability of biological entities to sense different smells, which enhances their ability to taste. Recent developments in electronic olfactory sensors have enabled implementation of real-time embedded systems that can sense various gases. Such systems are used in biosecurity applications, the food industry and to avoid hazards by detecting harmful gases [69, 70].

2.5.1. BIOLOGICAL OLFACTION

Biological olfaction sensing requires an odour delivery channel for the odour molecules to enter the olfactory system. Most of the biological entities sniff odour molecules using nasal cavity whereas a few insects depend on antennal lobes for this task. The sensitivity of olfaction sensing varies across different living beings as some insects and animals depend solely on olfaction for their very existence [71]. Extensive research on the human olfactory system has triggered immense interest from neuromorphic engineering to understand and reverse engineer this phenomenon.

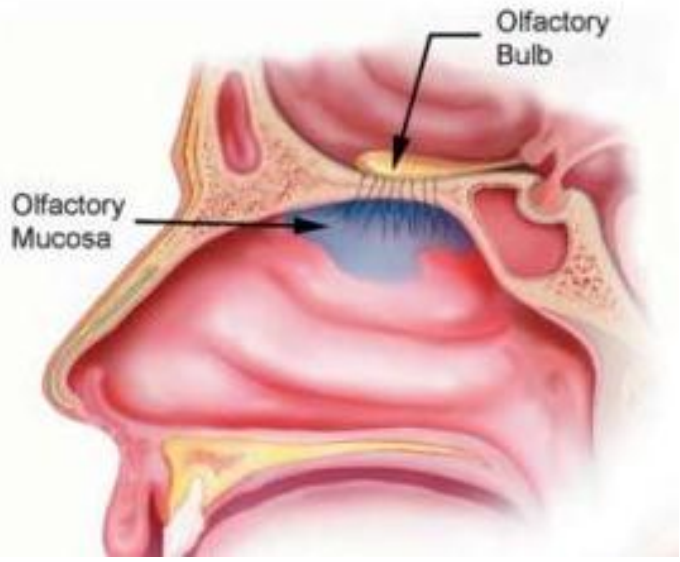

Figure 2.25. Cross-section of human olfactory system (Adapted from [71])

The odour molecules enter the olfactory system through the nasal cavity. The receptor neurons situated on the ciliary membrane are responsible for identification of odours based on the odorant molecules. The olfactory epithelium, a thin tissue in the nasal cavity, is a vital part of olfaction system. It comprises of three types of cells: the Odour Receptor Neurons (ORNs) and the dendrite-like projections called cilia, the supporting cells, and the basal cells that are responsible for the generation of new ORNs. The bones in the nose direct the inhaled airflow in such a way that the volatile compounds reach the ORNs in the olfactory epithelium.

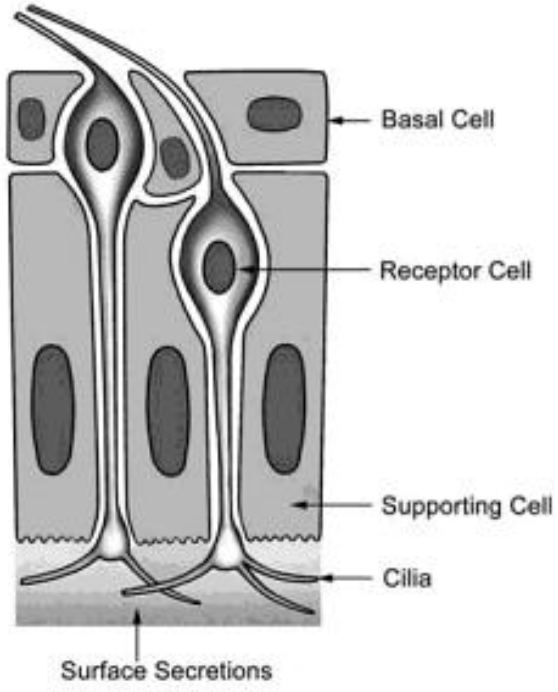

Figure 2.26.Cross-section of biological olfactory epithelium (Adapted from [72])

The number of ORNs in humans vary from 10^6 to 10^8 [73]. An ORN comprises of dendrite-like structures called cilia that project into the olfactory mucus, a Soma that is the main cell body and an axon that propagates action potentials from the soma to the olfactory bulb [72]. Specific ORNs are sensitive to only selective volatile compounds and are spatially distributed along the olfactory epithelium. Each ORN is responsive to a broad range of volatile compounds. The cribriform plate, a part of the ethmoid bone, lies between the olfactory epithelium and the olfactory bulb. The axons of ORNs fasciculate together and coarse through tiny holes in the cribriform plate and synapse with glomeruli. Glomeruli are second order neurons in the olfactory system that are spherical in structure and contain neuropil. The dendrites of the mitral cells synapse with the ORN axons in the neuropil of glomeruli. The ORNs that are sensitive to specific odours synapse to a common glomerulus.

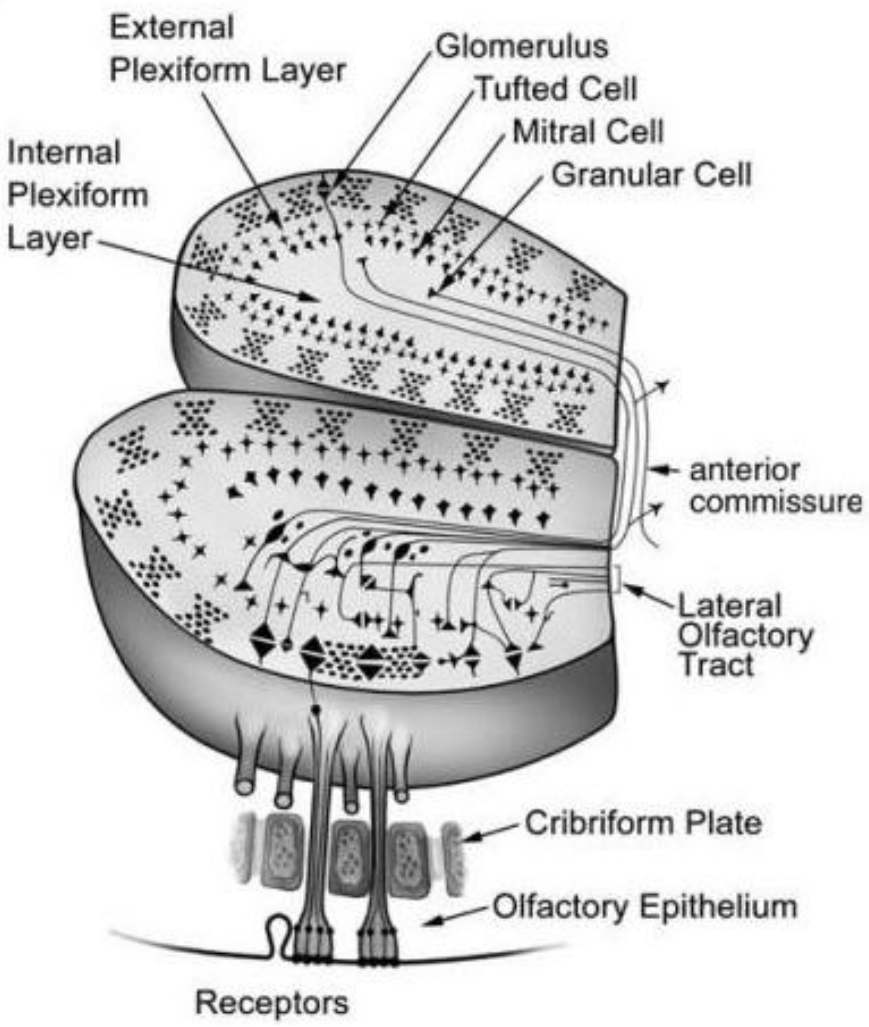

Figure 2.27. Detailed pathway for biological olfaction (Adapted from [72])

The primary processing of the olfactory signals is completed at the local neuronal circuits in the olfactory bulb; this data is further processed by the mitral cells that have the

narrower receptive range for volatile compounds compared to the ORNs [74, 75]. This second-stage processing by multiple glomeruli provides the basis to discriminate between olfactory qualities. The action potentials are propagated through the lateral olfactory tract to the olfactory cortex of the brain. The axons of the ORNs bind together to form the olfactory tract, which is the olfactory cranial nerve. This olfaction data is also used by pre-pyriform cortex that is a part of the limbic system of the brain.

2.5.2. BIOMIMETIC OLFACTION SENSORS

Technological advancements in electronic nose instrumentation have sparked interest from various fields for its ability to solve problems related to detecting hazardous gases, application in the food industry to determine food quality, environmental monitoring and many such applications related to odour detection and identification [76]. The conventional E-nose is a complex architecture with a bulky design that restricts its portability. It is necessary to have specialized gas sensor to detect a particular gas or odour. This limits the odour identification to the number of sensors used. Along with a large number of sensors, conventional olfactory sensing systems require sizeable odour delivery channels and a processing unit with an ADC and pattern recognition engine [77]. Conventional olfactory sensors also suffer from significant latency, sensor poisoning issues, and temperature and voltage variation dependence. These factors along with high manufacturing costs have largely restricted the use of such sensors to laboratory experiments.

The limitations of conventional olfactory sensors impeded its commercial application [78]. The successful application of neuromorphic concepts in vision and auditory sensing inspired research in the development of neuromorphic olfactory systems. To emulate the olfactory pathway, a general structure starting with an odour delivery channel followed by a sensor array, signal conditioning circuitry and spike-based output generator, is implemented using aVLSI [74]. The odour delivery channel acts like nasal cavity that directs the volatile compounds towards the sensor array and is designed accordingly. Numerous approaches have been proposed for the implementation of the sensor array, among which metal oxide sensors and polymer sensors are widely used. The signal conditioning circuit is responsible for ADC and signal modulation. The modulated signal is processed to generate spike-based output that describes the odour concentration.

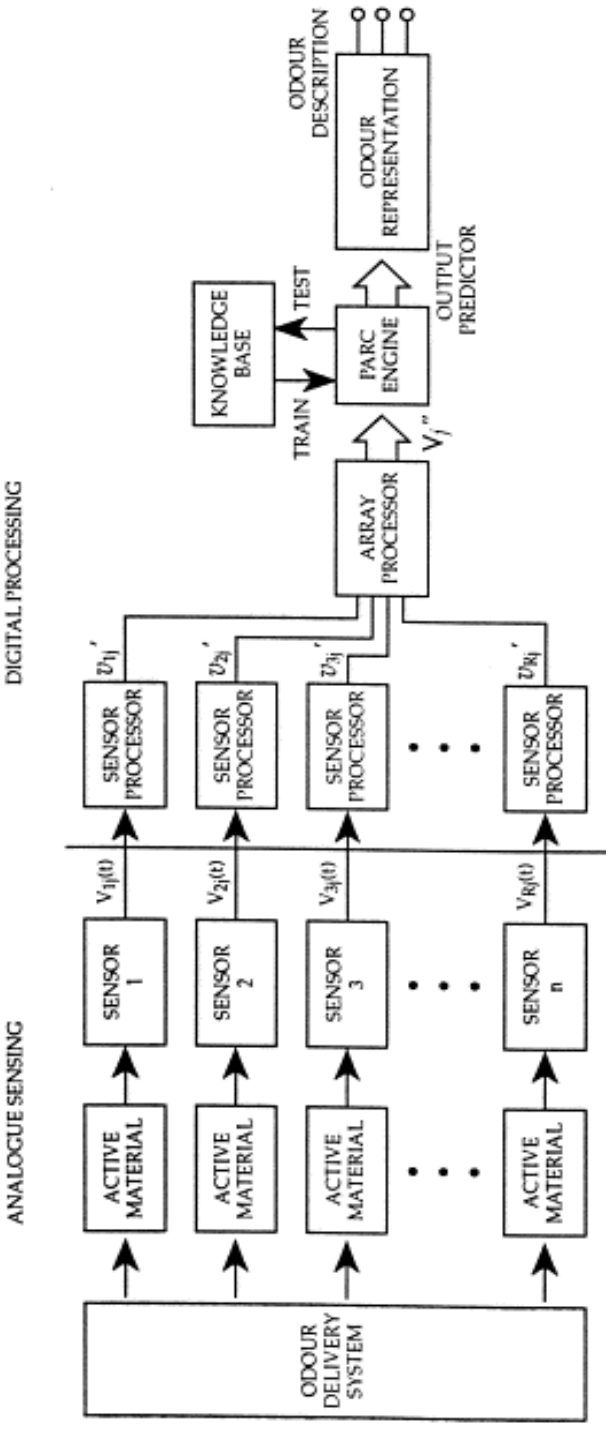

Figure 2.28. Typical biomimetic olfactory sensor design (Adapted from [74])

Developing on interface circuitry, sensor array design, and silicon olfactory pathway described in [70, 79] and [80], Thomas Koickal et al. developed the most cited neuromorphic olfactory system [77]. This implementation stressed on emulating all the functionalities of the olfactory pathway using aVLSI. The analogue VLSI design ensures low power consumption, low costs and minimal area for the hardware. By applying neuromorphic concepts, the

developed system can adapt and work efficiently in changing environmental conditions and perform complex odour detection. A block diagram representation of the olfactory system is given in Figure 2.29.

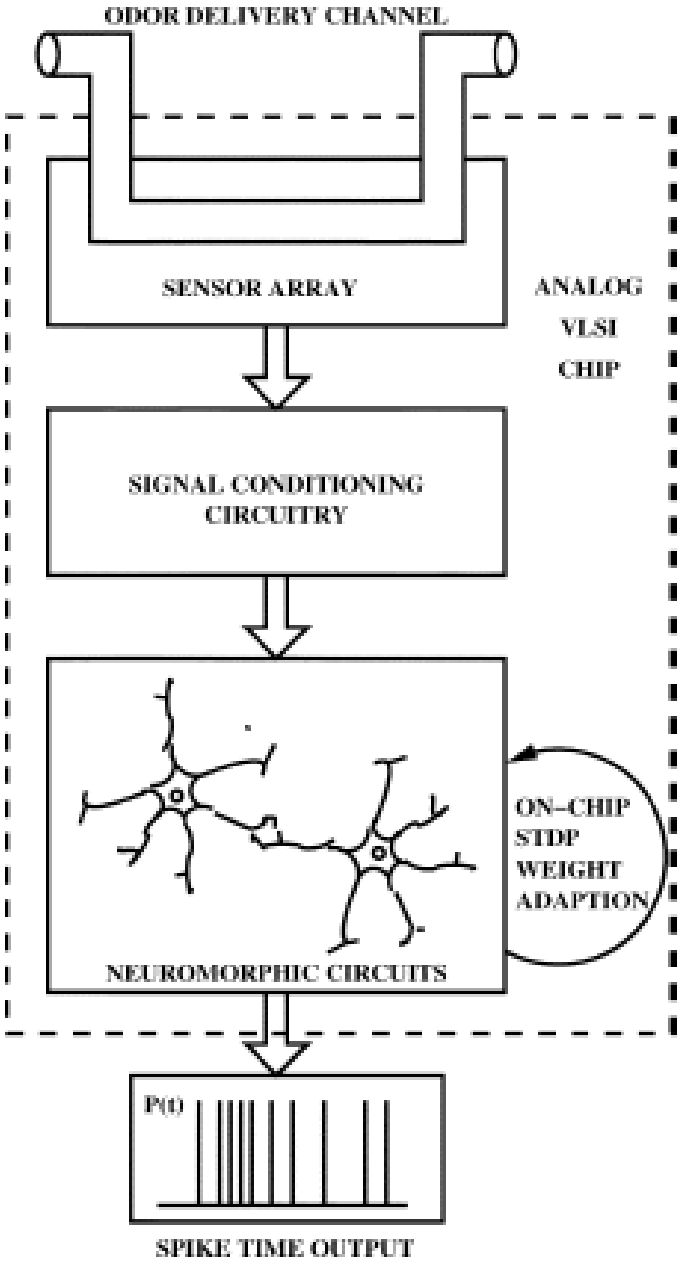

Figure 2.29. Block diagram of aVLSI implementation of adaptive olfactory system (Adapted from [77])

The on-chip resistive Carbon Black (CB) polymer chemosensor array is fabricated using Austria Micro Systems 0.6-µm CMOS process [77]. Each sensor cell comprises a programmable current source, a sensor and interface circuitry. A novel DC cancellation circuit and a difference amplifier are implemented in the sensor interface. This reduces variations caused by the baseline signals due to poisoning effect of the chemosensor array and different

operating current specifications for various sensor types. The output from the interface circuitry is given to the neuromorphic circuits that implement on-chip STDP learning. The dynamic exponential learning window function is implemented to emulate the biological olfactory characteristics. A data acquisition interface is used to obtain the spike-based output of the sensor. Although this implementation is highly cited in neuromorphic olfaction sensing, issues such as long-term weight storage, component mismatch and layout optimisation were identified for future development [78]. A crucial shortcoming of this implementation is the lack of AER interface to implement spike-based post-processing algorithms [81].

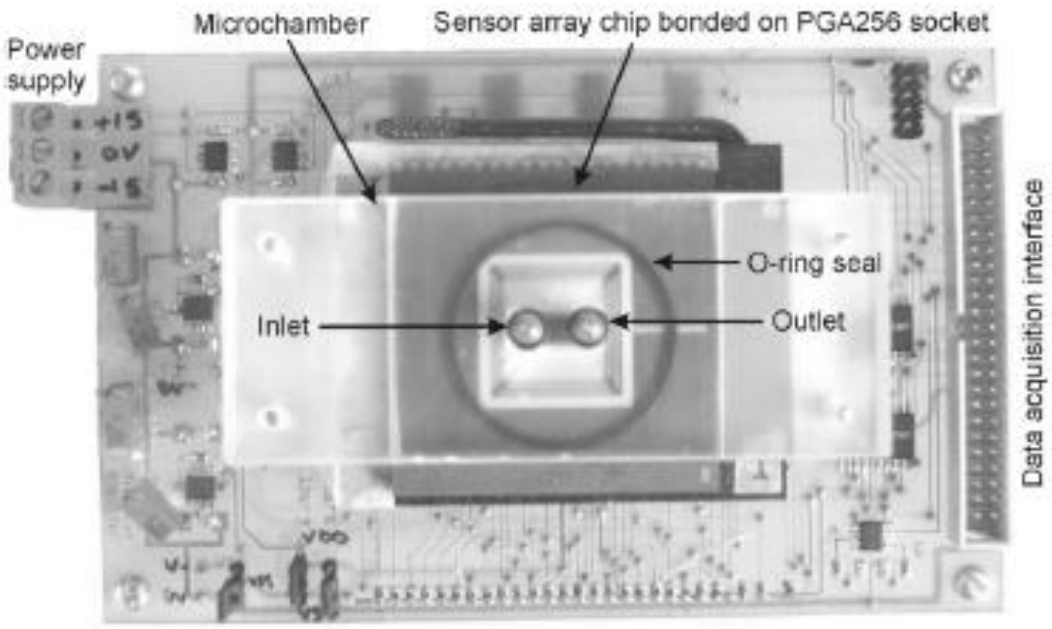

Figure 2.30 Sensor interface PCB (Adapted from [77])

This implementation inspired several promising developments in neuromorphic olfaction sensing. Hung-Yi Hsieh and Kea-Tiong Tang developed a VLSI implementation of the neuromorphic Spiking Neural Network (SNN) chip with 48 mitral cells, 48 STDP synapses and six cortical cells [82]. The proposed SNN chip consumes an average power of 3.6 µW and provides either a HIGH or an LOW output that represents if the input odour is identified. The mean testing accuracy of the chip is 87.59% and is comparable to the K-Nearest Neighbour pattern matching algorithm.

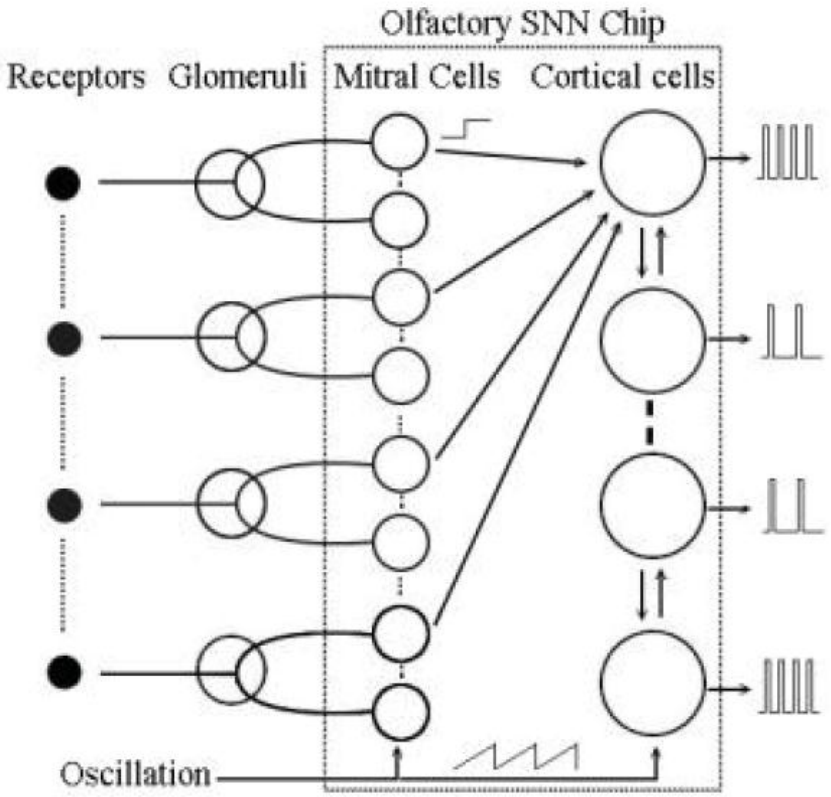

Figure 2.31. System implementation diagram for olfactory sensor based on SNN (Adapted from [82])

Kea-Tiong Tang has also contributed to the development of low-power signal processing chip for a portable E-nose system [83]. The front-end conductive polymer sensor array chip is composed of multi-walled carbon nanotubes. The chip comprises of interface circuitry, an ADC component, a memory module, and a microprocessor running a pattern recognition algorithm. The output of the signal processing chip is a distinct pattern that can be termed as a signature to identify and distinguish odours.

The power consumption of the chip is 2.81 mW on a continuous supply voltage of 1.8V. This chip is fabricated using TSMC 0.18 µm 1P6M CMOS technology. The identification of odour is implemented by comparing the ADC data to the library of gas signatures in the memory module. Although the success rate using testing is 100 %, this embedded software based approach using 8051 microcontrollers and KNN algorithm running on it is inefficient regarding response time compared to a neural network-based approach. A system implementing similar approach with LabVIEW for analysis and a DAQ interface was used in [84] to identify fruity odours. Other interesting approaches presented in [85-87] are also a part of comprehensive research by Kea-Tiong Tang in neuromorphic olfaction.

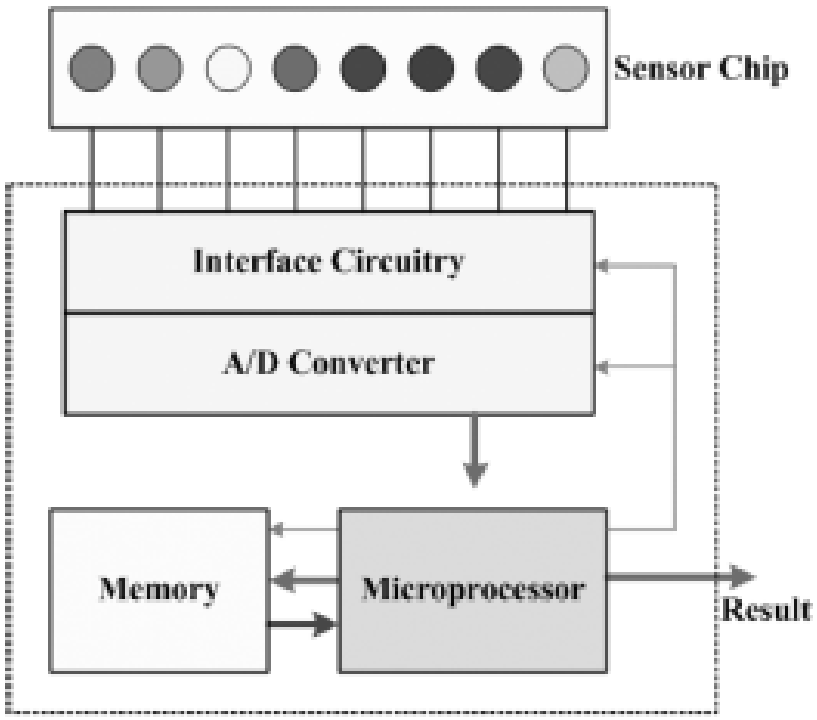

Figure 2.32. System architecture for electronic nose chip in [83]

A CMOS chip with 4 × 4 metal oxide gas sensor array is described in [88, 89]. This approach focused only on implementing the biological olfaction characteristics that can be emulated in silicon rather than developing a detailed model of the biological olfactory pathway. The main aim of this implementation was to implement the olfaction system on a single chip that can provide a different signature output for a particular gas. This signature is compared to the library of 2D spatio-temporal spike signatures for a match that enables simultaneous gas recognition and sensing.

This chip is fabricated using 0.35 µm CMOS technology with a 4 × 4 tin oxide sensor array as a front-end and has a power consumption of 23 mW. The drift insensitive and concentration-invariant generation of 2D spatio-temporal signatures is the highlight of this implementation. The proposed approach presented a correct detection rate of 94.9% when applied to detect propane, ethanol and carbon monoxide. Improvements marked for future improvements for this implementation focus on improving the response time of this system, its portability and adding an AER interface.

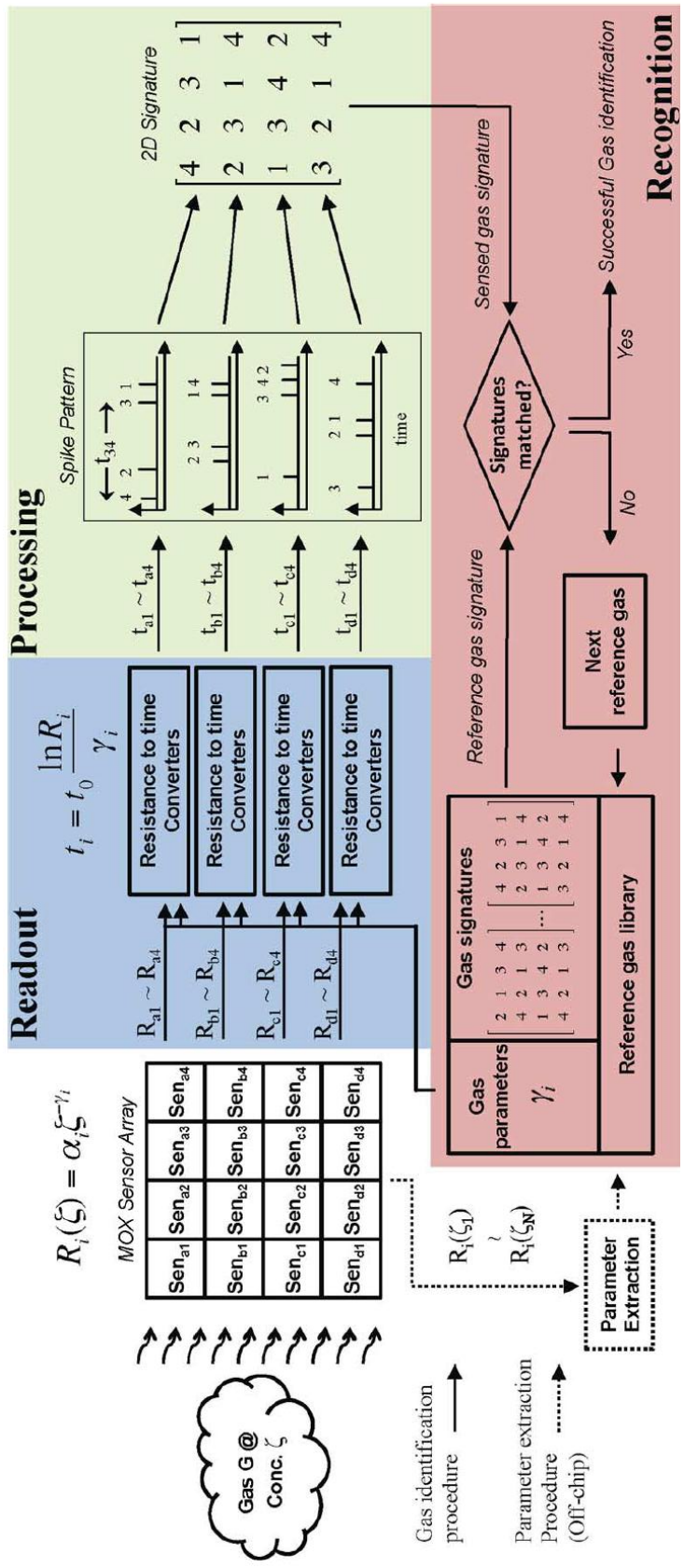

Figure 2.33. Key components and working of 4 × 4 gas sensor described in [88]

2.6. SUMMARY

This literature survey was focused on the working principles and output characteristics of neuromorphic vision, auditory and olfactory sensors. The implementation of an AER interface for neuromorphic vision and auditory sensors has underpinned further research towards development of processing algorithms for spike-based output. Chapter 4 presents more information on AER interfacing and interfacing of neuromorphic sensors. By determining the output and performance parameters for vision and auditory sensors, implementations like DVS, DAVIS and AEREAR2 have set benchmarks in their respective fields. This study has helped us to identify specific gaps in research related to neuromorphic olfactory sensors. Performance parameters for interfacing, sensor material, gas recognition engine and signal conditioning circuitry, are yet to be standardised. Thus, unlike vision and auditory sensing, where future development is directed towards a definite goal (like improving fill factor and resolution in vision or sound reconstruction in audition), there is still a wide scope for performance improvement in neuromorphic olfactory sensing.

CHAPTER 3. COMPARISON BETWEEN CURRENT STATE-OF-THE-ART NEUROMORPHIC VISION, AUDITORY AND OLFACTORY SENSORS

This chapter is adapted from the manuscript "A Review of Current Neuromorphic Approaches for Vision, Auditory and Olfactory Sensors ".The manuscript has been published in the journal Frontiers in 'Neuroscience: Neuromorphic Engineering' under the research topic "Benchmarks and Challenges for Neuromorphic Engineering". Some of the information in this section is redundant with the information in the literature review, but as this section is an extract from a publication, the redundant information has been included to maintain a step-by-step flow of the document.

3.1. CURRENT DEVELOPMENTS IN NEUROMORPHIC ENGINEERING

The field of neuromorphic engineering has been developing rapidly over the last decade. With the growing trend towards embedding intelligence in day-to-day devices, we are constantly making our surroundings smarter and more adaptive to our behaviour. However, this technological progression requires an ever increasing number of sensors and associated data storage [11]. Along with the data processing challenges, factors such as power consumption and financial viability limit the development of smart devices. Realising these limitations in the late 1980s, Carver Mead introduced the concept of neuromorphic engineering. This interdisciplinary field addresses the underlying concepts of neurobiological architecture and mimics its implementation using aVLSI. Neurobiological architecture is a low power consuming system which learns through exposure; these attributes, along with sparse output are crucial design criteria for neuromorphic systems [4].

Neuromorphic approaches have been applied in implementing neural processors, developing neural networks, and particularly in electronic sensing where novel methodologies have been developed [90]. In the mid-1980s, Max Delbrück, John Hopfield, Carver Mead, and Richard Feynman collaborated to exploit the non-linear current characteristics of transistors [3]. Carver Mead, further highlighted the excessive dissipation of energy through conventional computing methods and the limitation of using transistors merely as digital switching components. He proposed that the analogue physical properties of transistors could be

exploited to design adaptive and low power consuming sensors like silicon retina and cochlea [4]. With these models as inspiration, neuromorphic concepts have been applied to vision sensors, auditory sensors and olfactory sensors. Current sensor advances have been supported by massive parallelism, asynchronous processing and self-organization [12, 22].

As described in [91], analogue implementation of neural-like systems are capable of approaching equivalence to biological systems in terms of power consumption and efficiency. Most of the research in neuromorphic sensors has involved aVLSI; however, with rapidly changing technology, digital electronics has also been applied to implement neuromorphic concepts, particularly as it has proved to be robust to internal and external noise [13]. Systems implemented using digital electronics are easily programmed and upscaled [2]. Regardless of whether analogue or digital implementations are used, the lack of standards and benchmarks for the output of neuromorphic sensors may limit their development and adoption. In the same way that the interfacing for neuromorphic sensors uses standard Address Event Representation (AER) [92], a standardised method to evaluate sensor outputs could help establish appropriate benchmarks for further improvement. In this paper we review significant recent contributions to neuromorphic vision, auditory and olfactory sensing and compare them to identify potential benchmarks for neuromorphic sensors.

3.2. NEUROMORPHIC VISION SENSORS

Neuromorphic engineering concepts have been successfully implemented to emulate biological sensory systems with silicon retinas being a prominent example [11]. Currently, vision sensing depends on the conventional frame-based approach but regardless of whether the scene changes, these frames are captured continuously and this generates significant volumes of redundant data [27, 35]. However, reducing the frame capture rate may cause excessive information loss between consecutive frames, particularly for real-time applications such as machine vision and robotics. Such frame-based approaches also consume substantial power and make data management challenging [24]. Attempts were made to control the data output from these sensors by relaying information only for changed values of pixels. However, off-sensor processing and complex control strategies increased the overall power consumption of the system [35].

Mahowald and Mead implemented the first silicon retina model in [29], that was both adaptive and energy efficient, by emulating retina functionalities, especially the cone cells,

through analogue properties of transistors and introducing adaptive vision sensing. [33, 34], improved this model by adding the functionalities of inner retina and parvo-magno cells [33, 34]. These attempts could only model the retina in silicon, however, and did not provide a realistic implementation for practical use. In response, the neuromorphic community focused on the operating principle of the neurobiological architecture rather than modelling the overall sensory system. Specifically, this problem could be solved by realising the difference between temporal and spatial contrasts. With the developments in AER, pixels could operate individually as processing units and report any deviations in temporal contrast. The spiking output is similar to the action potentials generated by ganglion cells and consequently most retinomorphic sensors now use AER communication [24].

Tobi Delbruck built on the idea of adaptive photoreceptor circuits developed in [44] and introduced strategies for enhancing retinomorphic sensors. The 128 × 128 pixel Dynamic Vision Sensor (DVS) can be considered as the product of several improvements through [26, 43, 93] where the concepts of differentiating ON/OFF events with respect to lumosity change and relative lumosity change were implemented. DVS established a benchmark in neuromorphic vision sensing with its AER- based approach in which each individual pixel processed the normalised time derivative of the sensed light and provided an output in the form of spikes of the pixel addresses that detect lumosity change. As an alternative approach, frame-based temporal detection imagers [94, 95] were developed. The operating principle of these imagers was based on integration of the photocurrent between successive frames and computing of the difference between them. However these implementations have a limited speed response and a low-dynamic range, 100dB for [95] and 52dB for [94]. With features such as sub-millisecond precision, dynamic range > 120dB and low power consumption of 23mW, DVS was a path-breaking discovery and was used in various robotic and real-time systems [47, 48, 96].

With DVS, a benchmark was established for essential characteristics that a neuromorphic vision sensor should possess and gave a certain direction for further research in vision sensing. Developing on the basic idea of DVS, [97] enhanced the capabilities of DVS by improving the contrast sensitivity by one order of magnitude (down to 1.5%) and reducing power consumption to 4mW and fixed pattern noise to 0.9% and thus the overall pixel size of the sensor down to 30 × 31μm^2 per pixel. The QVGA (304 × 240 pixel) ATIS (Asynchronous Time-based Image Sensor) by [36], implemented PWM (Pulse Width Modulation) based intensity readout that improved the dynamic range (143-125 dB) at the cost of increased pixel

area of 30 × 30μm^2. The inclusion of DVS pixel and PWM intensity readout triples the sensor output data. [27] proposed a hybrid approach between frame-based and frame-free vision sensing. The 240 × 180 pixel DAVIS (Dynamic and Active-pixel Vision Sensor) arose in part from contributions by [51], in which the concept of integrating a synchronous active-pixel sensor with asynchronous DVS pixels was implemented.

The successful implementation of DAVIS set another benchmark that will inspire future work towards neuromorphic vision sensors that provides spatial details of static scenes while also responding to dynamic temporal changes with minimum latency. This will also drive efforts to improve the fill factor and dynamic range.

3.3. NEUROMORPHIC AUDITORY SENSORS

The conventional method of sensing auditory signals is sampling the data continuously for auditory input at an application specific Nyquist frequency. This data undergoes Analogue-to-Digital Conversion (ADC) and further digital processing to generate auditory frames. There is a significant power cost for high resolution ADC and digital processing of auditory frames. Although this sampling rate can be altered dynamically to reduce power consumption, there is a risk of losing critical information due to low sampling rate. For applications such as auditory scene analysis, it is necessary that such sensors use less power and generate sparse data [1].

Lyon and Mead, proposed an auditory sensor in [5] that models the human cochlea using aVLSI. This work addressed key concepts like automatic gain control, the use of cascaded second-order bandpass filters and the necessary quality factors for auditory applications such as delay, high-gain pseudoresonance and sharp roll-off. Although these researchers implemented the bio-physics of both outer and inner hair cells of the basilar membrane, this analogue cochlea model did not incorporate any biasing circuits for process, voltage and temperature variations. However, it was further improved by addressing issues such as device mismatch, stability and dynamic range [98]. By introducing ‘overlapping cochlear cascades’ [56], established a novel approach to the design of an aVLSI cochlea with dynamic range of 61dB that consumes 0.5 mW. These early works underpinned further studies in silicon cochlea design.

Crucially, the efforts in silicon cochlea research led to the development of an auditory processor for cochlear implants that operated on minimal power. Sarpeshkar and his colleagues

extending their work in [61, 62] and taking inspiration from other contributions [59, 60], developed an ultra-low power auditory processor for a bionic ear. This processor can theoretically operate on a 100 mAh rechargeable battery for several years and features automatic gain control and microphone pre-amplifier audio front end, so that the processor converts the input signal to the desired dynamic range. The digital output of the processor ensures its independence from voltage and temperature variations. It operates over 16 channels that are comprised of independently programmable bandpass filters. [54] claimed that such processors can be applied in systems needing low-powered portable speech recognition front ends.

Along with cochlear implants, auditory scene analysis is a crucial application for the silicon cochlea. The implementation of AER to communicate output spikes stimulated further research on developing a spatial auditory sensor. Building on the silicon cochlea described by [63] and a neuromorphic front end MEMS (Micro-Electro-Mechanical Systems) microphone explained in [64], [65] developed AER EAR, a matched pair of silicon cochlea with an AER interface. This auditory sensor models the basilar membrane bio-physics by cascading low-pass filters to provide output over 32 channels. The simplified inner hair cell circuit and spiking neurons ensured sparse asynchronous output; the design was tested for localization applications by computing the interaural time delay between the matched pair of silicon cochlea [66].

Further improvements including microphone pre-amplifiers and per-channel capability led to the development of AEREAR2 [1], a 64 channel binaural audition sensor that set a benchmark in neuromorphic audition. By integrating local DACs that enable the quality factors of individual channels to be adjusted, this sensor overcomes most of the drawbacks of AEREAR. With improved dynamic range, binaural structure, integrated microphone preamplifiers and biasing circuits for stability against voltage and temperature variance, this sensor provides precise timing of spikes over a USB interface. This approach was used in complex applications like speaker identification [67]. A thorough comparison between conventional cross-correlation approaches and spike-based sound localization algorithms shows that event-driven methods are about 40 times less computationally demanding [1]. Even more precise and efficient neuromorphic auditory systems will be developed by applying interesting approaches such as spike based audio front ends described in [68].

3.4. NEUROMORPHIC OLFACTORY SENSORS

The development of artificial olfaction devices started with [99] who applied mechanical concepts to measuring and determining odours. Since the development of the electronic nose [75], emphasis has been placed on developing olfactory sensors that are portable and precise. Conventional olfactory sensors are large with restricted portability and also impede reliability as the chemical constituents in a target gas vary rapidly. These factors along with high manufacturing costs have largely restricted the use of such sensors to laboratory experiments and industries [78].

The electronic nose has benefited from CMOS and MEMS technologies, advanced pattern matching methods and new sensing materials [81]. Biologically based olfaction systems have inspired a general structure for electronic nose systems that are composed of a sensor array, signal conditioning circuitry, and a pattern recognition unit [74]. By applying neuromorphic concepts, improvements were made to this structure by integrating all these units on a single chip and implementing neural networks for pattern recognition. Thomas Koickal and colleagues made a notable contribution to developing an adaptive neuromorphic olfaction chip. The CB polymer sensor array used in that system was fabricated using the Austria Micro Systems 0.6-µm CMOS process [77]. A novel design was implemented to cancel the baseline sensor variations due to sensor poisoning and variation in operating current specifications across different sensors. The neuromorphic implementation simplified the odour detection especially in the presence of background odour signals. This design proved to be a technological benchmark to stimulate further study in neuromorphic olfaction by introducing features like on-chip Spike Timing Dependent Plasticity (STDP) learning, reduced power consumption, and temporal spiking signals output. [100] developed a biomimetic mucosa that can generate spatio-temporal output but improvements were needed for reduced response times and odour delivery channel size in this design.

Researchers have focused on implementing the critical olfaction characteristics rather than emulating the entire biological olfactory pathway. A 4 × 4 tin oxide gas sensor array was designed [88] such that each row forms a group of sensors showing similar drift behaviour. It is possible to detect a wide range of chemical gases by assigning the same catalyst to each group of sensors. The firing delay in the spiking output from these sensors generates a unique sequence of drift-insensitive spikes [101]. This output represents a signature for a specific gas which is determined by matching it in a library of 2-D spatio-temporal spike signatures. This

approach reduces the computation challenges involved in pattern matching [102]. The entire gas recognition circuit is fabricated and implemented on a single CMOS chip and the power consumption is as low as 6.6mW with 94.9% identification accuracy.

E-Nose described in [83], consists of a conducting polymer sensor chip, interface circuitry, ADC and a microprocessor with a pattern recognition algorithm and an associated memory module. The output of this chip is a unique signature of the target gas, but the inclusion of a pattern matching algorithm instead of a neural network makes this approach computationally expensive. This approach was also used by [84] to identify and classify fruity odours and led to the development of a spiking neural network chip that implements the Spike Timing Dependent Plasticity (STDP) learning rule [82]. The sensor array used for sampling odour data is a commercial electronic nose (Cyranose 320). This work focused on the backend computation to identify odour and the developed chip can identify three different odours concurrently. The average power consumption is as low as 3.6μW and mean testing accuracy is 87.59%. NEUROCHEM is an important project lead by European universities that is focused on developing a large sensor array for neuromorphic olfactory systems [103]. This conductive polymer sensor array mimics the essential characteristics of biological Odour Receptor Neurons (ORNs) including redundancy and sensitivity to a wide range of volatile compounds.

The neuromorphic olfactory sensor literature indicates that there is considerable scope for improving these sensors. The CMOS chip by Thomas Koickal is a notable contribution in neuromorphic olfaction and can be considered as a highly cited research contribution in neuromorphic olfaction. Although there are several shortcomings in this implementation, it proposes a novel architecture for olfactory sensors. Improvements proposed in [88] are promising if the response time can be improved further. [78], also exposes gaps in interfacing, signal conditioning and pattern matching computations in neuromorphic olfaction.

While neuromorphic sensors offer benefits of low-power consumption and sparse output data generation, the means to process the spike-based data format is still limited. Decades of research in digital image processing and digital signal processing, has led to the development of advanced algorithms and hardware architectures that allowed efficient processing of conventional outputs (e.g. frame-based and audio samples). As techniques for high-level processing of event-based data are still under development, the large-scale application of neuromorphic sensors depends on the introduction of these techniques. However, advanced research in neuromorphic sensors has increased the application scope of these sensors in

intelligent embedded systems. Prototypes of neuromorphic vision and auditory sensors evolved into commercial products such as the DVS128 PAER and Dynamic Audio Sensor (DAS1). However, most of the systems that make use of neuromorphic sensing implement only a single type of sensor such as vision or auditory. [104] and [105] were among the first who targeted the development of platforms for interfacing multiple neuromorphic sensors. [106] implemented sensor fusion of Audio-Video (AV) neuromorphic sensors and presented an advanced version of the Koala robot that was first developed by [105] for object tracking. Development of neuromorphic processing boards under large scale projects such as CAVIAR, BrainScaleS and SpiNNaker, promotes the idea of sensor fusion and data correlation. By utilizing concepts like the spiking Deep Belief Network (DBN) [107], the idea of multi-sensor neuromorphic systems can be brought to fruition. Such systems can have numerous applications in fields such as robotics, biosecurity and environmental monitoring to name a few.

We have reviewed some of the most significant research contributions towards the improvement of neuromorphic vision, auditory and olfactory sensors. The distinctive properties of neuromorphic sensors, such as sparse data output and low power consumption have led to extensive research and commercialization. The concept of developing neuromorphic sensors by emulating neuro-biological sensing in silicon has been progressing for many years. More recently, path-breaking research in biological sensing has provided an impetus to developments in neuromorphic sensing, especially in vision and auditory sensors. Pioneering contributions such as DVS and DAVIS, and AEREAR2 have provided considerable progress towards a sensor design that simulates neuro-biological vision and auditory sensing. Accordingly, these have led to the development of several applications for these sensors aiming at replacing conventional sensors in vision and audition. What is lacking is research that provides benchmarks for olfactory sensor implementation and its performance evaluation. Subsequently, future development in neuromorphic sensing should focus on the correlation of inputs from different sensors and efficient pre-processing. With this review we have identified challenges for future research on neuromorphic olfaction, building on the advancements made in vision and audition. In addition to neuromorphic olfaction, future research directions should target neuromorphic sensing of parameters such as pressure, vibration, thermal and magnetic field as well as their inter-correlated sensor fusion functions which would be ideal for applications such as the Internet of Things (IoT).

CHAPTER 4. METHODOLOGY

As discussed in the literature review, neuromorphic sensors utilize the biological concept of spike-based communication. These sensors are interfaced to a PC through USB or DAQ to perform output data analyses. The application of neuromorphic sensors in standalone autonomous systems is restricted due to its reliance on computers as processing units. The prime focus of this research is to devise a digital interfacing methodology by utilizing established protocols. The proposed methodology aims to eliminate the use of a computer and simplify the interface between neuromorphic sensors and processing units such as FPGA and microcontrollers.

4.1. ADDRESS EVENT REPRESENTATION

The point-to-point communication between biological neurons is carried out by firing spikes that are called 'action potentials'. An essential component of these spikes is their spike timing, which is responsible for a typical neuronal behaviour to a stimulus. For example, when a sharp or a hot object is touched, the spikes generated by the tactile sensors and the timing of these spikes are responsible for a rapid response to the stimulus. AER is a spike-based communication technology, inspired from biological action potentials [92]. Although AER was first implemented in Carver Mead's lab at Caltech, it was effectively utilized for the first time in the implementation of DVS and AEREAR [11]. These asynchronous spikes represent crucial information such as the address of a source neuron, address of the destination neuron and the spike timing. A schematic representation of AER is given below in Figure 4.1.

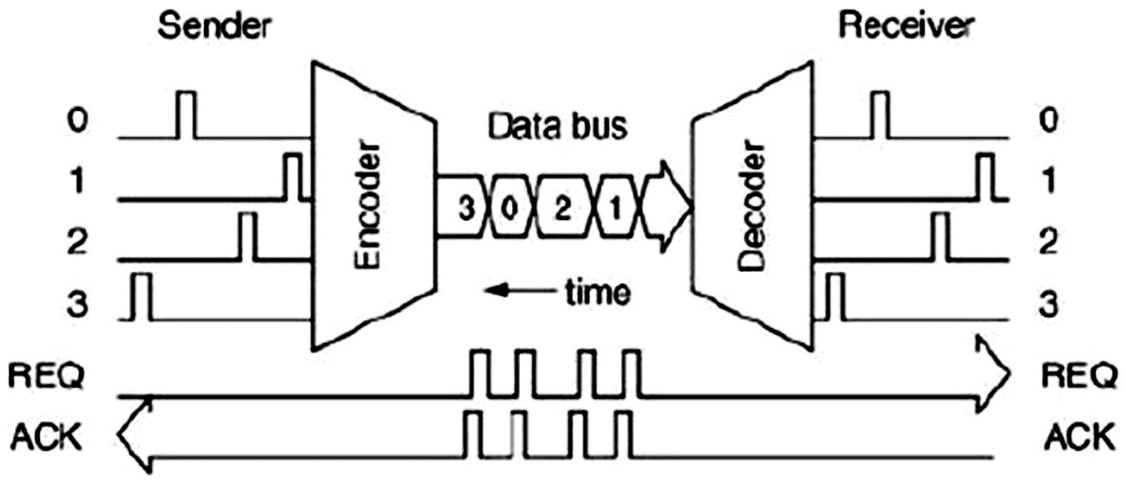

Figure 4.1. Conceptual diagram of working of AER (Adapted from [11])

4.1.1. PRINCIPLE OF OPERATION

A biological neuron fires at a rate of 1-10 Hz. When thousands and millions of neurons in a cluster spike, the spiking rate reaches about 1 KHz to low MHz range. The high speed of data transmission in silicon supports simultaneous transmission of action potentials from clusters of neurons. The operation principle of AER takes advantage of the inherent properties of digital implementation, to communicate the address of a neuron in a network by using an encoder at the source. A decoder is used at the receiving end, and appropriate synapses are therefore stimulated. This is accomplished using dedicated AER circuits that are embedded in most of the neuromorphic electronic systems. The AER circuits are responsible for both, multiplexing (or demultiplexing) the spikes generated by (or delivered to) an array of individual neurons. The address of the firing neuron is produced on the output transmission channel with a time-stamp that indicates the timing when the spike was generated. A neuron identifier is allocated to an address-event while transmitting the spike. This ensures that the inter-arrival time between spikes is preserved.

As neurons in a cluster spike asynchronously, multiple neurons can have the same firing time. Potential collision handling is accomplished by using arbitration techniques [18]. Demultiplexing circuits are used at the destination to decode the spike address at the destination. The input spike is scanned for an axon identifier by an asynchronous decoder and delivered to the relevant destination. The data received at the axons is further reported to the connected neurons. The implementation of self-timed AER encoders and decoders ensures that the inter-arrival time delay among the spikes is preserved during the transmission from source to destination [108, 109].

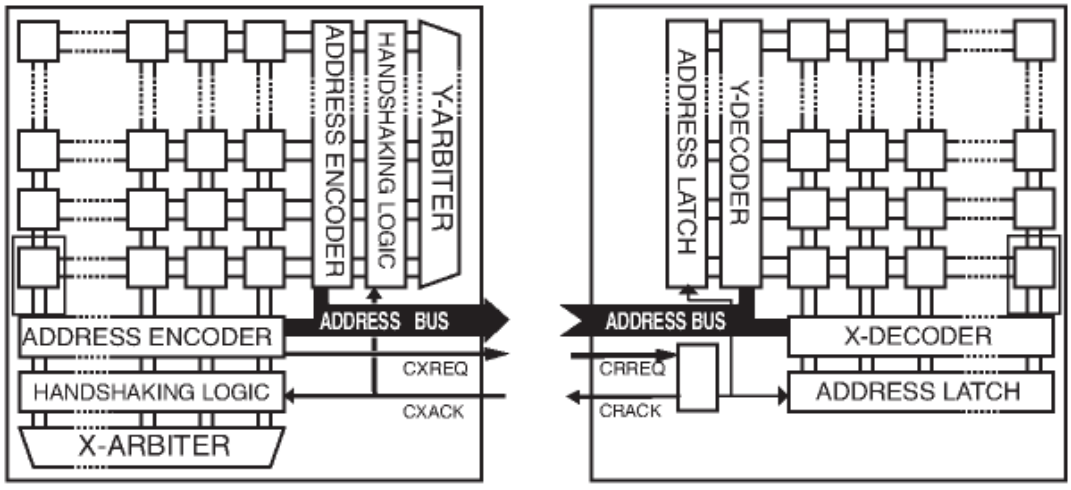

Figure 4.2. AER sender and receiver architecture (Adapted from [12])

4.1.2. APPLICATION OF AER FOR THIS PROJECT

This project is focused on interfacing neuromorphic vision, auditory and olfactory sensors with digital neuromorphic circuits. The physical and electrical protocol of AER supports single-sender/single-receiver architecture to establish a dedicated AER link for each sensor in this application [109]. The sensors will communicate with only one node i.e. the neuromorphic processing board. An address mapping function is required to appropriately deliver the output spikes of a neuron 'n' to an address 'a.' As the focus of this project is to develop a simplified standalone system, the functionality of the neuromorphic processing board will be hard-coded. Thus, any complexity related to programming the connectivity or maintaining an address translation table will be eliminated. The output spikes of these sensors will be directly delivered to the corresponding neurons of a neuromorphic processing chip. A standard 15 bit AER bus [12] will be used for this project.

4.2. PROPOSED APPROACH

It is necessary to identify appropriate sensors and neuromorphic processing boards that can support rapid-prototyping and AER interfacing to devise a simplified interfacing methodology. This section explains the selection criteria for sensors and processing boards.

4.2.1. FPGA BOARD SELECTION REQUIREMENTS

Recent advances in neuromorphic processing have resulted in the development of sophisticated processing boards under large-scale projects such as CAVIAR [10], BrainScaleS [9], and SpiNNaker [8]. These massively-parallel spike-based development boards are applied in various sensing-processing-learning-actuating systems. These digital neuromorphic circuits have thousands of silicon neurons and millions of synapses to perform large-scale synaptic operations. Such large-scale neural processing units support simulation of large-scale spiking neural networks, sensor-specific applications, scalable massively parallel systems [110].

Features such as on-board FPGA, multi-processor architecture, external memory interfacing and on-board learning unit have improved the performance of these neuromorphic circuits. An important criteria for the selection of an appropriate FPGA board for this project is multi-device support for connectivity over AER interface. Other inclusions such as USB

interface, on-board microcontroller, and PC independent operation are also necessary to implement the proposed interface.

4.2.2. AER SWITCH BOARD AS AER MULTIPLEXER/DEMULTIPLEXER

The implementation of CAVIAR project included the development of several AER-based processing boards that provided these functionalities. The AER SWITCH [10] is a board with five AER ports that support input-output operations. This board supports AER interfacing with up to four input devices and one output device with basic bit manipulation for input channel identification. The AER SWITCH is based on a Xilinx 9500 CPLD FPGA.

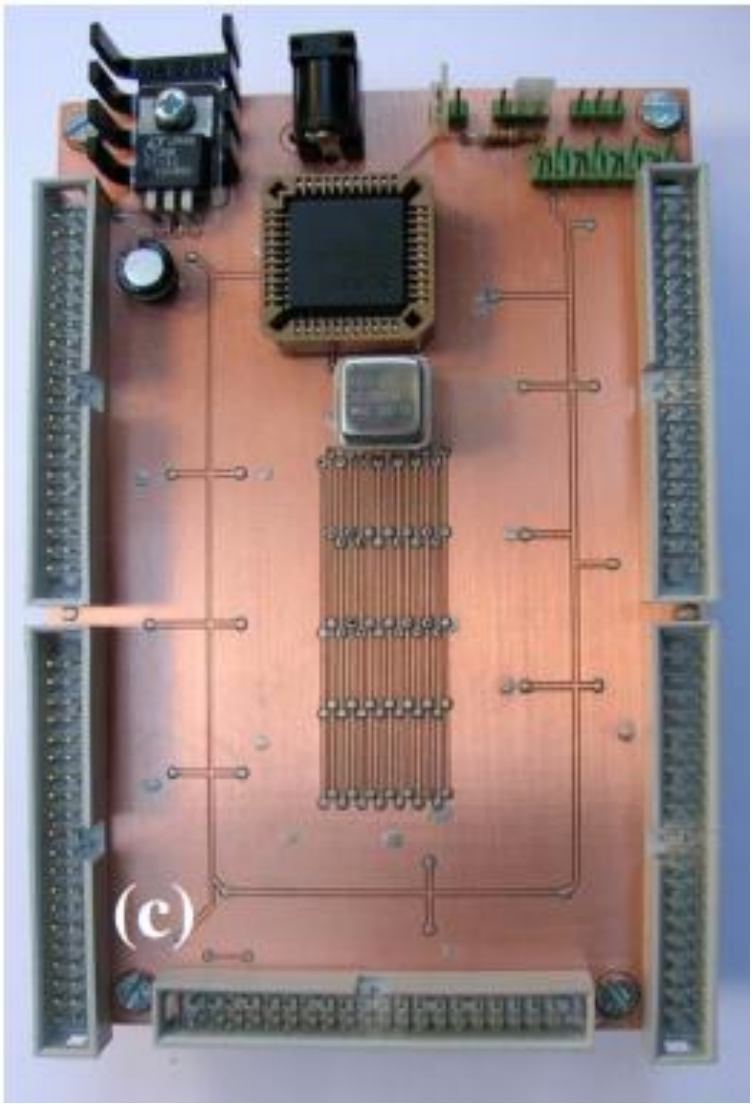

Figure 4.3. AER-SWITCH board (Adapted from [10])

4.2.3. USB-AER BOARD AS PROCESSING UNIT

The functionality of the AER SWITCH board is limited to AER data routing, therefore AER data processing cannot be executed on this board. The USB-AER board developed under CAVIAR project provides interfacing and processing configurations. This board is based on Spartan II 200 FPGA with an on-board C8051F320 USB microcontroller, which makes this board fully reconfigurable [10]. The two AER ports on this board (one input and one output) supports AER data traffic of up to 25 Mega events per second (Meps). The functionality of standalone mode operation by using MMC/SD (Memory Management Controller/Secure Digital) card for loading firmware appears to be the most appropriate board to use as a processing and learning unit. Other functionalities supported on USB-AER board are: (1) remapping of AER addresses by implementing a lookup table (AER mapper) (2) storing and time stamping events for offline AER data analysis and processing (AER data logger) (3) reproducing time-stamped events in real-time (AER data player).

Figure 4.4. USB-AER board (Adapted from [10])

A block diagram representation of the proposed processing module is as follows:

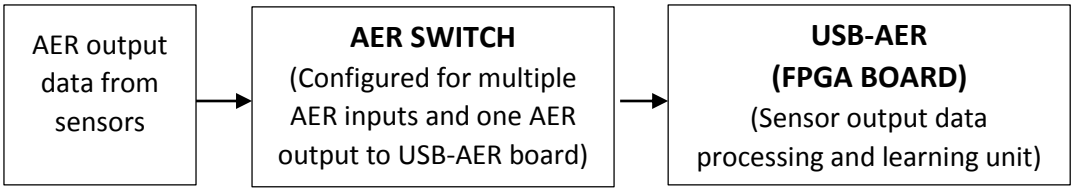

Figure 4.5. A block diagram representing the connection between AER-SWITCH and USB-AER

4.2.4. SENSOR SELECTION REQUIREMENTS

The recent developments in understanding biological sensory systems have inspired different approaches and design architectures to implement neuromorphic sensors. The application of neuromorphic concepts in electronic sensing are steadily evolving from simple aVLSI designs and laboratory experiments to commercially viable products. Thus, it is necessary to define the functional requirements for this project to facilitate appropriate selection of sensors. The FPGA board and AER adapter board selected for this project support AER interfacing using the standard 40-pin CAVIAR connectors only. So, it is crucial that the sensors support standard 40-pin CAVIAR connectors. An implicit requirement for the sensors to be used in this project is the spike-based output. Sensors with standard AER protocol, mentioned in [12], are more suitable for this project. Other functional requirements for selection of sensors are, organised bit-wise AER output data format, commercially tested performance, on-board pre-processing and sparse output data.

4.2.5. INTERFACING OF VISION SENSOR

Among the commercially available neuromorphic vision sensors, the DVS and the DAVIS are the most widely used. These sensors provide both, AER and USB interface to extend their connectivity to standalone devices and computers. The AER interface on both the sensors follows a standard 15-bit AER data format. However, the AER interface of the DVS is a parallel AER implementation that transmits the data in a single operation. Such an implementation is called Simple AER protocol [109]. The DVS128 PAER [111] is a commercial sensor part of the DVS prototype family and that uses 15 bit simple AER protocol where bits 14 down-to 8 denotes the Y address of spiked pixels; bit 7 down-to 1 denote the X address of spiked pixels, and bit 0 is used as a polarity bit [112]. Features such as simple AER interfacing, direct connection pin layout and compact and portable makes this vision sensor most suitable for this research.

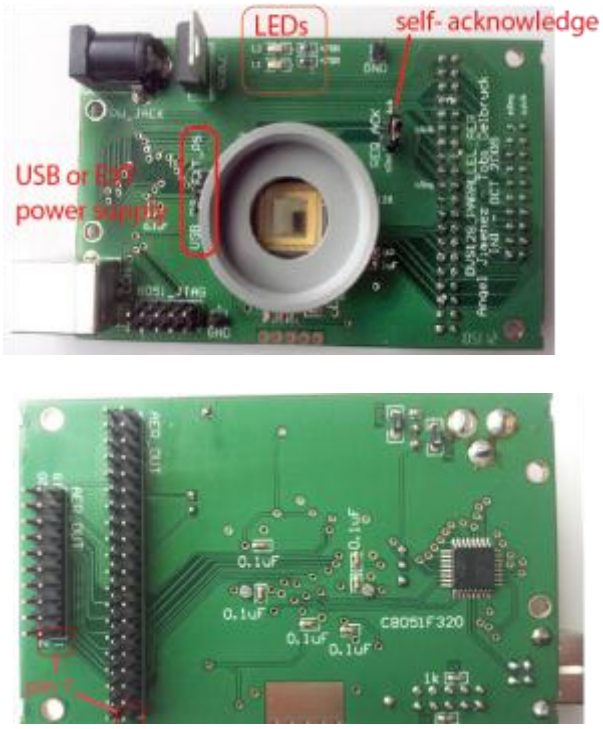

Figure 4.6. DVS128 PAER commercial vision sensor based on DVS pixel design (Adapted from [111])

The specifications of the DVS128 PAER sensor match the requirements of this project. The 40 pin standard AER interface on the rear side of DVS128 PAER can be directly connected to AER SWITCH by using a standard 40 pin CAVIAR connector [108]. Thus, the standalone system can be provided with a vision sensor.

Figure 4.7. Interfacing of neuromorphic vision sensor with USB-AER FPGA board

4.2.3. INTERFACING OF AUDITORY SENSOR

DAS1, also known as AEREAR2, is a commercially available neuromorphic auditory sensor from iniLabs Zurich. The paper [1], describes the design and implementation of this device in detail. The simple AER protocol implemented on DAS1 is similar to DVS128 PAER, except for the AER bus width, which in this case is 10 bits [113]. Bits 9 and 8 represent the spiking neuron, bits 7 down-to 2 denote the channel, bit 1 denotes left/right ear, and bit 0 is used to specify the filter type [112].

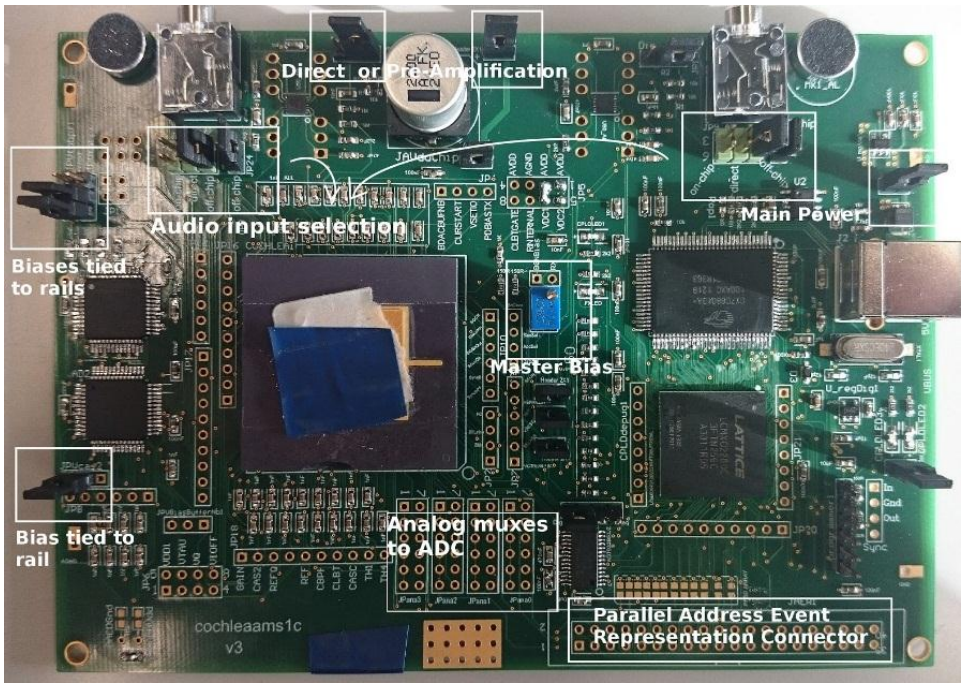

Figure 4.8. DAS1 commercial neuromorphic auditory sensor (Adapted from [113])

The supportive features of DAS1 such as the simplified AER interfacing, the wide application scope (e.g. localisation), the low-power consumption and the binaural structure make this sensor suitable for a standalone system. As the pin layout of both, DAS1 and DVS128 PAER is based on parallel AER connectors, standard CAVIAR AER connector is used to interface DAS1 with AER SWITCH.

Figure 4.9. Interfacing of neuromorphic auditory sensor with USB-AER FPGA board

4.2.4. INTERFACING OF OLFACTORY SENSOR

A neuromorphic olfactory sensor mentioned in [77] is a CMOS chip implementation that provides spike-based output data stream over a data acquisition interface. The olfactory sensor developed in [88] utilizes neuromorphic concepts to generate an output in the form of a 2D signature of the target gas. Usually, these sensors are connected to a PC over a data acquisition interface for output data analysis. The inclusion of PC as a processing unit restricts the use of olfactory sensors in standalone portable systems.

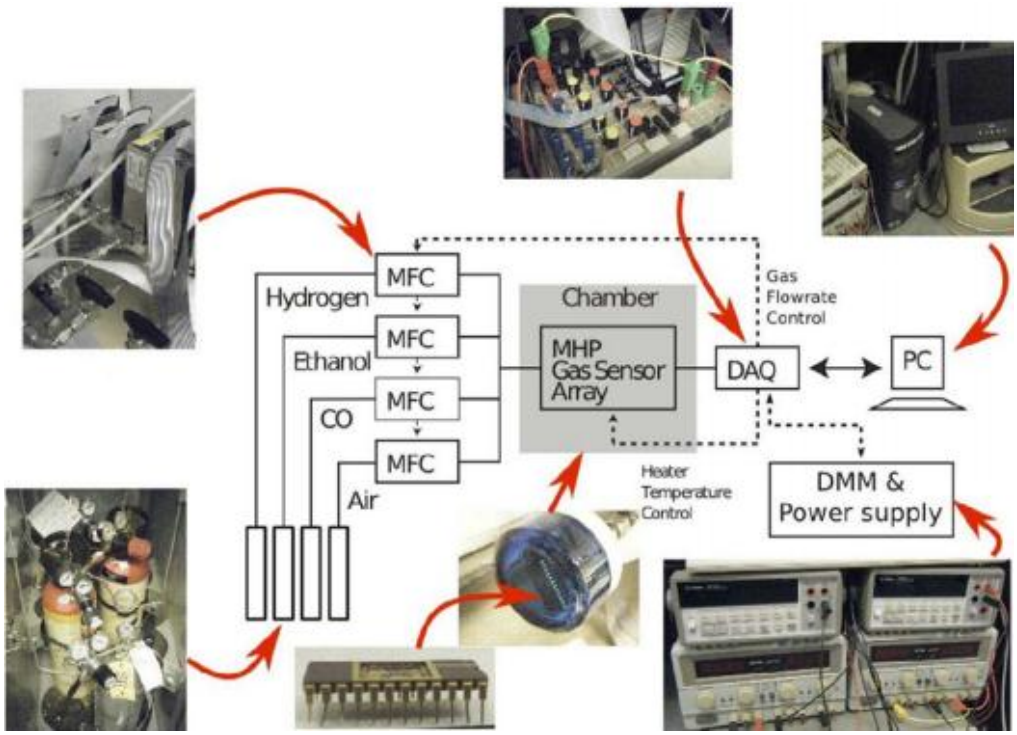

Figure 4.10. Typical interfacing method for CMOS olfactory sensor in [114]

After further investigation on interfacing methods, it was found that the neuromorphic olfactory sensor described in [77] provides a spike-based output over a standard AER interface. Similarities between the format of the output data and the interface enable the connection of this sensor to other neuromorphic devices using AER bus. Thus, the AER SWITCH board can be used to connect this olfactory sensor to the USB-AER FPGA board. A high-level block diagram for this connection is given below.

Figure 4.11. Interfacing of neuromorphic olfactory sensor with USB-AER FPGA board using AER SWITCH board

4.3. SUMMARY

This chapter showed how the neuromorphic sensors are connected to the digital neuromorphic processing hardware. The spike-based output of these sensors is transmitted through an AER interface. The data is processed as per the input stimuli and programmed instructions. The synaptic weight changes are monitored in order to implement learning

algorithms. The processed data can be relayed to a simple digital computing device such as a microcontroller that can further control actuators and activate other control circuits. These functionalities are implemented using digital logic. A block diagram of the proposed approach is given in Figure 4.12.

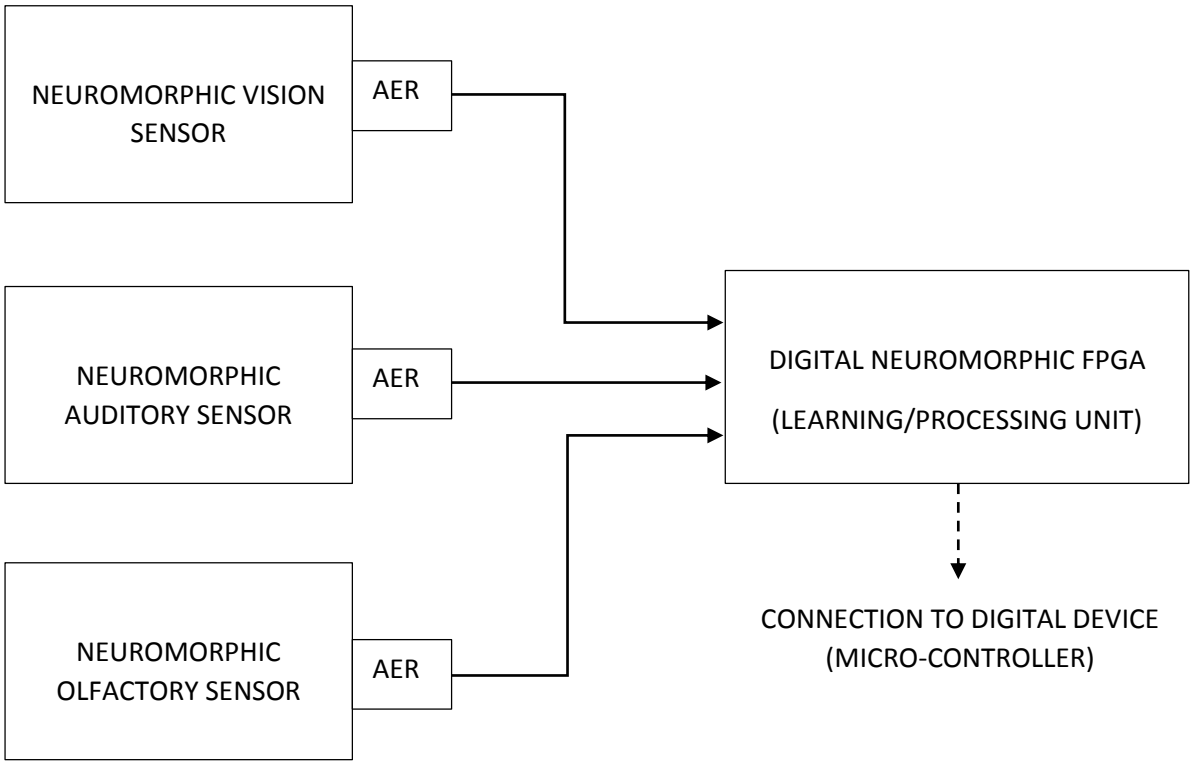

Figure 4.12. Block diagram of the proposed interfacing method

The proposed approach enables interfacing of neuromorphic sensors with a digital neuromorphic FPGA such as the CAVIAR USB-AER FPGA board with CAVIAR AER SWITCH as an intermediate layer for AER mapping. This reconfigurable neuromorphic FPGA board processes the sensory data and manipulates it in application of the learning algorithm. It then relays the output to the connected control device. This approach makes the use of neuromorphic sensors in a standalone autonomous system possible, for example, by interfacing sensors such as [105] [107] [77].

CHAPTER 5. JAVA SIMULATION AND MODELLING

In the previous chapter, we proposed a methodology to establish an interface between the neuromorphic vision, auditory and olfactory sensors and digital neuromorphic circuitry. A cost-efficient way to determine the working of this methodology is by emulating the functionality of the proposed interface in a programming environment.

Most of the popular simulation tools in neuromorphic engineering are developed in JAVA because of the availability of several mathematical and data representation packages and open-source licencing. Easy data acquisition from external hardware and real-time processing abilities have encouraged the development of specialized AER tools in JAVA such as jAER [115]. jAER was initially developed to allow USB interfacing and output data analysis of DVS and AEREAR. Later, functionalities of jAER were extended to allow interfacing and output data analysis of DAVIS, ATIS, AEREAR2 and most of the AER devices with a USB interface. The prime focus of JAVA modelling for this research is to demonstrate the viability and application of the proposed interfacing methodology.

5.1. JAVA BASED MODEL OF OLFACTORY SENSOR

The interfacing methodology proposed in Chapter 4 can be applied for any neuromorphic sensor that provides a spike-based output through AER interface. However, for simulation and modelling, we have focused on emulating the output from an olfactory sensor, similar to the implementations mentioned in [77] and [88]. The simulation starts with a supervised learning process to assign sensitivity of a sensor array element for a particular gas; learning data is collected from the user and stored. The neuron class is designed in JAVA to monitor multiple parameters such as spike timing and learning data. Random sensor arrays are selected to replicate detection of multiple gases. The output data processing on the FPGA board is implemented as a JAVA function that plots a graph of changing gas concentration by comparing the sensor output data with the learning data. A correct graph proves that by relaying digital AER data from a neuromorphic sensor to an FPGA, we can eliminate the requirement of a PC for data computation and analysis.

The olfactory system structure for this simulation is inspired from [88] and designed as an 8 × 8 sensor array. Each sensor element is assumed to be an ORN that is sensitive to a

specific gas. These ORNs are implemented as an array of buttons that can be selected to assign the learning data. The sensor array of 64 ORNs is shown in Figure 5.1.

Figure 5.1. ORN sensor array panel for JAVA simulation system

The simulation window comprises 4 panels: 1) Control panel – includes the title of simulation, control buttons (Next, Simulate and Exit) and display messages. 2) Sensor array panel – includes 8 × 8 sensor array. 3) Output data panel – displays the spike-based sensor output data in the form of address events. 4) Graph panel - plots a graph of changing gas concentrations based on output data processing.

The simulation window is shown in Figure 5.2.

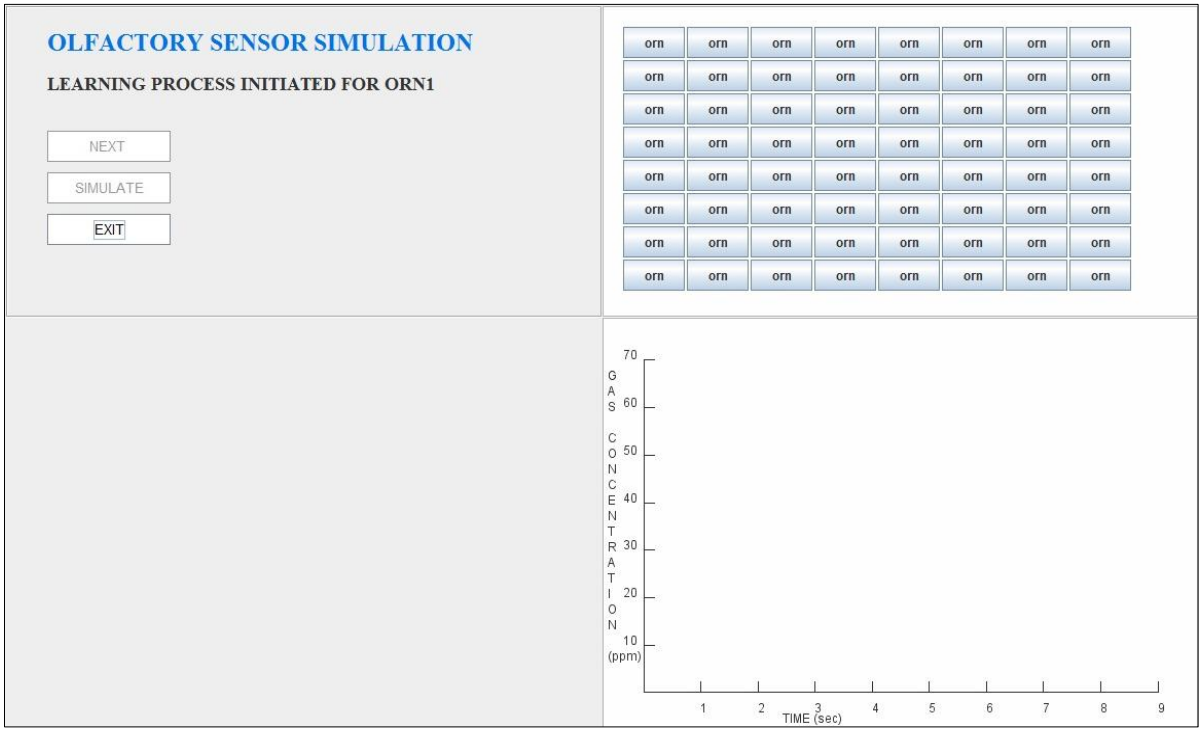

Figure 5.2. JAVA simulation system window

The supervised learning process for this simulation is implemented by requesting the user to specify the sensitivity of an ORN to a particular gas. Currently, this model supports storage of learning data for four gases. When the simulation is started, the user is asked to select ORNs that are sensitive to gas 1. The selection of ORNs will enable the button and changes its colour to red. The sensor element is now named ORN1. Figure 5.3 shows the selected ORNs for gas 1.

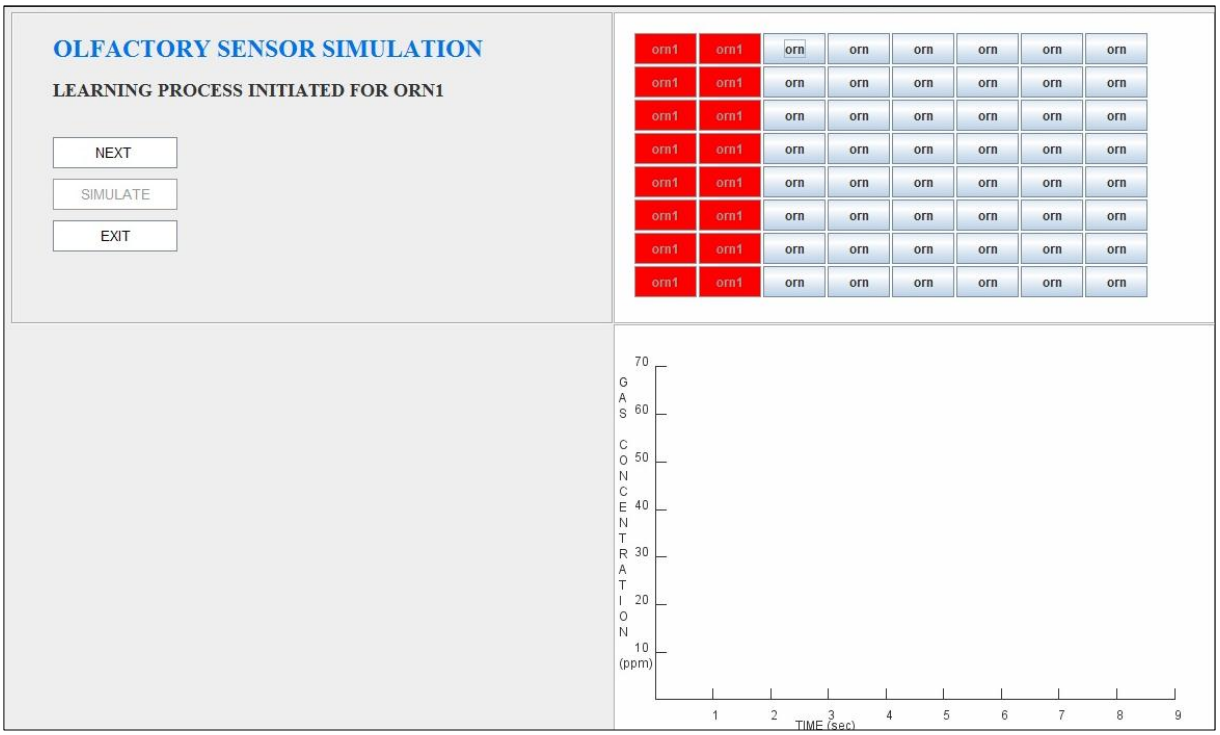

Figure 5.3. Selection of ORN for supervised learning for gas1

Any number of ORNs can be assigned to represent sensitivity to a specific gas. It is necessary for the user to select at least one array element to enable the 'NEXT' button and proceed with the simulation. Subsequently, the user can select ORNs for gas 2 and 3. The ORNs selected for gas 2 are highlighted in blue colour and the ORNs for gas 3 are highlighted in green colour. The remaining ORNs are auto-selected to be sensitive to gas 4 and highlighted in orange colour. This selection of ORNs and assignment of sensitivity constitutes the learning data. The supervised learning method requires the user to specify and monitor the learning data which is implemented here. Such learning algorithms are stored onboard when implemented in hardware on FPGA. Figure 5.4 to Figure 5.6 show learning processes for gas2, gas3 and gas4.

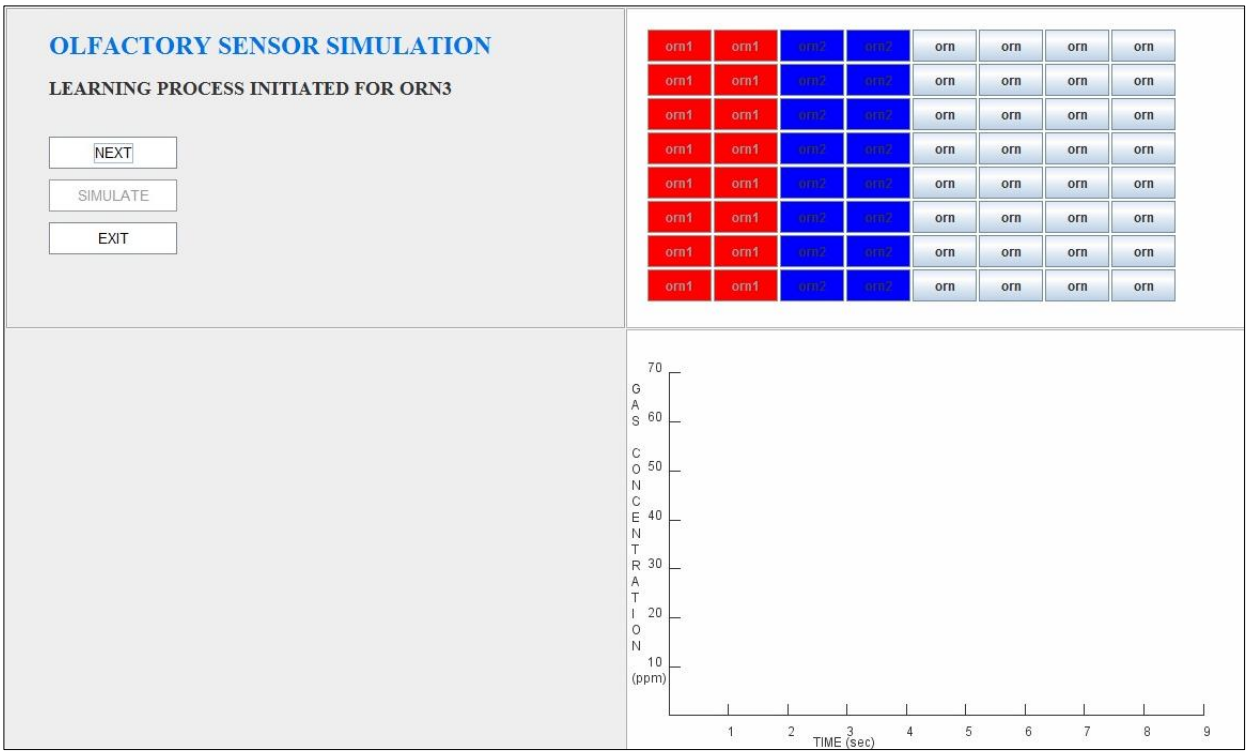

Figure 5.4. Selection of ORN for supervised learning for gas2

The supervised learning process for gas 3 is shown in Figure 5.5. 16 ORNs are selected to demonstrate sensitivity to gas 3 and are highlighted in green colour.

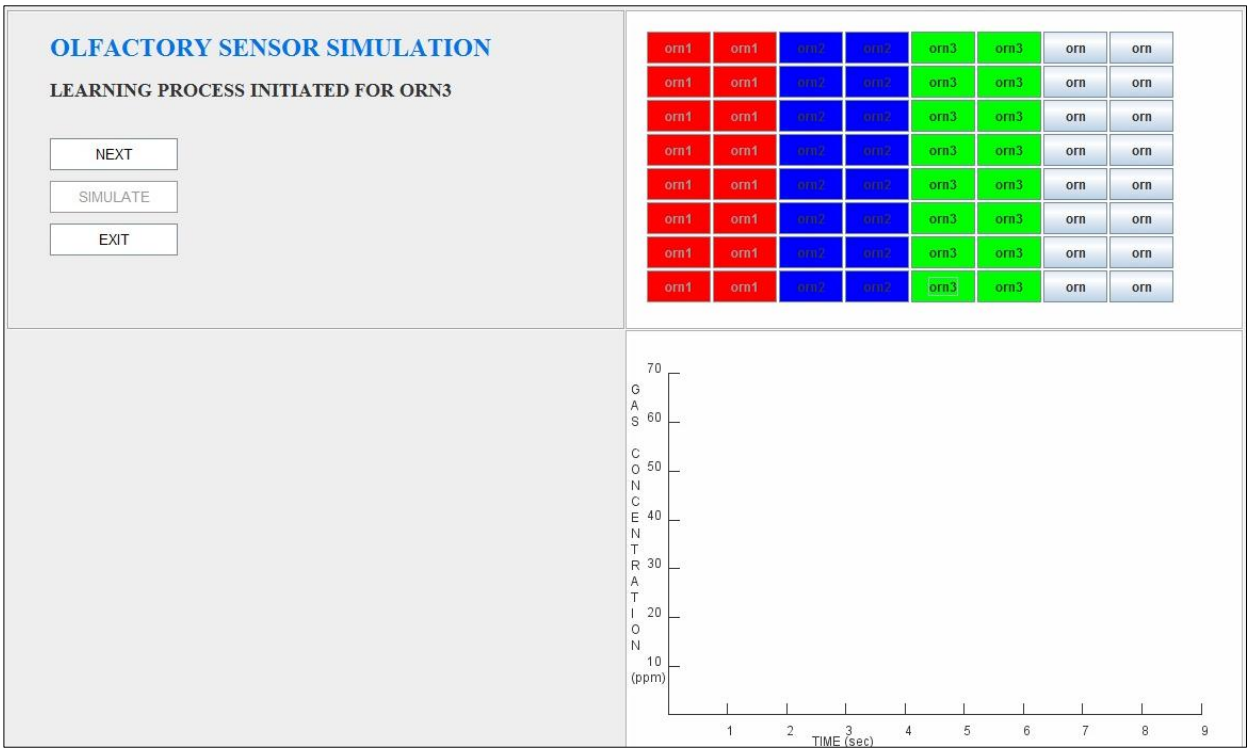

Figure 5.5. Selection of ORN for supervised learning for gas3

As shown in Figure 5.6, the sensitivity of remaining ORNs is automatically allocated to gas 4. These ORNs are highlighted in yellow colour.

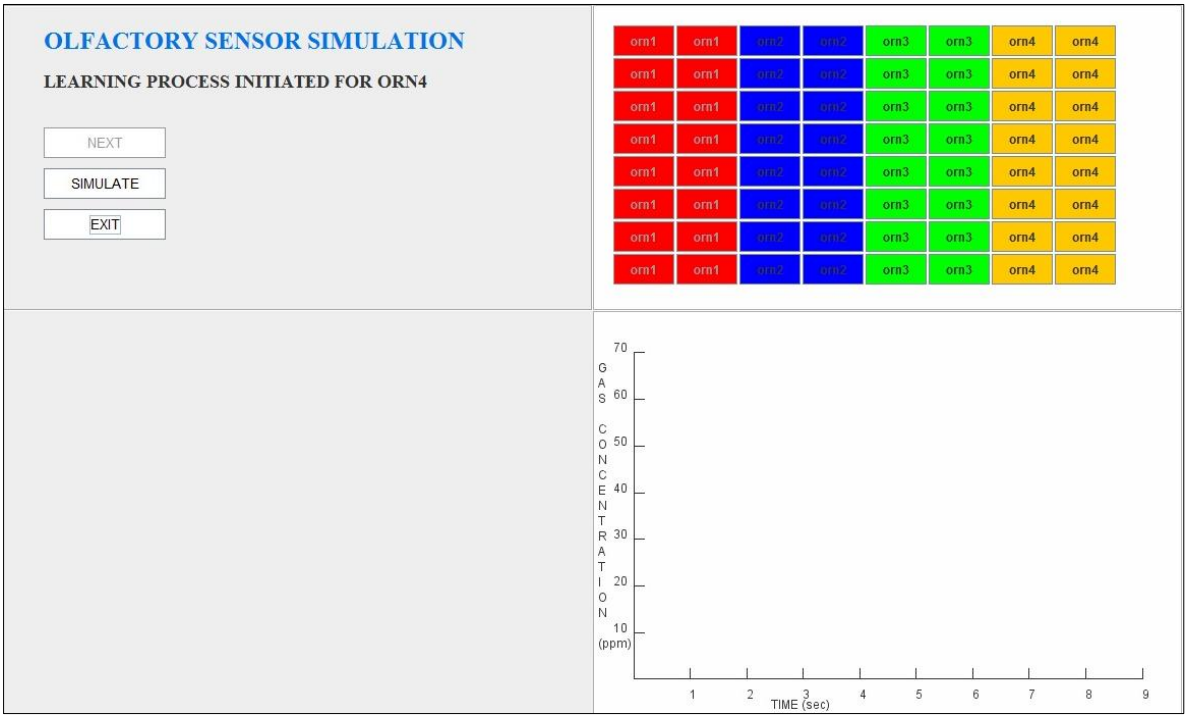

Figure 5.6. Selection of ORN for supervised learning for gas4

The aim of this simulation is to demonstrate the interfacing of neuromorphic sensors with digital neuromorphic processors. The methodology proposed in chapter 4, describes the neuromorphic vision, auditory and olfactory sensors that provide a spike-based output over an AER interface. Such an output represents the addresses of neurons that have spiked due to the occurrence of an event. Hence, an AER mapping function, a learning algorithm and an appropriate data manipulation and control logic should be implemented on neuromorphic FPGA board to process the spike-based output data.

The gas concentration graph and the output spike data are the two key elements that constitute the result of this simulation. The supervised learning process in the simulation is analogous to the implementation of the learning algorithm on USB-AER FPGA board. The output spike data displayed in the spike data panel signifies that the ORNs selected were compared to the learning data to identify the detected gas. Considering the result of the simulation (at time = 9 secs) shown in Figure 5.11, the number of ORNs spiked for each gas is appropriately displayed under the spike address in Figure 5. 7. This proves that the learning function is implemented correctly.

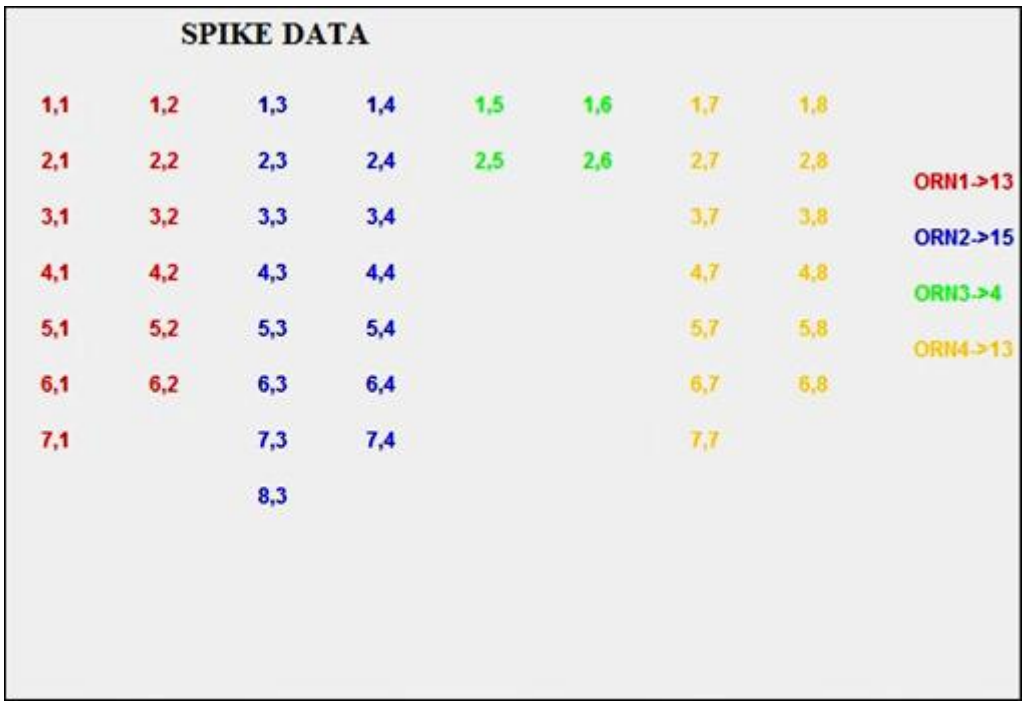

Figure 5. 7. Output spike data at time=9 sec

The computation principle implemented in this function depends on the parameters such as spike timing and learning data. The result of this computation represents the concentration of a specific gas at an instance. This is represented graphically by plotting a graph of varying concentration of gases against time. A graph based on the spike data at time = 9 sec is shown in the Figure 5. *8*.

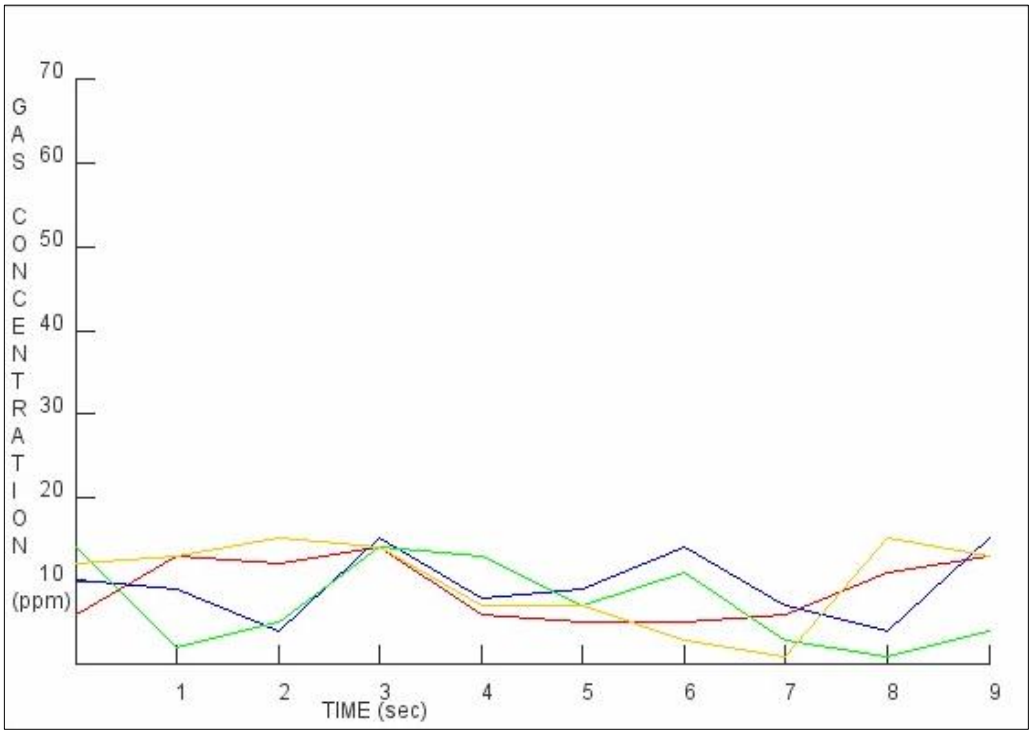

Figure 5. 8. Gas concentration graph at time=9 sec

5.2. SIMULATION AND RESULT ANALYSIS

After the supervised learning process is completed, the 'SIMULATE' button is enabled, and the model is ready to accept spike data for computation. In an olfactory sensor, sensor array elements are activated when their sensitive, volatile compounds are detected. This is replicated by random activation of array elements at an interval of 1 second to emulate the detection of changing gas concentrations. The random function of array elements is handled by JAVA engine and does not involve any manual intervention. The addresses of activated (spiked) ORNs are passed as parameters to the supervised learning function. The working principle of spike-based communication is adopted by studying the implementation of AER in neuromorphic sensors and the AER SWITCH board.

The spike addresses are analysed and compared with the learning data to identify the gas sensitivity of the spiked ORNs and the change in concentration of that gas. The concentration of a gas in this simulation is denoted by the number of spiked ORNs for that specific gas at that instance. Thus, change in concentration of a gas is computed by determining the increase/decrease in the number of spiked ORNs for that gas over a period. The spike data, along with the number of activated ORNs for each gas is displayed in the bottom-left panel. The change in concentration with respect to time is plotted in the form of a graph. It is assumed that each sensor element is capable of detecting 1ppm for a specific gas. As shown in Figure 5. *9*, the simulation starts with initial values at time=0 sec.

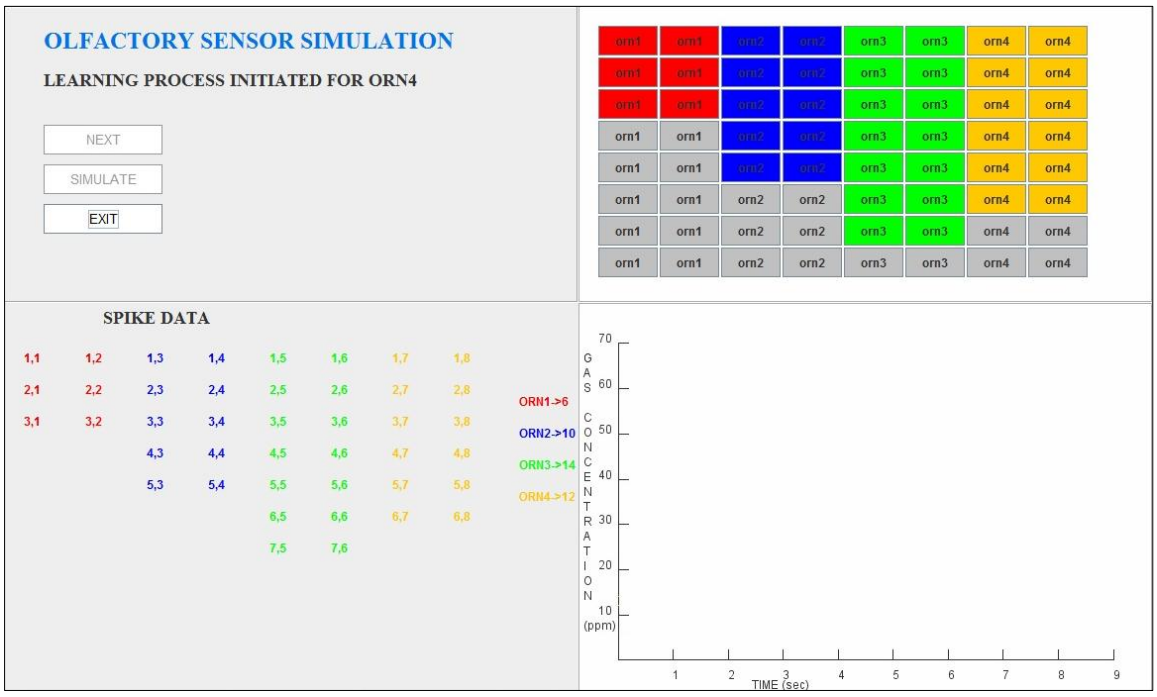

Figure 5. 9. Initial values for simulation. Simulation at time=0 sec

Figure 5.10 shows the state of the simulation system at a time interval of 5 sec.

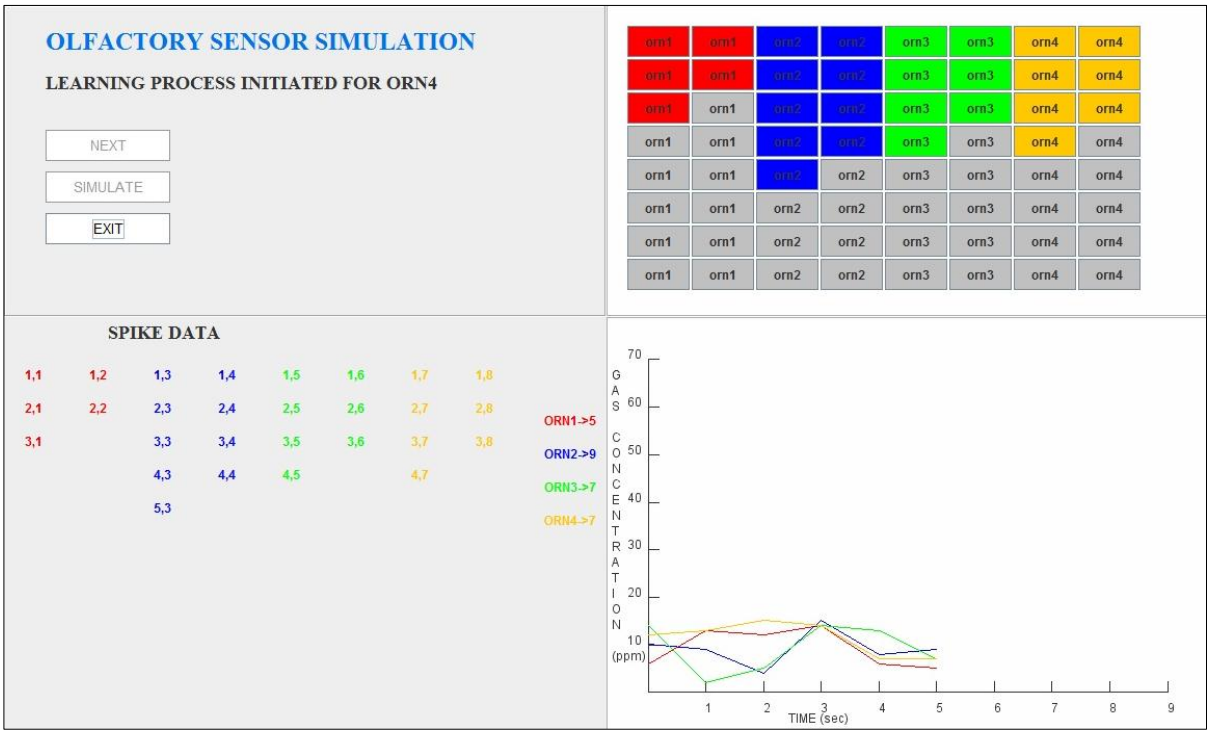

Figure 5.10. Simulation at time=5 sec

Figure 5.11 shows the simulation results with the graph representing gas concentrations and output spike data at time = 9 secs.

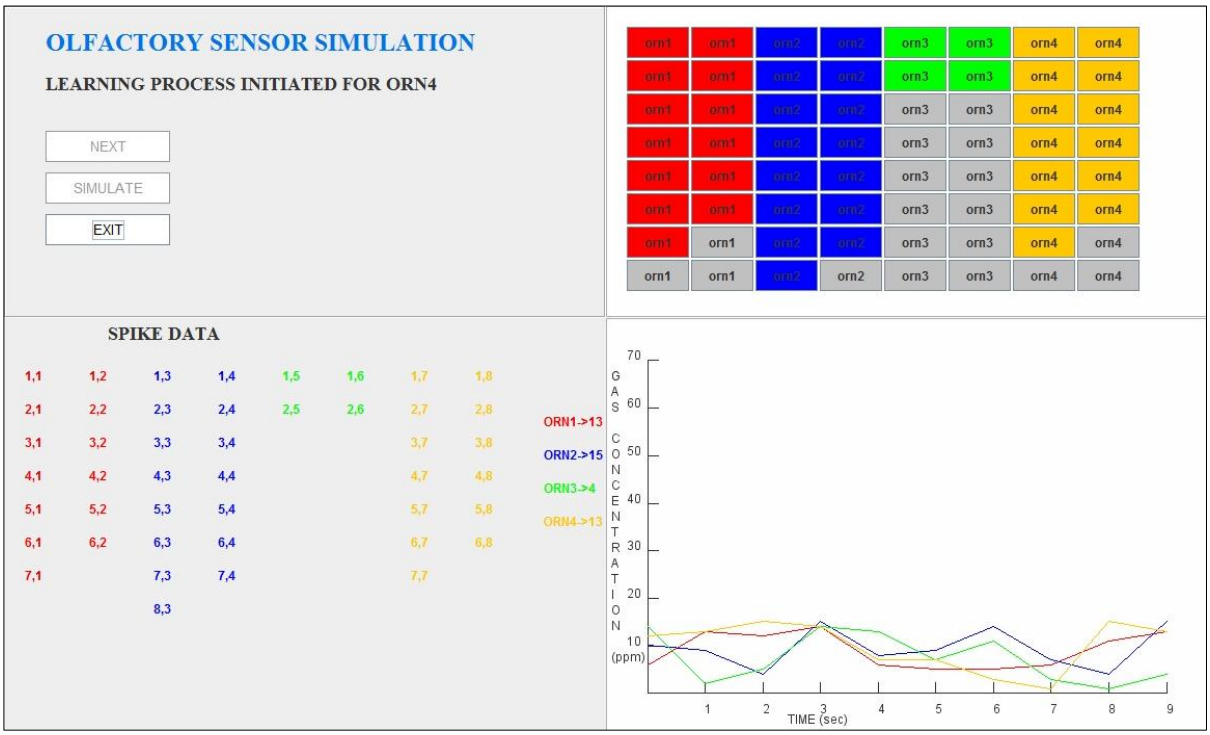

Figure 5.11. Simulation at time=9 sec

The results obtained from this simulation can be validated by comparing the number of ORNs selected by the JAVA engine at an instance with the corresponding graph value. This data is shown in a tabular format below.

TIME (SEC)	ORNs SELECTED FOR GAS1	GRAPH VALUE FOR GAS1	ORNs SELECTED FOR GAS2	GRAPH VALUE FOR GAS2	ORNs SELECTED FOR GAS3	GRAPH VALUE FOR GAS3	ORNs SELECTED FOR GAS4	GRAPH VALUE FOR GAS4
0	6	6	10	10	14	14	12	12
5	5	5	9	9	7	7	7	7
9	13	13	15	15	4	4	13	13

Table 5. 1 Validation of simulation results at different time instances

The coherent data in the above table confirms that the results of the simulation model are correct and error-free. For example, at time = 0 sec, the random number of ORNs for gas 1 generated by JAVA engine is equivalent to the graph reading, i.e. 6. The digital format of the output spike data is preserved throughout the simulation as the spike-data is passed as parameters to different functions without any conversions. This proves that the proposed interface can be implemented in hardware as mentioned in section 4.3. The representation of activated sensor elements in AER format, digital processing of the AER data, implementation of the supervised learning process and emulation of an olfactory system output are some of the highlights of this model.

As the prime focus of this research is to demonstrate digital interfacing, the functionality of an olfactory sensor is implemented in a simple form. However, the functions and classes of this simulation model can be reused to plot a similar concentration graph when an external olfactory sensor is interfaced to a PC. These properties provide a foundation for an olfactory system simulation and testing software and can be further enhanced for doctoral studies.

5.3. COMPARISON WITH NENGO SIMULATION MODEL

A comparison with a standard simulation tool can help to identify the pros and cons of the JAVA simulation model. Nengo is a neural simulation tool designed at the University of Waterloo, Canada. This tool allows both, graphical and scripting packages to design and

simulate large-scale neural systems. Nengo tools can be used to create ensembles of neurons representing a system, with the ability to alter properties of individual neurons. Synaptic connections between these ensembles allow them to perform a specific computation that can be defined in Nengo workspace. The Neural Engineering Framework is implemented to solve neurological simulation problems in Nengo. The scripting language used for Nengo is Python and the simulation runs on JAVA engine. Nengo has been used in a wide range of neuromorphic designs and dynamic applications like the implementation of complex high-level cognitive algorithms, various learning-based systems, motor control, action selection, working memory and planning with problem solving [116].

To compare the JAVA model with a de-facto standard simulation tool, a simulation for the olfactory system as described in [88] was designed in Nengo. The Nengo simulator graphical tools are used to set up the model. The output generated by an olfactory sensor is modelled as an output vector function. This spike-based output data is provided to an ensemble of 16 Leaky Integrate and Fire (LIF) neurons based on 4 ×4 sensor array design in [88]. The 16 neurons are arranged in a 2-dimensional array; this enables the generation of two controls for the input vector. These controls are used to vary the concentration of two gases with 0 as the minimum value and 1 as maximum.

Nengo provides with numerous tools to represent the simulation output in the form of graphs and spikes. In this simulation, an output graph, a voltage grid of neurons and a spike raster for the system are enabled to represent the computations on an FPGA. The concentration of gases computed by the ensemble of neurons is dynamically represented in the graph. The spike raster displays the spikes generated when the threshold voltage is exceeded. The spike trains can be dense or sparse depending upon the varying input control. A voltage grid shows the 16 neurons with the grey coloured neurons representing threshold voltage and the spiking neurons are represented in yellow.

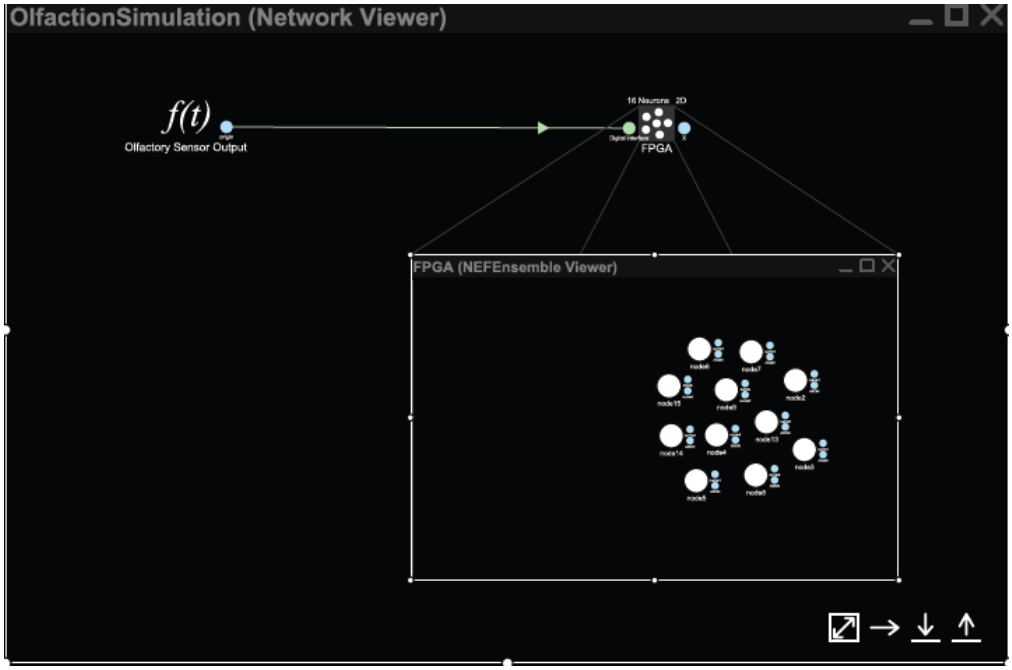

Figure 5. 12. Nengo simulation network with 2D array of 16 neurons

Figure 5. *12* shows the simulation window for the designed Nengo network. The two input controls at the olfactory sensor function are used to vary the value of input function for FPGA, which is analogous to varying the concentration of two gases. Figure 5.13 shows the change in output graph as the concentration of gas 2 is increased. Sparse spike trains are observed depending on the gas concentration exceeding the threshold.

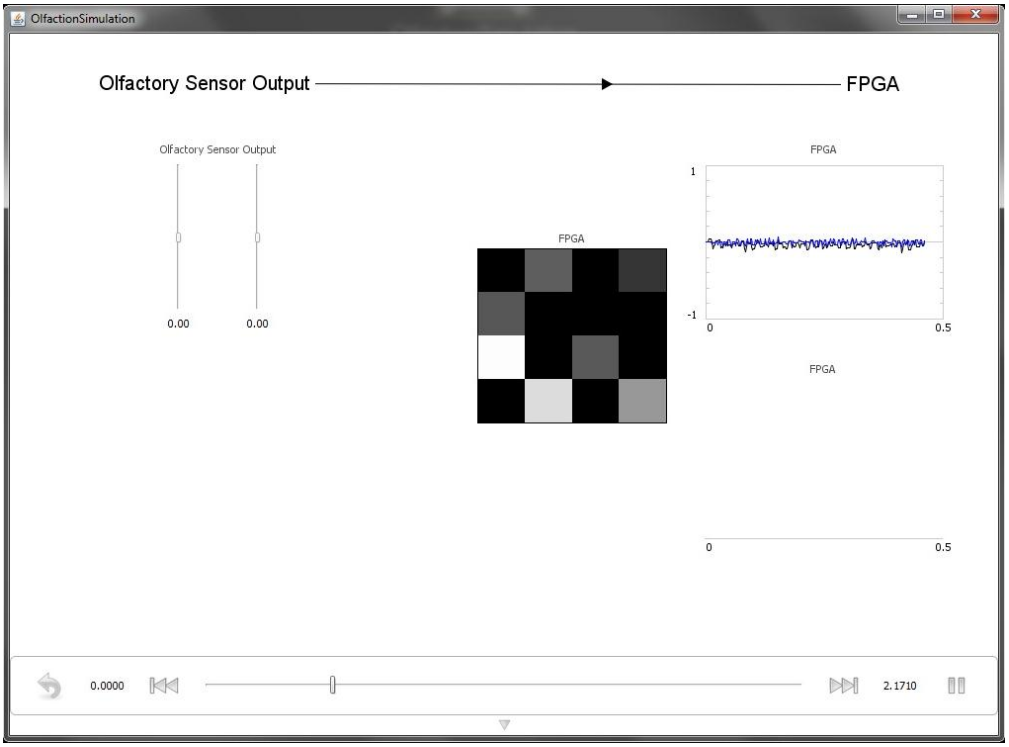

Figure 5.13. Nengo generated simulation window with two controls for concentration of gases as input and voltage grid, output values and spike raster for output

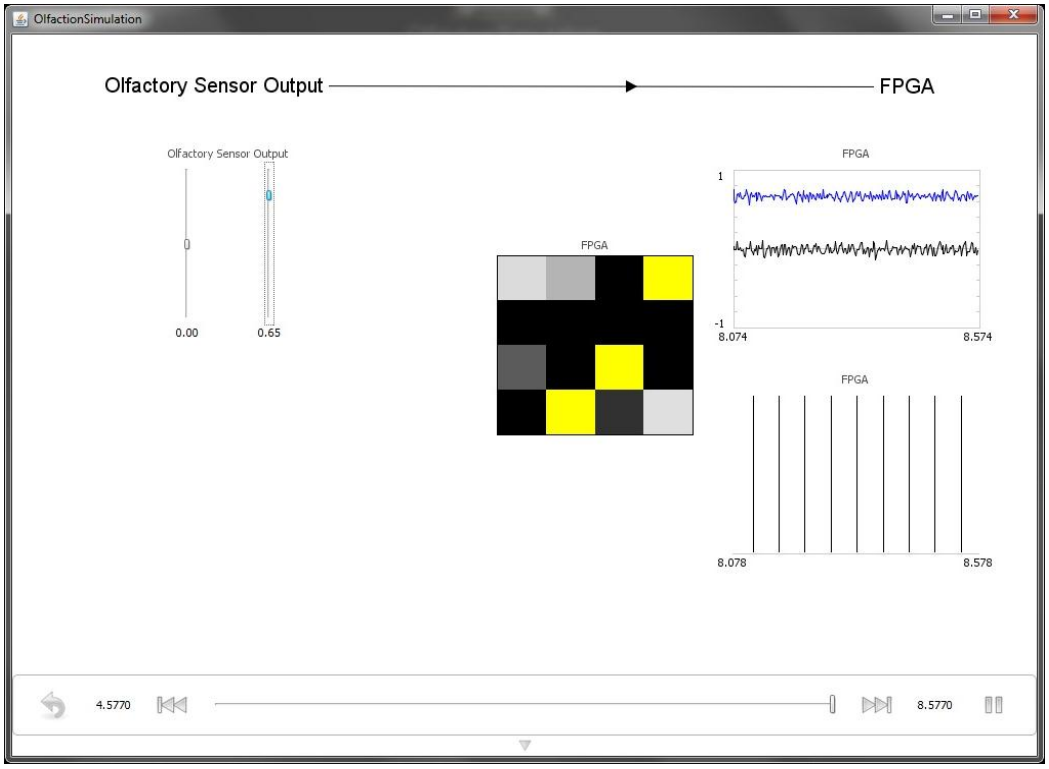

Figure 5.14. Output response for increase in gas2 concentration

Figure 5.14 to Figure 5.16 shows the output values in terms of a graph, a spike raster and a voltage grid for changing input for two gases.

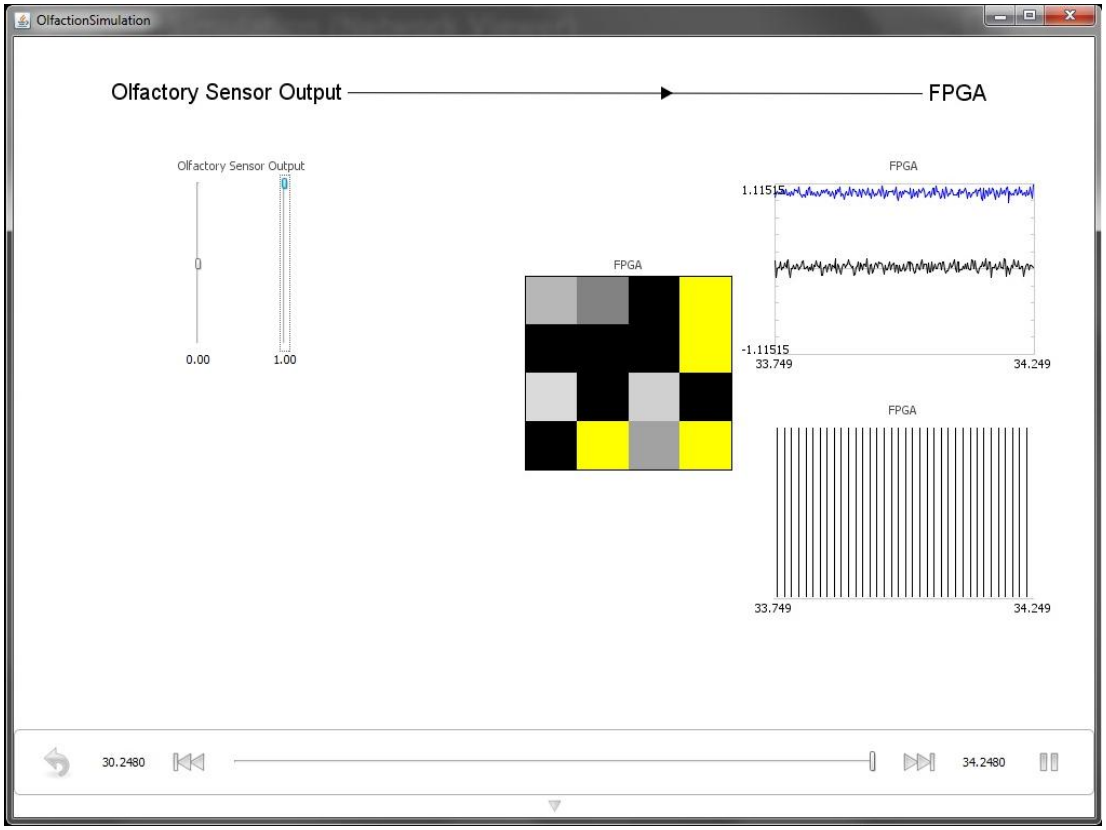

Figure 5.15. Output response for maximum concentration of gas2

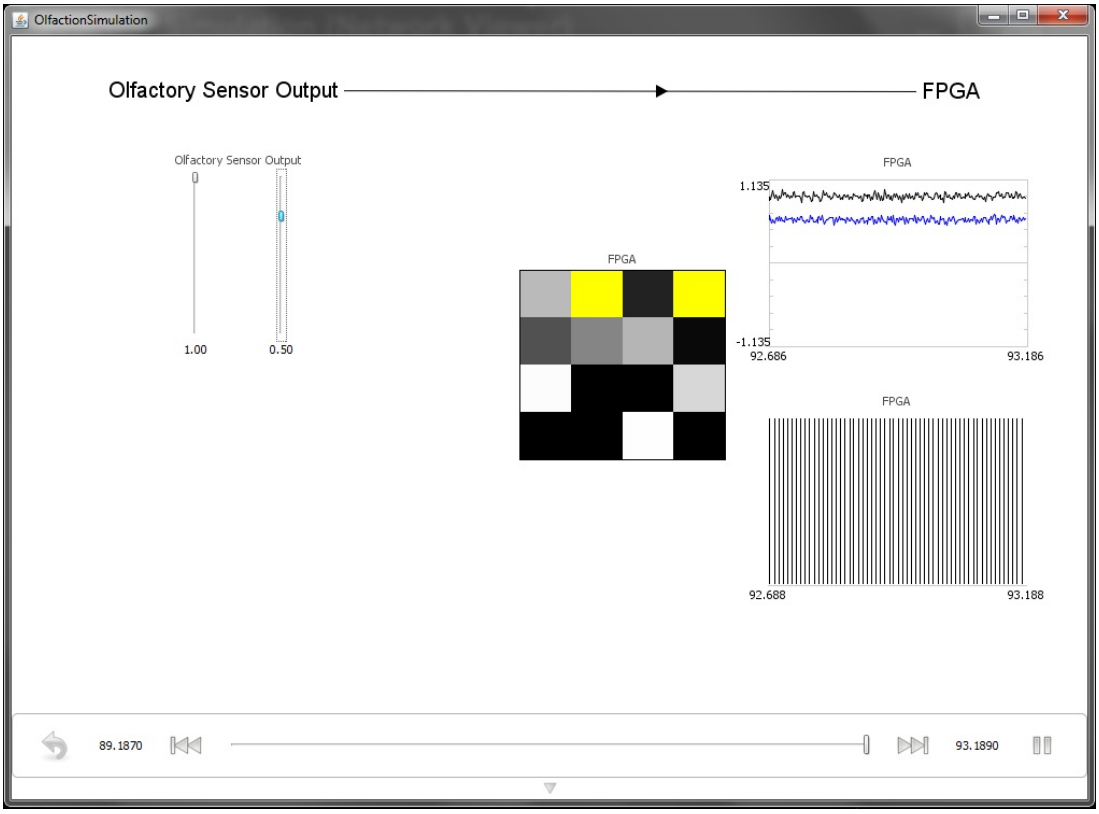

Figure 5.16. Output response for increase in gas concentration of gas1 and gas2

Figure 5.17 shows an overlapping graph when the controls for both gas 1 and gas 2 are brought at a stable value.

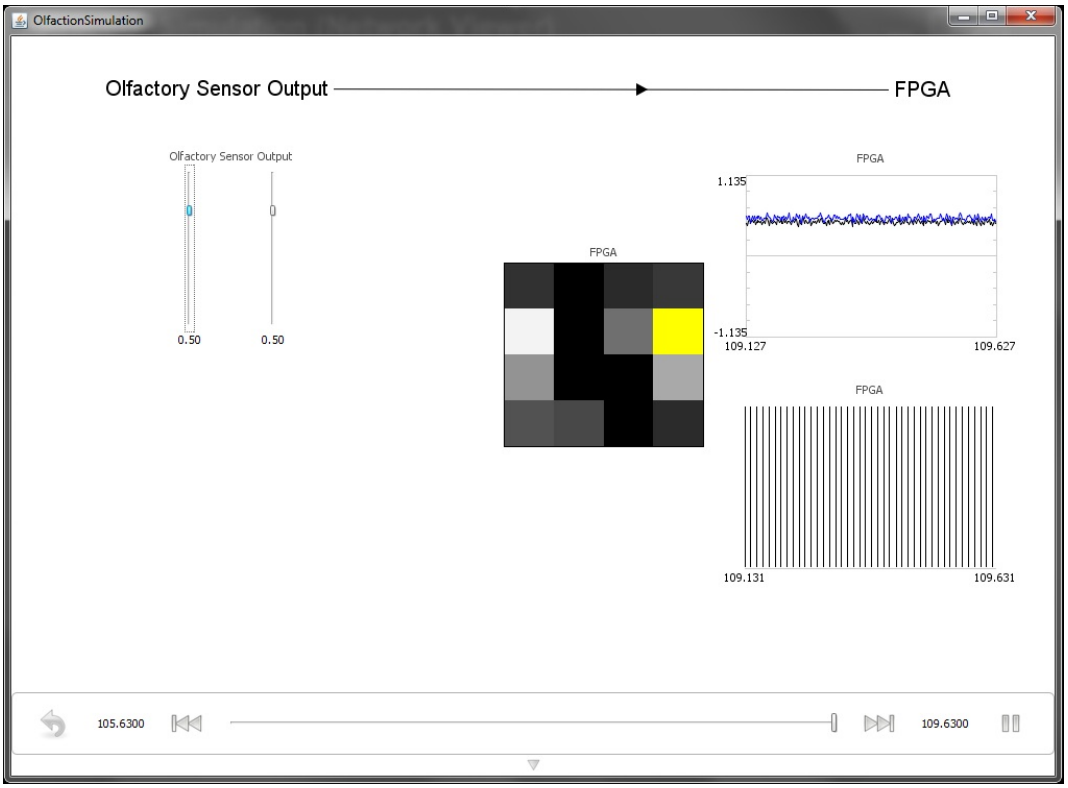

Figure 5.17. Output response for stable concentration of gas1 and gas2

The results of the Nengo simulation model were monitored over three output parameters, a graph, a voltage grid and a spike raster. The simulation demonstrated the effect of the changing values of gas concentrations on the output parameters. Although the changing concentration of gases was correctly depicted through the output graph, the scope of this Nengo simulation environment is limited to detecting the range of concentration level of a gas from maximum to minimum and not in terms of ppm values. Also, there is no provision to monitor the spiking data that can be used for result validation.

The design of simulation models in Nengo requires explicit definition for neuronal behaviour and properties of neuronal systems at an abstraction level of an individual neuron. Thus, system-level simulations are detailed yet they are complex to design which restricts Nengo to a general-purpose neural simulator and cannot be used for specialized systems. The olfactory system described in [88] does not implement highly detailed biological olfactory model but only emulates its essential characteristics. Thus, the parameters such as type of neurons, membrane time constant and the firing rates have been set to default values.

Simplification in the implementation of the learning algorithms and the inclusion of AER data monitor in the JAVA simulation model extends the usability of this simulator for specialized neuromorphic systems. The JAVA model allows implementation of the supervised learning rule and AER based data processing. The design of this model encourages the reuse of several classes and functions for output data processing when an external neuromorphic sensor is connected. These functionalities are not extended in Nengo. Thus, current JAVA implementation provides a promising base for further enhancements such as neuron-level detailing.

CHAPTER 6. CONCLUSION

Neuromorphic engineering is a rapidly evolving discipline that utilises unconventional concepts to solve complex problems related to electronic sensing, data processing and network architectures. This interdisciplinary science takes inspiration from neurobiological architecture to solve these complex problems. Traditional electronic devices that are based on the Von Neumann architecture tend to consume excessive power due to the complex data processing strategies. Electronic sensors based on these principles generate a huge amount of redundant data that increases processing complexity. Over the last decade, extensive research in neuromorphics has produced promising results in sensing, data processing and network technology. With features such as low-power consumption, spike-based data handling and a hybrid implementation with both analogue and digital components, application scope for neuromorphic sensors is steadily widening.

Neuromorphic sensors like DVS, DAVIS, AEREAR2 and [77] [88], have set performance benchmarks in vision, auditory and olfactory sensing. The application of neuromorphic concepts in electronic sensing has assisted in overcoming the drawback of conventional sensors. However, a lack of processing algorithms and dedicated processing units for spike-based output has restricted their potential application in standalone autonomous systems. Current methods of interfacing neuromorphic sensors are dependent on high end computers for output data processing. This dependency has restricted the portability of these sensors, and the inclusion of such a computer as a processing unit also increases the overall cost of the system. Consequently, neuromorphic sensors have not yet made an impact in large-scale industrial applications and are currently utilised only in limited areas.

This research started with a focus on simplifying the interface between neuromorphic vision, auditory and olfactory sensors and digital neuromorphic circuits. An important aspect of this research was to preserve the digital format of the spike-based data throughout data transmission and processing. Thus, AER, a specialised communication protocol for neuromorphic sensors was used. Sensors such as DVS, DAVIS and AEREAR2 provide an AER interface that can be exploited to establish direct connectivity to a neuromorphic FPGA board. In recent years, several efficient multi-function digital neuromorphic processing boards under projects such as SNAP, BrainScaleS, SpiNNaker and CAVIAR were designed.

The proposed methodology utilises digital neuromorphic processing boards designed under the project CAVIAR. One of the main goals of this research was to explore possible methods for sensor fusion. Thus, AER SWITCH board that supports connection with multiple AER devices and AER mapping functionalities is used to connect the sensors. After careful consideration of features such as sensor output format, compatibility and interfacing abilities the sensors chosen for this research are: DVS128-PAER for vision, DAS1 for audition and the CMOS adaptive sensor described in [77] for olfaction. The AER SWITCH communicates sensor output to a USB-AER FPGA board that acts as the processing unit for this standalone system. This method for interfacing promotes sensor fusion in a standalone autonomous system based on neuromorphic concepts.

The methodology proposed in this thesis is a theoretical solution and must be tested for its viability in a real-time application. The digital interface of these sensors with a neuromorphic processing unit is simulated using JAVA. This simulation emulated the olfactory sensor output in the form of spike addresses and processed the spike data using JAVA classes and supervised learning techniques. The digital format of the data was preserved, and processed results were plotted in the form of graphs that denote a change in concentration for four gases. Assuming that the neuromorphic processing implemented in this simulation emulates the behaviour of a neuromorphic FPGA board, we can expect similar interfacing in hardware to deliver the correct results. Nengo, a de-facto standard neural simulation tool, was used to design a similar model for validation and comparison. The JAVA model forms a strong foundation for future enhancements and can be reused for output data processing of an external olfactory sensor.

Thus, the main research question of simplifying the interface between neuromorphic sensors and neuromorphic processors has been answered in this thesis through a detailed methodology. Along with simplification of the interface, this research has contributed towards:

- The development of a platform to implement neuromorphic sensor fusion and output data correlation.
- Extending the portability of the neuromorphic sensors by eliminating the dependency on computers for output data processing.
- As a result, these sensors can be easily incorporated in intelligent systems for standalone operation.

- The cost of processing spike-based output data can be reduced drastically and the application scope for these sensors can be extended.
- The JAVA simulation developed to verify the methodology, provides a strong foundation for further research in neuromorphic olfaction systems with spiking output.

6.1. APPLICATION

The neuromorphic sensors, particularly, the DVS, DAVIS, AEREAR2 have been tested and applied in their specialised scope of application. For example, neuromorphic vision sensors like DVS and DAVIS have been widely used for applications such as particle tracking. Similarly, AEREAR2 has shown promising results for localisation applications. However, it has been observed that very few implementations such as [105-107] have taken advantage of sensor fusion and output correlation. Furthermore, these implementations require MATLAB for analysis and processing. Thus, such systems are dependent on desktop computers for processing which impedes their portability.

By applying the interfacing methodology proposed in this thesis, multiple neuromorphic sensors can be connected to a digital neuromorphic processor to form a standalone autonomous system. Such a technique boosts portability for neuromorphic sensors and enables easy deployment in intelligent embedded systems and Internet of Things (IoT). Specifically in this project, we proposed an interface for DVS128PAER (vision), DAS1 (auditory) and a neuromorphic CMOS olfactory sensor with digital neuromorphic FPGA board. The low-power consumption and self-calibrating structure based learning architecture can be exploited to design solar powered embedded systems to be deployed in hostile regions. These systems can also be used extensively in industrial robotics and robots used in rescue operations. This type of sensor fusion in an intelligent embedded system will be well-suited for biosecurity and environmental monitoring applications.

6.2. FUTURE DIRECTIONS

During the literature review, it was observed that substantial research has been conducted in neuromorphic vision and auditory sensing. Sensors like DVS, DAVIS and AEREAR2, are widely accepted as benchmarks in neuromorphic vision and audition.

However, research in neuromorphic olfaction is still in its infancy, and there are very few implementations that have contributed towards setting a specific benchmark in this field. Neuromorphic olfactory sensing is implemented as a system and comprises several sub-systems such as sensor array, signal conditioning circuitry and a pattern recognition algorithm.

The neuromorphic olfactory sensors developed in [77] and [88] have provided promising results for further research to improve their performance. The olfactory sensor chip described in [77] emulates multiple features of the biological olfactory system and includes on-board signal conditioning circuitry and STDP learning. As pointed out by Koickal et.al further research in "long term weight storage, component mismatch, layout optimization and decoding of spike outputs" should be considered to improve the overall performance of the chip [77]. Yamani et.al designed an olfactory system that implements a spike latency coding structure to generate a unique sequence of spikes from the sensor array [108]. Further improvements would be targeted towards easy interfacing of the sensor in a stand-alone system and increasing the number of ORNs per glomeruli with minimum complexity. A continuation of this project will be aimed towards implementing an olfactory system with a research focus on providing an AER interface and determining efficient pattern recognition technique for such systems.

The JAVA simulation model designed for this research project can be enhanced to include STDP learning rather than supervised learning rules. The properties and real-time behaviour of the olfactory sensor array can be integrated into the olfactory sensor model. Identification of gases can also be implemented if the olfactory sensor is based on [89] that generates 2D spike signature. Current results have provided a strong base to extend this project for a doctoral scope.

REFERENCES

[1] L. Shih-Chii, A. van Schaik, B. A. Minch, and T. Delbruck, "Asynchronous Binaural Spatial Audition Sensor With 2 × 64 × 4 Channel Output," *Biomedical Circuits and Systems, IEEE Transactions on*, vol. 8, pp. 453-464, 2014.

[2] R. Sarpeshkar, "Brain power - borrowing from biology makes for low power computing [bionic ear]," *Spectrum, IEEE*, vol. 43, pp. 24-29, 2006.

[3] G. Indiveri and T. K. Horiuchi, "Frontiers in neuromorphic engineering," *Frontiers in neuroscience*, vol. 5, 2011.

[4] C. Mead, "Neuromorphic electronic systems," *Proceedings of the IEEE*, vol. 78, pp. 1629-1636, 1990.

[5] R. F. Lyon and C. Mead, "An analog electronic cochlea," *Acoustics, Speech and Signal Processing, IEEE Transactions on*, vol. 36, pp. 1119-1134, 1988.

[6] T. S. Lande, *Neuromorphic systems engineering: neural networks in silicon* vol. SECS 447. Boston: Kluwer Academic, 1998.

[7] T. Delbruck, "Frame-free dynamic digital vision," in *Proceedings of Intl. Symp. on Secure-Life Electronics, Advanced Electronics for Quality Life and Society*, 2008, pp. 21-26.

[8] S. B. Furber, D. R. Lester, L. Plana, J. D. Garside, E. Painkras, S. Temple, *et al.*, "Overview of the spinnaker system architecture," *Computers, IEEE Transactions on*, vol. 62, pp. 2454-2467, 2013.

[9] J. Schemmel, A. Grübl, S. Hartmann, A. Kononov, C. Mayr, K. Meier, *et al.*, "Live demonstration: A scaled-down version of the BrainScaleS wafer-scale neuromorphic system," in *Circuits and Systems (ISCAS), 2012 IEEE International Symposium on*, 2012, pp. 702-702.

[10] R. Serrano-Gotarredona, M. Oster, P. Lichtsteiner, A. Linares-Barranco, R. Paz-Vicente, F. Gómez-Rodríguez, *et al.*, "CAVIAR: A 45k neuron, 5M synapse, 12G connects/s AER hardware sensory–processing–learning–actuating system for high-speed visual object recognition and tracking," *Neural Networks, IEEE Transactions on*, vol. 20, pp. 1417-1438, 2009.

[11] R. Jung, "Neuromorphic Electronic Design," in *Biohybrid Systems*, ed Weinheim, Germany: Wiley-VCH Verlag GmbH & Co. KGaA, 2009, pp. 31-51.

[12] S.-C. Liu, *Event-Based Neuromorphic Systems*: John Wiley & Sons, 2015.

[13] R. Sarpeshkar, "Analog versus digital: extrapolating from electronics to neurobiology," *Neural computation,* vol. 10, pp. 1601-1638, 1998.

[14] C. Mead and M. Ismail, *Analog VLSI implementation of neural systems* vol. 80: Springer Science & Business Media, 2012.

[15] L. S. Smith and A. Hamilton, *Neuromorphic systems: engineering silicon from neurobiology* vol. 10: World Scientific, 1998.

[16] R. J. Douglas, M. Mahowald, and K. A. Martin, "Hybrid analog-digital architectures for neuromorphic systems," in *Neural Networks, 1994. IEEE World Congress on Computational Intelligence., 1994 IEEE International Conference on*, 1994, pp. 1848-1853.

[17] E. Oja, "Simplified neuron model as a principal component analyzer," *Journal of mathematical biology,* vol. 15, pp. 267-273, 1982.

[18] P. Hafliger, "Neuromorphic Electronics," unpublished, 2010.

[19] N. Srinivasa and J. M. Cruz-Albrecht, "Neuromorphic adaptive plastic scalable electronics: analog learning systems," *Pulse, IEEE,* vol. 3, pp. 51-56, 2012.

[20] E. M. Izhikevich, "Which model to use for cortical spiking neurons?," *IEEE transactions on neural networks,* vol. 15, pp. 1063-1070, 2004.

[21] F. Rosenblatt, "Principles of neurodynamics. perceptrons and the theory of brain mechanisms," DTIC Document1961.

[22] R. Douglas, M. Mahowald, and C. Mead, "Neuromorphic analogue VLSI," *Annual review of neuroscience,* vol. 18, pp. 255-281, 1995.

[23] L. Abbott and T. B. Kepler, "Model neurons: From hodgkin-huxley to hopfield," in *Statistical mechanics of neural networks*, ed: Springer, 1990, pp. 5-18.

[24] C. Posch, T. Serrano-Gotarredona, B. Linares-Barranco, and T. Delbruck, "Retinomorphic Event-Based Vision Sensors: Bioinspired Cameras With Spiking Output," *Proceedings of the IEEE,* vol. 102, pp. 1470-1484, Oct 2014.

[25] J. E. Dowling, *The retina: an approachable part of the brain*: Harvard University Press, 1987.

[26] P. Lichtsteiner, C. Posch, and T. Delbruck, "A 128 × 128 120dB 30mW asynchronous vision sensor that responds to relative intensity change," in *Solid-State Circuits Conference, 2006. ISSCC 2006. Digest of Technical Papers. IEEE International*, 2006, pp. 2060-2069.

[27] C. Brandli, R. Berner, Y. Minhao, L. Shih-Chii, and T. Delbruck, "A 240 × 180 130dB 3µs Latency Global Shutter Spatiotemporal Vision Sensor," *IEEE Journal of Solid-State Circuits*, vol. 49, pp. 2333-2341, 2014.

[28] T. Delbruck, "Investigations of analog VLSI visual transduction and motion processing," California Institute of Technology, 1993.

[29] M. A. Mahowald and C. Mead, "The Silicon Retina," *Scientific American*, vol. 264, pp. 76-82, May 1991.

[30] M. Mahowald, *An analog VLSI system for stereoscopic vision*: Springer Science & Business Media, 1994.

[31] C. A. Mead and M. A. Mahowald, "A silicon model of early visual processing," *Neural networks*, vol. 1, pp. 91-97, 1988.

[32] C. Mead, "Adaptive retina," in *Analog VLSI implementation of neural systems*, ed: Springer, 1989, pp. 239-246.

[33] K. A. Zaghloul and K. Boahen, "Optic nerve signals in a neuromorphic chip I: Outer and inner retina models," *IEEE Trans Biomed Eng*, vol. 51, pp. 657-666, 2004.

[34] K. A. Zaghloul and K. Boahen, "Optic nerve signals in a neuromorphic chip II: testing and results," *IEEE Trans Biomed Eng*, vol. 51, pp. 667-675, 2004.

[35] P. Lichtsteiner, C. Posch, and T. Delbruck, "A 128 × 128 120dB 15µs Latency Asynchronous Temporal Contrast Vision Sensor," *IEEE Journal of Solid-State Circuits*, vol. 43, pp. 566-576, 2008.

[36] C. Posch, D. Matolin, and R. Wohlgenannt, "A QVGA 143dB Dynamic Range Frame-Free PWM Image Sensor With Lossless Pixel-Level Video Compression and Time-Domain CDS," *Solid-State Circuits, IEEE Journal of*, vol. 46, pp. 259-275, 2011.

[37] P.-F. Rüedi, P. Heim, F. Kaess, E. Grenet, F. Heitger, P.-Y. Burgi, *et al.*, "A 128 × 128 pixel 120dB dynamic-range vision-sensor chip for image contrast and orientation extraction," *Solid-State Circuits, IEEE Journal of*, vol. 38, pp. 2325-2333, 2003.

[38] U. Mallik, M. Clapp, E. Choi, G. Cauwenberghs, and R. Etienne-Cummings, "Temporal change threshold detection imager," in *ISSCC. 2005 IEEE International Digest of Technical Papers. Solid-State Circuits Conference, 2005.*, 2005.

[39] E. Culurciello and A. G. Andreou, "CMOS image sensors for sensor networks," *Analog Integrated Circuits and Signal Processing,* vol. 49, pp. 39-51, 2006.

[40] X. Qi, X. Guo, and J. G. Harris, "A time-to-first spike CMOS imager," in *Circuits and Systems, 2004. ISCAS'04. Proceedings of the 2004 International Symposium on*, 2004, pp. IV-824-7 Vol. 4.

[41] Q. Luo and J. G. Harris, "A time-based CMOS image sensor," in *Circuits and Systems, 2004. ISCAS'04. Proceedings of the 2004 International Symposium on*, 2004, pp. IV-840-3 Vol. 4.

[42] J. Kramer, "An on/off transient imager with event-driven, asynchronous read-out," in *Circuits and Systems, 2002. ISCAS 2002. IEEE International Symposium on*, 2002, pp. II-165-II-168 vol. 2.

[43] P. Lichtsteiner, T. Delbruck, and J. Kramer, "Improved ON/OFF temporally differentiating address-event imager," in *Electronics, Circuits and Systems, 2004. ICECS 2004. Proceedings of the 2004 11th IEEE International Conference on*, 2004, pp. 211-214.

[44] T. Delbruck and C. A. Mead, "Adaptive photoreceptor with wide dynamic range," in *Circuits and Systems, 1994. ISCAS '94., 1994 IEEE International Symposium on*, 1994, pp. 339-342 vol.4.

[45] T. Delbrück and C. Mead, "Analog VLSI adaptive logarithmic wide-dynamic-range photoreceptor. vol. 4, 339-342. 1994. London," in *1994 IEEE International Symposium on Circuits and Systems*.

[46] P. Lichtsteiner and T. Delbruck, "A 64 × 64 AER logarithmic temporal derivative silicon retina," *Research in Microelectronics and Electronics,* vol. 2, pp. 202-205, 2005.

[47] C. Brandli, T. A. Mantel, M. Hutter, M. A. Hopflinger, R. Berner, R. Siegwart, *et al.*, "Adaptive pulsed laser line extraction for terrain reconstruction using a dynamic vision sensor," *Front Neurosci,* vol. 7, p. 275, 2014-January-17 2013.

[48] D. Drazen, P. Lichtsteiner, P. Häfliger, T. Delbrück, and A. Jensen, "Toward real-time particle tracking using an event-based dynamic vision sensor," *Experiments in Fluids,* vol. 51, pp. 1465-1469, 2011/11/01 2011.

[49] R. Berner and T. Delbruck, "Event-based pixel sensitive to changes of color and brightness," *Circuits and Systems I: Regular Papers, IEEE Transactions on,* vol. 58, pp. 1581-1590, 2011.

[50] T. Serrano-Gotarredona and B. Linares-Barranco, "A 128 × 128 1.5% Contrast Sensitivity 0.9% FPN 3μs Latency 4mW Asynchronous Frame-Free Dynamic Vision Sensor Using Transimpedance Preamplifiers," *Solid-State Circuits, IEEE Journal of,* vol. 48, pp. 827-838, 2013.

[51] R. Berner, C. Brandli, Y. Minhao, L. Shih-Chii, and T. Delbruck, "A 240 × 180 10mW 12μs latency sparse-output vision sensor for mobile applications," in *VLSI Circuits (VLSIC), 2013 Symposium on*, 2013, pp. C186-C187.

[52] S.-C. Liu and T. Delbruck, "Neuromorphic sensory systems," *Current Opinion in Neurobiology,* vol. 20, pp. 288-295, Jun 2010.

[53] P. C. Loizou, "Mimicking the human ear," *Signal Processing Magazine, IEEE,* vol. 15, pp. 101-130, 1998.

[54] R. Sarpeshkar, C. Salthouse, S. Ji-Jon, M. W. Baker, S. M. Zhak, T. K. T. Lu, *et al.*, "An ultra-low-power programmable analog bionic ear processor," *Biomedical Engineering, IEEE Transactions on,* vol. 52, pp. 711-727, 2005.

[55] L. Watts, D. Kerns, R. F. Lyon, and C. Mead, "Improved implementation of the silicon cochlea," *Solid-State Circuits, IEEE Journal of,* vol. 27, pp. 692-700, 1992.

[56] R. Sarpeshkar, R. Lyon, and C. Mead, "A Low-Power Wide-Dynamic-Range Analog VLSI Cochlea," *Analog Integrated Circuits and Signal Processing,* vol. 16, pp. 245-274, 1998/08/01 1998.

[57] T. J. Hamilton, J. Tapson, C. Jin, and A. Van Schaik, "Analogue VLSI implementations of two dimensional, nonlinear, active cochlea models," in *Biomedical Circuits and Systems Conference, 2008. BioCAS 2008. IEEE*, 2008, pp. 153-156.

[58] T. J. Hamilton, C. T. Jin, A. van Schaik, and J. Tapson, "An active 2-d silicon cochlea," *IEEE Trans. Biomed. Circuits and Systems*, vol. 2, pp. 30-43, 2008.

[59] M. W. Baker and R. Sarpeshkar, "A low-power high-PSRR current-mode microphone preamplifier," *Solid-State Circuits, IEEE Journal of*, vol. 38, pp. 1671-1678, 2003.

[60] C. D. Salthouse and R. Sarpeshkar, "A practical micropower programmable bandpass filter for use in bionic ears," *Solid-State Circuits, IEEE Journal of*, vol. 38, pp. 63-70, 2003.

[61] R. Wang, R. Sarpeshkar, M. Jabri, and C. Mead, "A Low Power Analog Front-end Module for Cochlear Implants," 1997.

[62] M. W. Baker, T. K. T. Lu, C. D. Salthouse, S. Ji-Jon, S. Zhak, and R. Sarpeshkar, "A 16-channel analog VLSI processor for bionic ears and speech-recognition front ends," in *Custom Integrated Circuits Conference, 2003. Proceedings of the IEEE 2003*, 2003, pp. 521-526.

[63] A. van Schaik, E. Fragnière, and E. Vittoz, "Improved silicon cochlea using compatible lateral bipolar transistors," *Advances in neural information processing systems*, pp. 671-677, 1996.

[64] A. Van Schaik and S. Shamma, "A neuromorphic sound localizer for a smart MEMS system," *Analog Integrated Circuits and Signal Processing*, vol. 39, pp. 267-273, 2004.

[65] V. Chan, S. C. Liu, and A. van Schaik, "AER EAR: A matched silicon cochlea pair with address event representation interface," *IEEE Transactions on Circuits and Systems I-Regular Papers*, vol. 54, pp. 48-59, Jan 2007.

[66] T. Yu, A. Schwartz, J. Harris, M. Slaney, and L. Shih-Chii, "Periodicity detection and localization using spike timing from the AER EAR," in *Circuits and Systems, 2009. ISCAS 2009. IEEE International Symposium on*, 2009, pp. 109-112.

[67] C.-H. Li, T. Delbruck, and S.-C. Liu, "Real-time speaker identification using the AEREAR2 event-based silicon cochlea," in *Circuits and Systems (ISCAS), 2012 IEEE International Symposium on*, 2012, pp. 1159-1162.

[68] T. J. Koickal, R. Latif, L. Gouveia, E. Mastropaolo, S. Wang, A. Hamilton, *et al.*, "Design of a spike event coded RGT microphone for neuromorphic auditory systems," in *Circuits and Systems (ISCAS), 2011 IEEE International Symposium on*, 2011, pp. 2465-2468.

[69] J. W. Gardner and P. N. Bartlett, *Electronic noses: principles and applications* vol. 233: Oxford University Press New York, 1999.

[70] J. Covington, S. Tan, J. Gardner, A. Hamilton, T. Koickal, and T. Pearce, "Combined smart chemFET/resistive sensor array," in *Sensors, 2003. Proceedings of IEEE*, 2003, pp. 1120-1123.

[71] T. C. Pearce, S. S. Schiffman, H. T. Nagle, and J. W. Gardner, *Handbook of machine olfaction: electronic nose technology*: John Wiley & Sons, 2006.

[72] R. L. Doty, *Handbook of olfaction and gustation*: John Wiley & Sons, 2015.

[73] K. C. Persaud, S. Marco, and A. Gutiérrez, *Neuromorphic olfaction*. Boca Raton, FL: CRC Press, 2013.

[74] B. Raman, J. L. Hertz, K. D. Benkstein, and S. Semancik, "Bioinspired Methodology for Artificial Olfaction," *Analytical Chemistry,* vol. 80, pp. 8364-8371, 2008/11/15 2008.

[75] K. Persaud and G. Dodd, "Analysis of discrimination mechanisms in the mammalian olfactory system using a model nose," 1982.

[76] T. Pearce, "Computational parallels between the biological olfactory pathway and its analogueThe Electronic Nose': Part II. Sensor-based machine olfaction," *Biosystems,* vol. 41, pp. 69-90, 1997.

[77] T. J. Koickal, A. Hamilton, T. Su Lim, J. A. Covington, J. W. Gardner, and T. C. Pearce, "Analog VLSI Circuit Implementation of an Adaptive Neuromorphic Olfaction Chip," *Circuits and Systems I: Regular Papers, IEEE Transactions on,* vol. 54, pp. 60-73, 2007.

[78] S.-W. Chiu and K.-T. Tang, "Towards a Chemiresistive Sensor-Integrated Electronic Nose: A Review," *Sensors*, vol. 13, p. 14214, 2013.

[79] T. C. Pearce, C. Fulvi-Mari, J. Covington, F. S. Tan, J. W. Gardner, T. J. Koickal, *et al.*, "Silicon-based neuromorphic implementation of the olfactory pathway," in *Neural Engineering, 2005. Conference Proceedings. 2nd International IEEE EMBS Conference on*, 2005, pp. 307-312.

[80] T. J. Koickal, A. Hamilton, S. L. Tan, J. Covington, J. Gardner, and T. Pearce, "Smart interface circuit to ameliorate loss of measurement range in chemical microsensor

arrays," in *Instrumentation and Measurement Technology Conference, 2005. IMTC 2005. Proceedings of the IEEE*, 2005, pp. 548-550.

[81] J. W. Gardner, P. K. Guha, F. Udrea, and J. A. Covington, "CMOS Interfacing for Integrated Gas Sensors: A Review," *Sensors Journal, IEEE,* vol. 10, pp. 1833-1848, 2010.

[82] H. Hung-Yi and T. Kea-Tiong, "VLSI Implementation of a Bio-Inspired Olfactory Spiking Neural Network," *Neural Networks and Learning Systems, IEEE Transactions on*, vol. 23, pp. 1065-1073, 2012.

[83] T. Kea-Tiong, C. Shih-Wen, C. Meng-Fan, H. Chih-Cheng, and S. Jyuo-Min, "A Low-Power Electronic Nose Signal-Processing Chip for a Portable Artificial Olfaction System," *Biomedical Circuits and Systems, IEEE Transactions on*, vol. 5, pp. 380-390, 2011.

[84] K.-T. Tang, S.-W. Chiu, C.-H. Pan, H.-Y. Hsieh, Y.-S. Liang, and S.-C. Liu, "Development of a portable electronic nose system for the detection and classification of fruity odors," *Sensors*, vol. 10, pp. 9179-9193, 2010.

[85] K.-T. Tang, C.-H. Li, and S.-W. Chiu, "An electronic-nose sensor node based on a polymer-coated surface acoustic wave array for wireless sensor network applications," *Sensors*, vol. 11, pp. 4609-4621, 2011.

[86] C.-H. Pan, H.-Y. Hsieh, and K.-T. Tang, "An analog multilayer perceptron neural network for a portable electronic nose," *Sensors*, vol. 13, pp. 193-207, 2012.

[87] K.-T. Tang and R. M. Goodman, "Electronic Olfaction System on a Chip," in *SCI2001/ISAS2001 International Conference on Information Systems, Analysis and Synthesis*, 2001, pp. Pages-534.

[88] N. Kwan Ting, F. Boussaid, and A. Bermak, "A CMOS Single-Chip Gas Recognition Circuit for Metal Oxide Gas Sensor Arrays," *Circuits and Systems I: Regular Papers, IEEE Transactions on*, vol. 58, pp. 1569-1580, 2011.

[89] K. T. Ng, F. Boussaid, and A. Bermak, "A frequency-based signature gas identification circuit for SnO_2 gas sensors," in *Circuits and Systems (ISCAS), Proceedings of 2010 IEEE International Symposium on*, 2010, pp. 2275-2278.

[90] E. Chicca, F. Stefanini, C. Bartolozzi, and G. Indiveri, "Neuromorphic Electronic Circuits for Building Autonomous Cognitive Systems," *Proceedings of the IEEE,* vol. 102, pp. 1367-1388, 2014.

[91] J. Hasler and B. Marr, "Finding a roadmap to achieve large neuromorphic hardware systems," *Frontiers in neuroscience,* vol. 7, 2013.

[92] K. A. Boahen, "Point-to-point connectivity between neuromorphic chips using address events," *Circuits and Systems II: Analog and Digital Signal Processing, IEEE Transactions on,* vol. 47, pp. 416-434, 2000.

[93] P. Lichtsteiner and T. Delbruck, "A 64 × 64 AER logarithmic temporal derivative silicon retina," in *Research in Microelectronics and Electronics, 2005 PhD*, 2005, pp. 202-205.

[94] N. Cottini, M. Gottardi, N. Massari, R. Passerone, and Z. Smilansky, "A 33W 64 × 64 Pixel Vision Sensor Embedding Robust Dynamic Background Subtraction for Event Detection and Scene Interpretation," *Solid-State Circuits, IEEE Journal of,* vol. 48, pp. 850-863, 2013.

[95] M. Gottardi, N. Massari, and S. A. Jawed, "A 100W 128 × 64 pixels contrast-based asynchronous binary vision sensor for sensor networks applications," *Solid-State Circuits, IEEE Journal of,* vol. 44, pp. 1582-1592, 2009.

[96] P. F. Ruedi, P. Heim, F. Kaess, E. Grenet, F. Heitger, P. Y. Burgi, *et al.*, "A 128 × 128 pixel 120dB dynamic-range vision-sensor chip for image contrast and orientation extraction," *IEEE Journal of Solid-State Circuits,* vol. 38, pp. 2325-2333, 2003.

[97] T. Serrano-Gotarredona and B. Linares-Barranco, "A 128 × 128 1.5% Contrast Sensitivity 0.9% FPN 3 μs Latency 4 mW Asynchronous Frame-Free Dynamic Vision Sensor Using Transimpedance Preamplifiers," *IEEE Journal of Solid-State Circuits,* vol. 48, pp. 827-838, 2013.

[98] L. Watts, D. A. Kerns, R. F. Lyon, and C. A. Mead, "Improved implementation of the silicon cochlea," *Solid-State Circuits, IEEE Journal of,* vol. 27, pp. 692-700, 1992.

[99] R. Moncrieff, "An instrument for measuring and classifying odors," *Journal of applied physiology,* vol. 16, pp. 742-749, 1961.

[100] J. A. Covington, J. W. Gardner, A. Hamilton, T. Pearce, and S.-L. Tan, "Towards a truly biomimetic olfactory microsystem: an artificial olfactory mucosa," *Nanobiotechnology, IET*, vol. 1, pp. 15-21, 2007.

[101] N. Kwan Ting, G. Bin, A. Bermak, D. Martinez, and F. Boussaid, "Characterization of a logarithmic spike timing encoding scheme for a 4 × 4 tin oxide gas sensor array," in *Sensors, 2009 IEEE*, 2009, pp. 731-734.

[102] N. Kwan Ting, F. Boussaid, and A. Bermak, "A frequency-based signature gas identification circuit for SnO_2 gas sensors," in *Circuits and Systems (ISCAS), Proceedings of 2010 IEEE International Symposium on*, 2010, pp. 2275-2278.

[103] M. Bernabei, K. C. Persaud, S. Pantalei, E. Zampetti, and R. Beccherelli, "Large-scale chemical sensor array testing biological olfaction concepts," *Sensors Journal, IEEE*, vol. 12, pp. 3174-3183, 2012.

[104] J. Rajapakse and R. Acharya, "Neuromorphic model for information fusion," in *Acoustics, Speech, and Signal Processing, 1991. ICASSP-91., 1991 International Conference on*, 1991, pp. 2397-2400.

[105] V. Bečanović, R. Hosseiny, and G. Indiveri, "Object tracking using multiple neuromorphic vision sensors," in *RoboCup 2004: Robot Soccer World Cup VIII*, ed: Springer, 2005, pp. 426-433.

[106] V. Y.-S. Chan, C. T. Jin, and A. van Schaik, "Neuromorphic Audio–Visual Sensor Fusion on a Sound-Localizing Robot," *Frontiers in Neuroscience*, vol. 6, p. 21, 02/08

[107] P. O'Connor, D. Neil, S.-C. Liu, T. Delbruck, and M. Pfeiffer, "Real-time classification and sensor fusion with a spiking deep belief network," *Frontiers in neuroscience*, vol. 7, 2013.

[108] V. Dante, P. Del Giudice, and A. Whatley, "PCI-AER–hardware and software for interfacing to address-event based neuromorphic systems," *The Neuromorphic Engineer*, vol. 2, pp. 5-6, 2005.

[109] F. Gomez-Rodriguez, R. Paz, A. Linares-Barranco, M. Rivas, L. Miro, S. Vicente, *et al.*, "AER tools for communications and debugging," in *Circuits and Systems, 2006. ISCAS 2006. Proceedings. 2006 IEEE International Symposium on*, 2006, p. 4 pp.

[110] R. Serrano-Gotarredona, M. Oster, P. Lichtsteiner, A. Linares-Barranco, R. Paz-Vicente, F. Gomez-Rodriguez, *et al.*, "AER building blocks for multi-layer multi-chip neuromorphic vision systems," in *NIPS*, 2005.

[111] iniLabs. (2015). *User Guide: DVS128_PAER*. Available: http://inilabs.com/support/hardware/dvs128paer/

[112] iniLabs. (2015). *Address-Event Representation (AER) protocol*. Available: http://inilabs.com/support/hardware/aer/

[113] iniLabs. (2015). *User Guide: DAS1*. Available: http://inilabs.com/support/hardware/das1/

[114] J. Al Yamani, F. Boussaid, A. Bermak, and D. Martinez, "Glomerular latency coding in artificial olfaction," *Frontiers in neuroengineering*, vol. 4, 2011.

[115] T. Delbrück, B. Linares-Barranco, E. Culurciello, and C. Posch, "Activity-driven, event-based vision sensors," in *Circuits and Systems (ISCAS), Proceedings of 2010 IEEE International Symposium on*, 2010, pp. 2426-2429.

[116] T. Bekolay, J. Bergstra, E. Hunsberger, T. DeWolf, T. C. Stewart, D. Rasmussen, *et al.*, "Nengo: a Python tool for building large-scale functional brain models," *Frontiers in neuroinformatics*, vol. 7, 2013.